管秉贤论著

汇集

Ⅲ. 黑潮源地和赤道区域的环流结构及其与中国近海海气相互关系的研究

中国科学院海洋研究所

1990

目　录

1．北太平洋西部赤道区域的海流结构及其变异

2．中国东南近海冬季逆风海流的证据

3．黑潮大弯曲与 El Nino 关系初探

4．东海黑潮主要特征及变异

5．棉兰老冷涡的变异及其与 El Nino 的关系

6．台湾和菲律宾以东海域冬季海流结构及变异

7．台湾和菲律宾以东海域的深层环流

8．巴士海峡及其附近夏季环流分布特征

9．副热带逆流二十年研究概况

10．北太平洋西部低纬海域海流结构和海气相互关系的若干特征

11．国内关于 El Nino 及其对海洋和气候的影响研究概述

CURRENT STRUCTURE AND ITS VARIATION IN THE EQUATORIAL AREA OF THE WESTERN NORTH PACIFIC OCEAN*

Guan Bingxian(管秉贤)
(Institute of Oceanology, Academia Sinica, Qingdao, China)

Abstract

Based on the current measurement data from the R/V Ryofu Maru of JMA in the equatorial area along 137°E (1972—83) and 155°E (1972—79) the structures of the zonal velocity of the Equatorial Undercurrent (EUC) and the North Equatorial Countercurrent (NECC) and their variations are systematically analyzed in detail.

At 155°E, the current at the equator and 100—300 m depth was a typical eastward EUC, it intensified in 1973—75, i.e., in the non-El Niño period. While the corresponding current at 137°E was mostly westward, and the origin of the EUC shifted to north of the equator around 0.5—1.5°N owing to the influence of the New Guinea Coast. The EUC origin disappeared in early July, 1982. Comparing with the EUC disappearance at 159°W, the average speed of an eastward travelling wave would be ~1.1m/s.

The velocity core of the NECC at 137°E generally shifted northward in winter and southward in summer, and was stronger in summer and weaker in winter. The fluctuations of the NECC were closely related to those of the wind stress curl over the region 2—10°N, 160°E—150°W.

INTRODUCTION

The western tropical Pacific Ocean is a heat pool and has been known as the origin of inducing the El Niño in the eastern equatorial Pacific Ocean, which is an extreme hydroclimatic anomaly. Theoretical and modeling studies suggest that oceanic circulation, especially equatorial circulation, has an important role in the formation of such an anomaly by altering the patterns of sea-surface temperature through advection (Meyers & Donguy, 1984). Among which the western equatorial North Pacific is a key region for the study of the equatorial ocean circulation because it is the origin of the eastward and the end of the westward equatorial currents.

Since the sixties, oceanographers, especially the Japanese and French have made many important contributions to the study of the circulation of the western equatorial and/or tropical Pacific Ocean (for example, Akamatsu & Sawara, 1969; Chaen, 1982; Colin et al., 1973; Donguy & Henin, 1983; Donguy et al., 1984;Masuzawa, 1967; Masuzawa & Nagasaka, 1975; Nagasaka, 1980, 1983; Nagasaka & Sawara, 1972; Tsuchiya, 1961; etc.).

But the circulation of the western equatorial Pacific Ocean is found to be less studied than the circulation of the central and eastern equatorial Pacific Ocean. Therefore, the

---

*Project Supported by the Science Fund of the Chinese Academy of Sciences.
Presented at IAMAP/IAPSO Joint Assembly (August 5—16, 1985 Honolulu, Hawaii).
Contribution No. 1331 from the Inst. of Oceanol., Academia Sinica. Received Feb. 25, 1986.

circulation of the western equatorial Pacific Ocean is worth further and thorough study, especially for elucidation on the mechanism of the El Niño.

Based on the upper 500m current measurement data from the R/V Ryofu Maru of JMA in the equatorial area along 137°E (in winter and summer, 1972—83) and 155°E (in summer, 1972—79) the structures of the zonal velocity of the Equatorial Undercurrent (EUC) and the North Equatorial Countercurrent (NECC) and their variations (especially in the period of 1982—83 El Niño Event), are systematically analyzed in detail. Fig.1 shows the section location chart of the Ryofu Maru, JMA, in 1972—83.

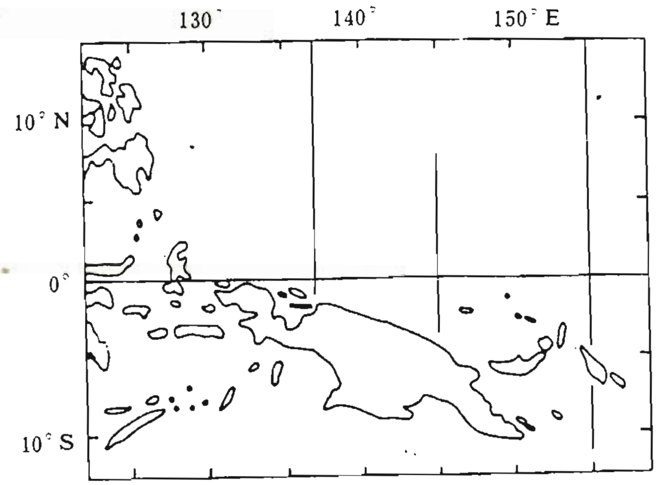

Fig. 1 Section location chart, Ryofu Maru, 1972—83 (137°, 145°,and 155°E)

The main results are as follows:

STRUCTURES OF THE CURRENTS AT THE EQUATOR AND OF THE EUC

The structures of the currents at the equator at 155°E and 137°E, owing to their different geographical locations relative to the western boundary and the New Guinea Coast, are quite different. Meridional distributions of zonal velocity components (cm.s^{-1}, positive eastward) at 155°E and 137°E in summer, 1973 are shown in Fig. 2a, b, respectively.

At 155°E, the current at the equator and thermoclinic depth (~100—300 m)was a stronger and typical eastward EUC, symmetrial with respect to the equator. Above the EUC was the surface layer current, the direction of which was occasionally eastward or westward. Below the EUC was the westward Equatorial Intermediate Current (EIC, Hisard and Rual, 1970). While at 137°E, the current at the equator and thermoclinic depth was mostly westward. The eastward current was observed north of the equator, around 0.5° ~ 1.5°N. Sometimes it appeared as an isolated current core, and sometimes extended northward with the NECC. It is weaker and of smaller scale compared with the EUC at 155°E. It is the origin or embryonic form of the EUC east of 137°E. In the following discussion, we name it "the origin of the EUC" (after Nagasaka & Sawara, 1972).

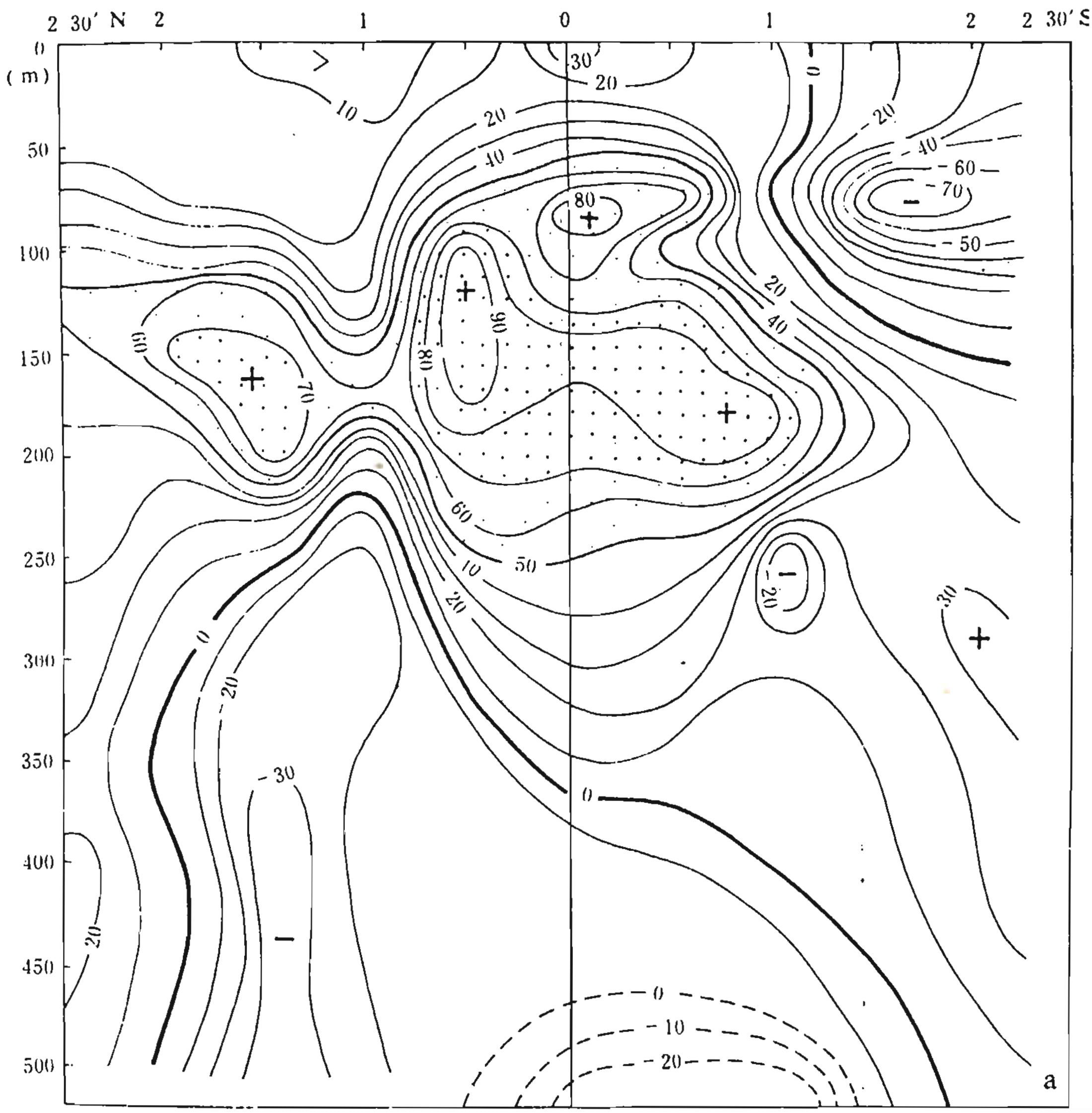
2 30′ N
2
1
0
1
2
2 30′ S
0
(m)
50
100
150
200
250
300
350
400
450
500
a

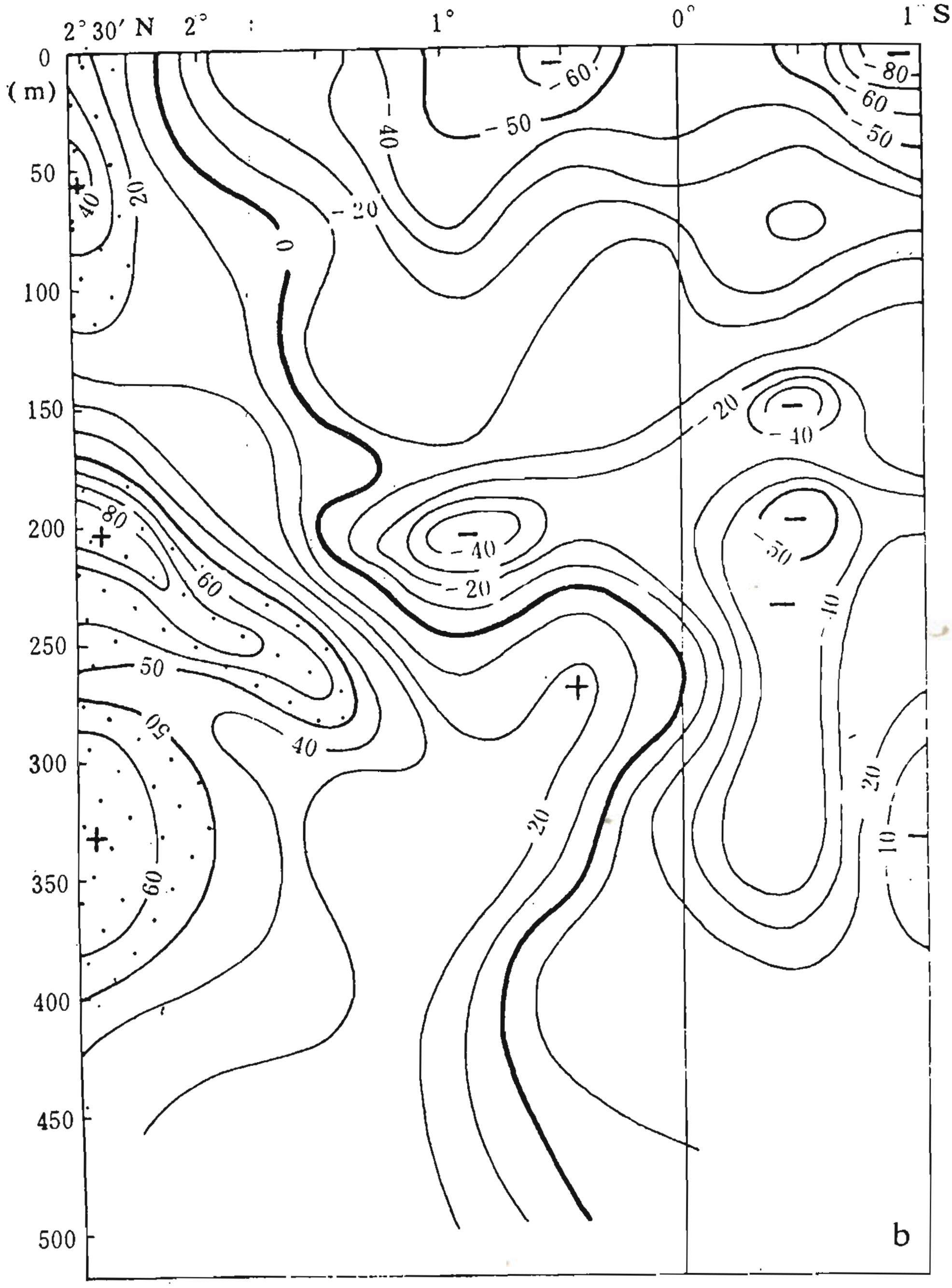

Fig. 2 Meridional distribution of zonal velocity components (cm · s^{-1}, positive eastward) at 155°E (a) and 137°E (b) in summer, 1973.

SEASONAL AND INTERANNUAL VARIATIONS

The structures of the zonal velocity components at the equator and 155°E and 137°E sections revealed many pronounced seasonal and interannual variations.

1. Fig. 3 shows the zonal velocity components on the equator at 155°E in summer, 1972—1979. It is evident that the velocity of the EUC in the summers of 1973 and 1975 (no observation in 1974) may reach a maximum of 80—90 cm · s^{-1} at 100—250m depths. Therefore, the EUC at 155°E intensified in the post-and pre-El Niño period of 1972 and 1976, respectively. During this period, stronger than normal equatorial trade winds caused a build-up of the sea level in the western Pacific that strengthened the EUC.

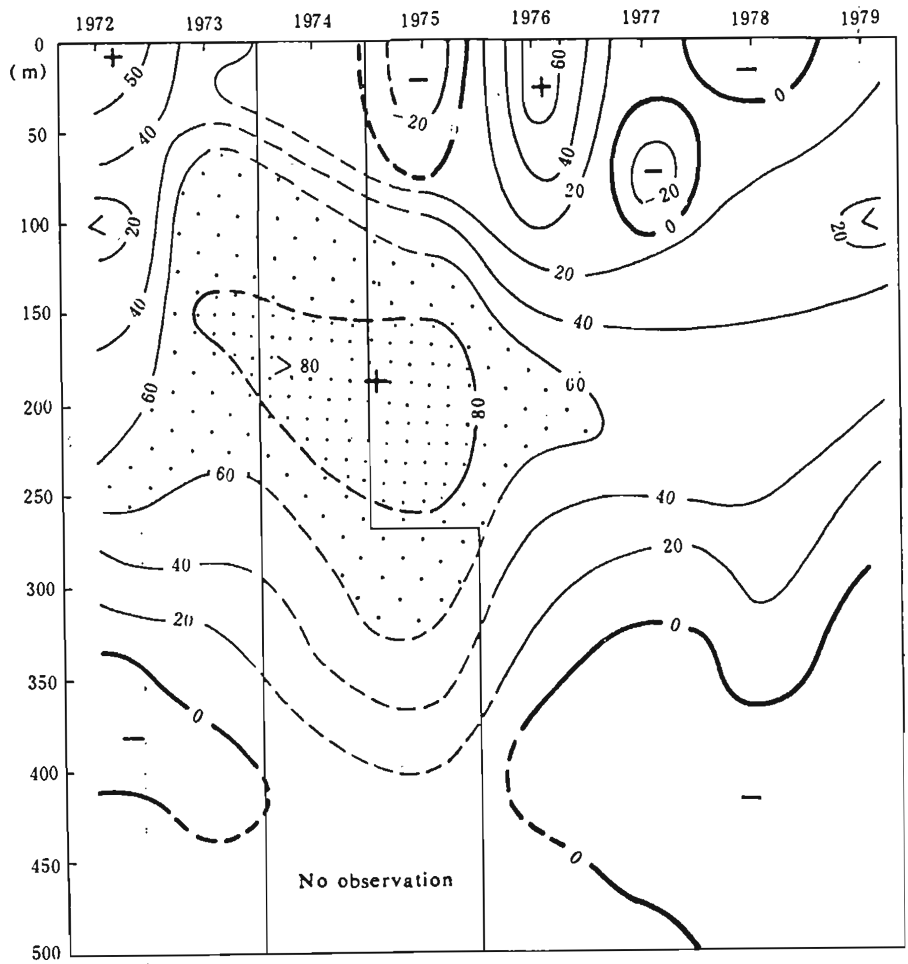

Fig. 3 Zonal velocity component (cm · s^{-1}, positive eastward) on the equator at 155°E in summer, 1972—1979.

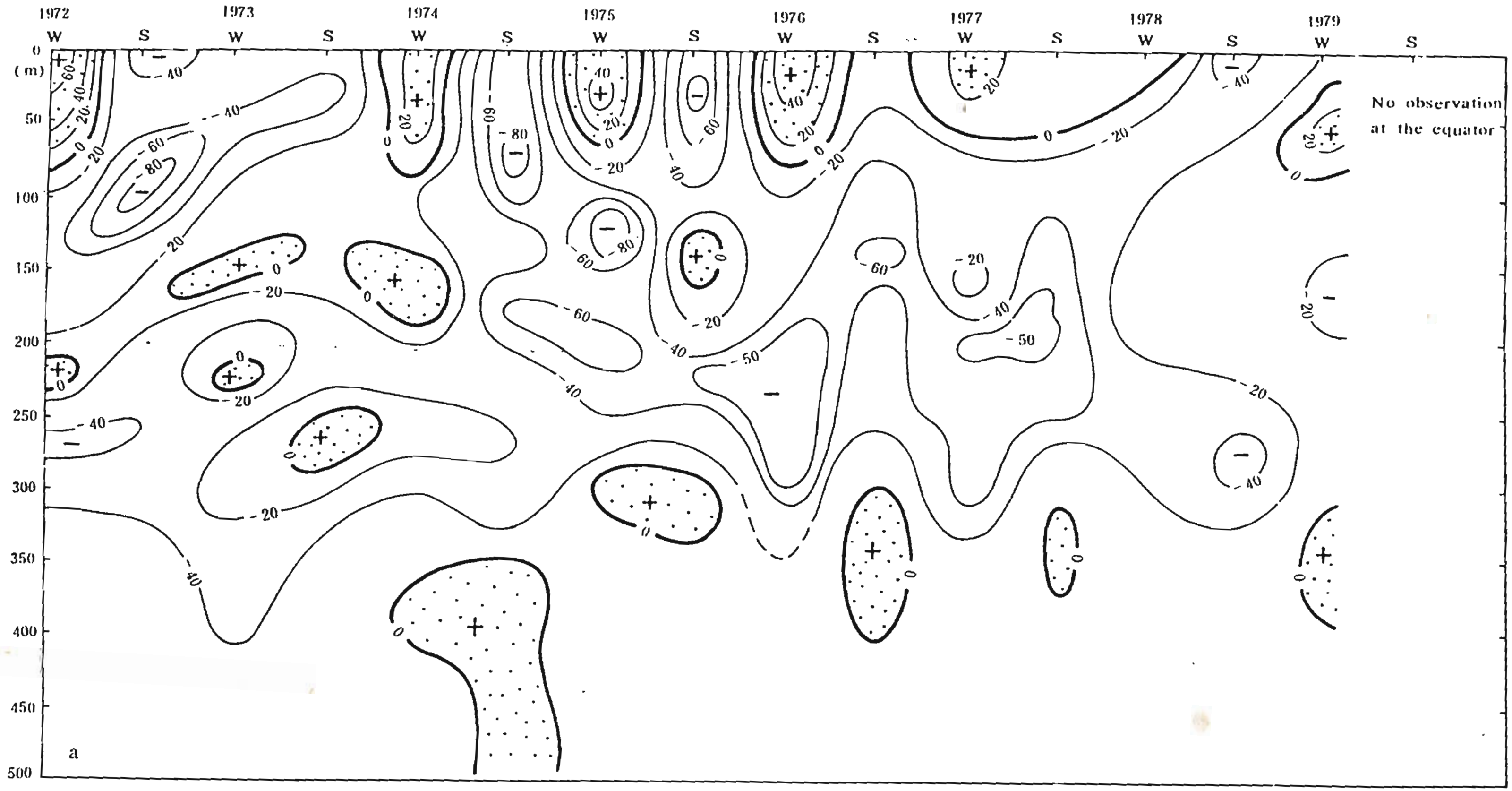
1972 1973 1974 1975 1976 1977 1978 1979
W S W S W S W S W S W S W S W S
0
(m)
50
100
150
200
250
300
350
400
450
500
No observation
at the equator
a

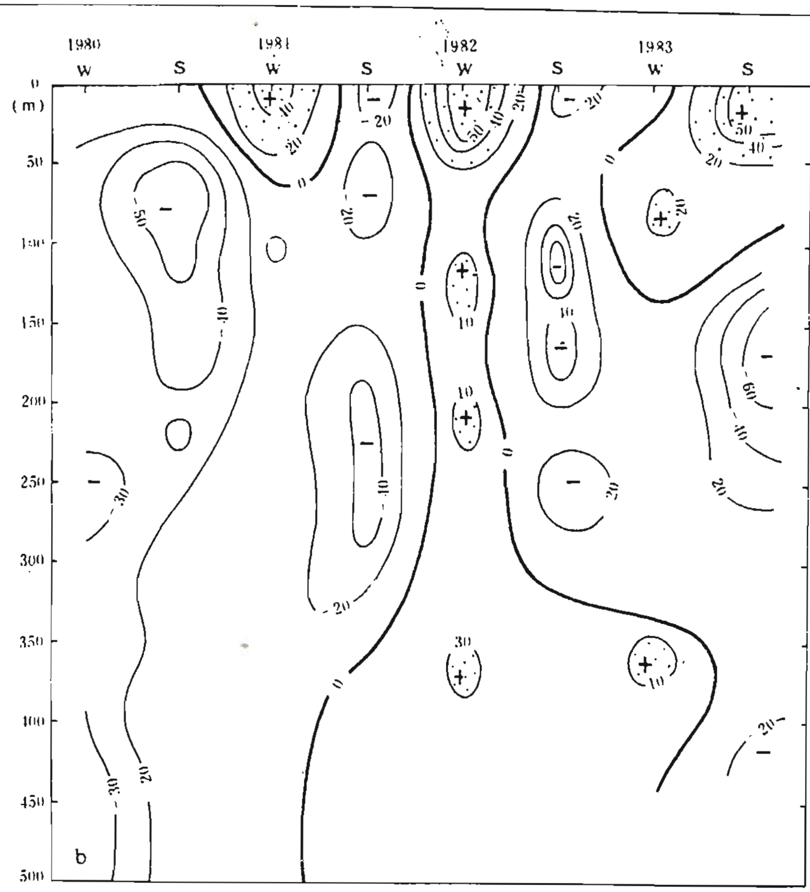

Fig. 4 Zonal velocity components (cm· s^{-1}· positive eastward) on the equator at 137°E in winter and summer. 1972—1979 (a) and 1980—1983 (b).

2. Fig. 4 shows the zonal velocity components on the equator at 137°E in winter and summer, 1972—1979 and 1980—1983, respectively. In this period, except for the upper 100 m layer (in which the current moved occasionally eastward or westward) the current at the thermoclinic depth (100—300 m) mostly flowed westward. Data are not available at the equator in the summer of 1979. The sole exception of eastward current in 0—360 m depths was observed in winter, 1982, but its velocity was rather weak, around 10 cm · s^{-1} at the thermoclinic depth. Below the 300 m depth, it was still predominant with weak westward current, but sometimes weak eastward flow appeared. Therefore, in 100—500 m depth, it was extremely dominated with westward current either in summer or in winter.

(1) The directions of the surface layer current varied with the seasons. Fig. 5 shows the fluctuations of the zonal velocity components averaged in the 10—50 m layer on the equator at 137°E in winter and summer, 1972—83. With few exceptions, the currents mostly flowed eastward in winter (it is the so-called "New Guinea Coastal Current") and westward in summer (it is the South Equatorial Current (SEC)). The seasonal average velocities are eastward in winter and westward in summer, and stronger in summer (27.5 cm · s^{-1}) and weaker in winter (18.2 cm · s^{-1}).

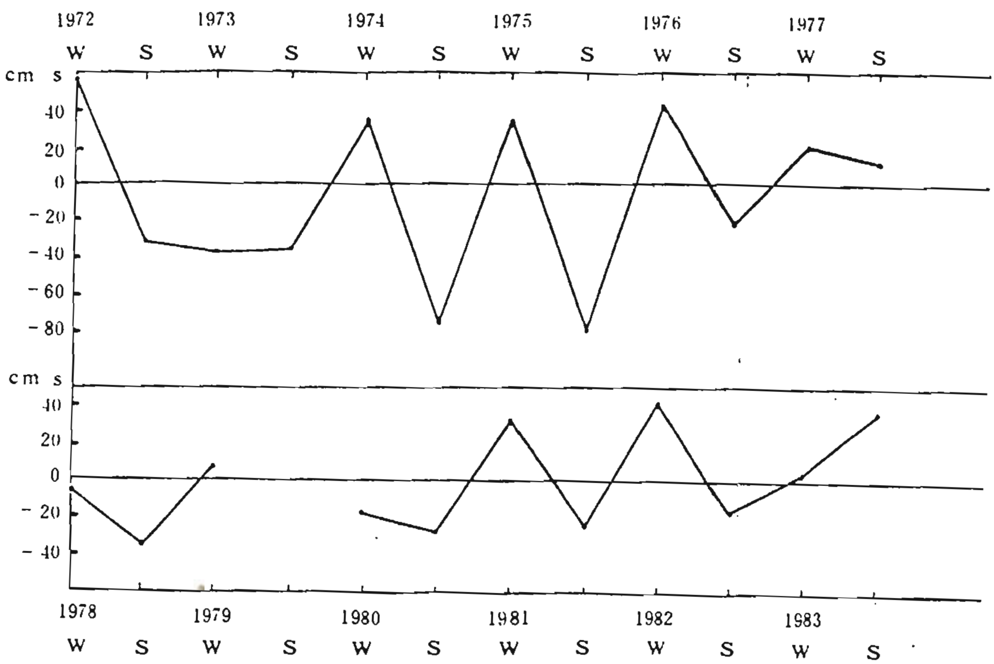

Fig. 5 Fluctuations of the zonal velocity components (cm· s^{-1}, positive eastward) averaged in the 10—50 m layer on the equator at 137°E in winter and summer, 1972—83.

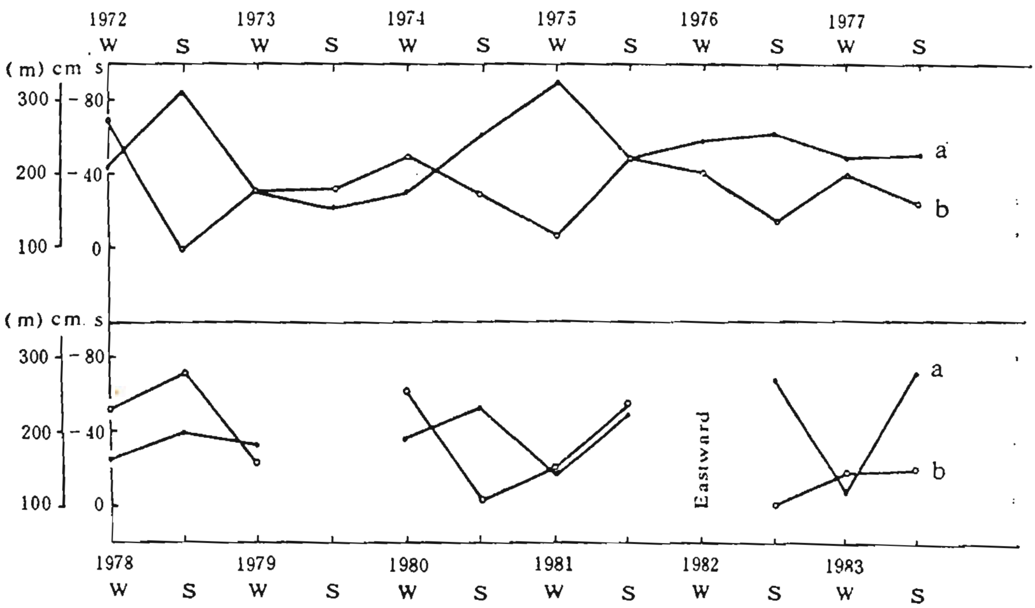

Fig. 6 Fluctuations of the maximum westward velocity components in the 100—300 m layer on the equator at 137°E in winter and summer, 1972—83.

(2) The westward velocities in the 100—300 m layer revealed significant seasonal variations, too. Fig. 6 shows the maximum westward velocity component in this layer on the equator at 137°E in winter and summer, 1972—83. Its average velocity was -38.5 $cm \cdot s^{-1}$ in winter and -55.6 $cm \cdot {}^{-1}$ in summer. Such a seasonal variation (stronger in summer than in winter) coincides with that of the SEC, an evidence for identification of the westward current being the SEC.

ORIGIN OF THE EUC AT 137°E

As mentioned above, during the period 1972—83 (with the exception of the summer of 1982, which will be analysed separately) the origin of the EUC shifted to north of the equator around 0.5°—1.5°N. Such stationary northward displacement can not be produced by the north-south oscillation of the EUC itself, or by the effect of the meridional component of the wind (Gill, 1982). It is suggested that such displacement may probably have been caused by the boundary effect of the New Guinea Coast on the EUC. It is less than 90 nautical miles from the equator at 137°E to the New Guinea Coast. As a result of the boundary obstruction, the water will pile up along the coast, depressing the thermocline in the vicinity of the coast. The associated additional poleward pressure gradient corresponds to an increase of the current north and a reduction south of the equator. In other words, the core of the origin of the EUC was shifted northward (Gill, 1982). Fig. 7 shows the current vectors at thermoclinic depths at 137°, 145° and 155°E, respectively. It is clear the eastward EUC began to appear, at least at 145°E, where the distance from the equator to the coast is ca. 240 nautical miles, hence the coastal effect would be much reduced than that at 137°E.

In the winters and summers of 1972—83, the origin of the EUC also had pronounced fluctuations. Either the location or the strength of its core varied seasonally and interannually. The case in the summer of 1982 was especially noteworthy. Fig. 8 shows the meridional distribution of zonal velocity components at 137°E in summer, 1982. It is evident from the figure that in the range of 1°S—2°N the westward current occupied the whole water column at the 100—300 m depth. The maximum westward velocity reached 69.2 $cm \cdot {}^{-1}$ at 0—2N. Therefore, the origin of the EUC was virtually absent in the observation period June 30—July 2, 1982, at and close to the equator. In other words, the reversal of zonal current (from eastward to westward) in the main thermocline appeared at 137°E in early July, 1982.

The area of equatorial low-level westerly wind anomalies first appeared in the far western equatorial Pacific (~ 140°E) in June, 1982, then progressed steadily eastward for an entire year until it reached the eastern Pacific (Rasmusson et al., 1983). The disappearance of the origin of the EUC at 137°E in early July of 1982 is closely related to the first appearance of the anomalous westerly wind in the western Pacific in June, 1982. In the 1982—83 El Niño event, the EUC at the equator and 159°W disappeared and a westward flow appeared in September, 1982 (Firing et al., 1983). Therefore, from 137°E to 159°W the disappearance of the EUC propagated eastward with an average velocity of ca. 1.1 $m \cdot s^{-1}$. At 110°W the onset time of the EUC disappearance was nearly 4.5 months later than at 159°W. So the average eastward propagation velocity of this phenomenon from 159°W to 110°W wound be 0.5 $m \cdot s^{-1}$ (Halpern, 1983).

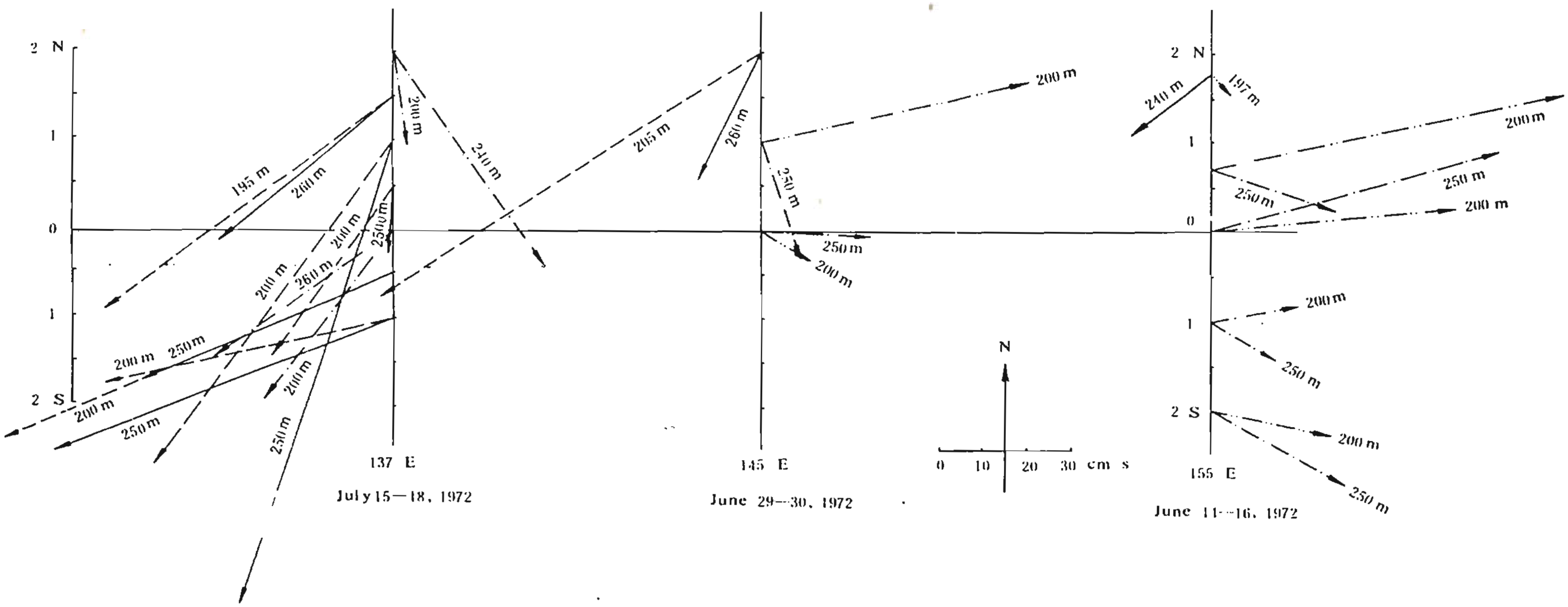

Fig. 7 Current vectors at the thermoclinic depth (ca. 200, 250 m) in summer, 1972.

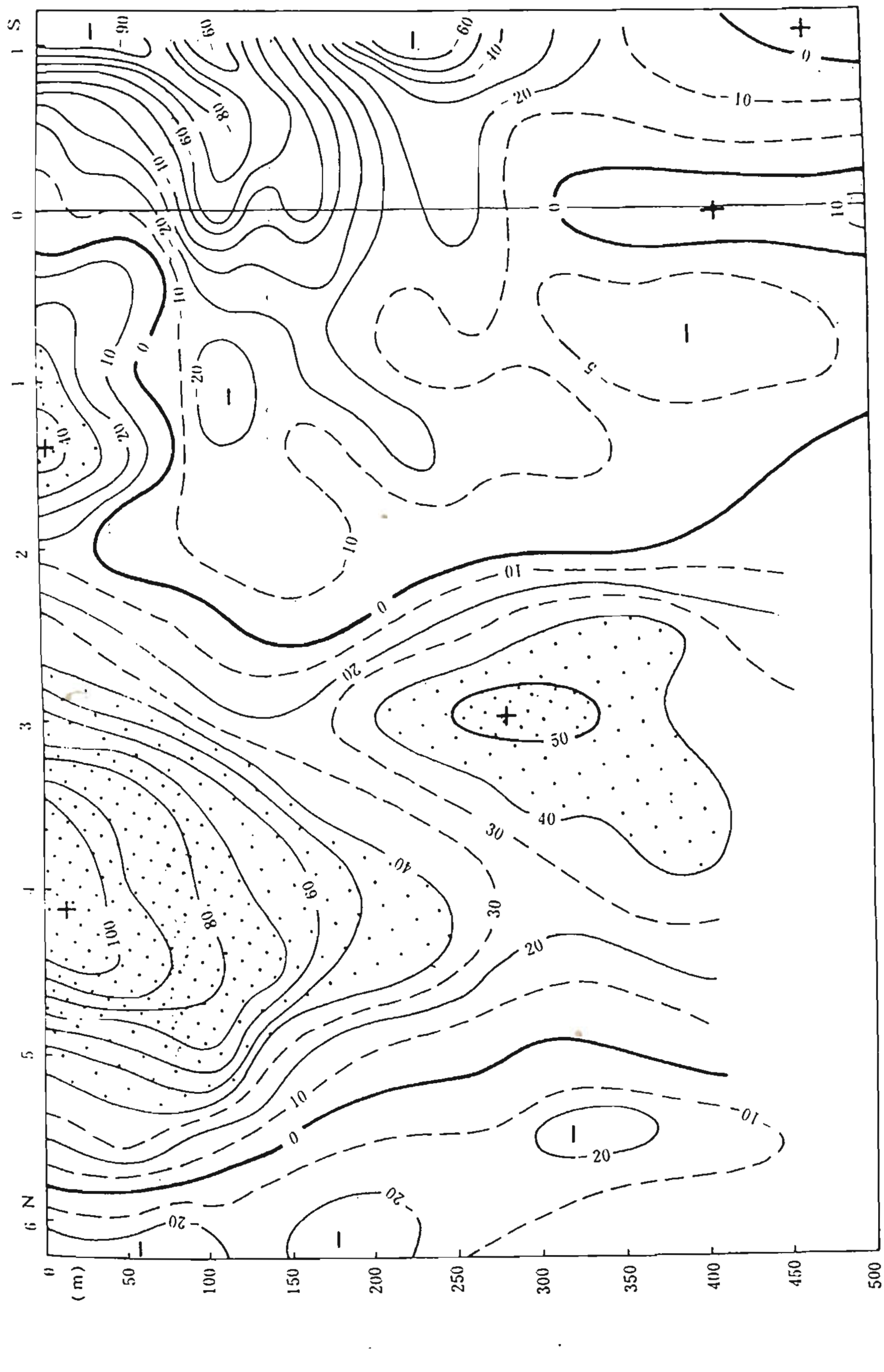

Fig. 8 Meridional distribution of zonal velocity component (cm · $^{-1}$, positive eastward) at 137°E in summer, 1982. The origin of the EUC was virtually absent in the period June 30—July 2 at and close to the equator (1°S—2°N).

Therefore, in the 1982—83 El Niño event, the ocean current anomalies that appeared from the far western equatorial Pacific to the eastern Pacific were comparable to the corresponding atmospheric anomalies. Both included reversals in the normal direction of flow. The phenomenon of ocean current anomalies also propagated from west to east, with an average speed ca. $1.0\sim0.5\ m\cdot s^{-1}$. In addition, the average speeds of an eastward travelling wave from the far western equatorial Pacific to the eastern equatorial Pacific are reconcilable each other.

NORTH EQUATORIAL COUNTERCURRENT AND ITS VARIATIONS

In the winters and summers of 1980—83, the NECC was the most powerful current in the area of 8°—0°N. It had the highest speed, widest width and deepest penetration. Fig. 9 shows the meridional distribution of zonal velocity components at 137°E in winter (a) and summer (b), 1981. Generally, it has only one current core (nucleus) in the horizontal direction. Sometimes double cores appeared with a some weak region in between. But in the vertical direction, there are two eastward current cores, one deeper and the other shallower. Underneath the NECC, and on the southern side, the deep eastward current core with its centre around 3°N , is the Northern Subsurface Countercurrent (NSCC, Tsuchiya, 1975). On the northern side of and underneath the NECC (200—500 m), the other core with its centre around 5°—6°N, on the contrary, is a westward current which was first recognized by Tsuchiya (1961) on the temperature and dynamic sections.

On both sides of the NECC are the North Equatorial Current (NEC) and SEC. The upper layer current north of the NECC is generally a westward flow, i.e., NEC. But at greater depth, especially around 8°N, a relatively strong and deep penetrating eastward current often appeared as in 1981 (Fig. 9a, b). Sometimes, it was still dominated with westward current as in 1982 and 1983 (figure not shown).

Therefore, the current structure in the Equatorial area of the western North Pacific has some outstanding feastures. Though similar in general with that in the central and eastern Pacific, and chiefly in line with the traditional idea, it is more complicated. With the location, depth and strength of the maximum velocity of the zonal component (i.e. the current core) as indexes, the seasonal and interannual variations of the NECC at 137°E in 1972—83 are shown in fig.10.

1. In the great majority of cases, the current core shifted northward (the average location was ca. 5.3° N) in winter and southward (ca. 3.8° N) in summer, quite regularly oscillated in the range 6°—3°N. The maximum speed of the N-S oscillation of the NECC axis may reach 55 km/mon, or 2 km/day.

2. The average depth of the current core is about 90 m, it deepens as its strength weakens, and vice versa.

3. On an average, the velocity of the current core was higher in summer (ca. 111.8 $cm\cdot s^{-1}$) than in winter (ca. 105.4 $cm\cdot s^{-1}$). The maximum (188.7 $cm\cdot s^{-1}$) appeared in summer, 1980. The second-maximum appeared in summer, 1976 (144.6 $cm\cdot s^{-1}$) and in winter, 1977 (135.0 $cm\cdot s^{-1}$). It is worth noting that, in the period 1972—83, there appeared three El Niño events, i.e., the 1972—73, 1976—77, and 1982—83 events. Except for the summer of 1976 and the winter of 1977, the core velocity of the NECC was not so strong.Especially, since the core velocity reached the peak value in summer, 1980, the velocity continued to decrease and remained at a low-level till the end of the obser-

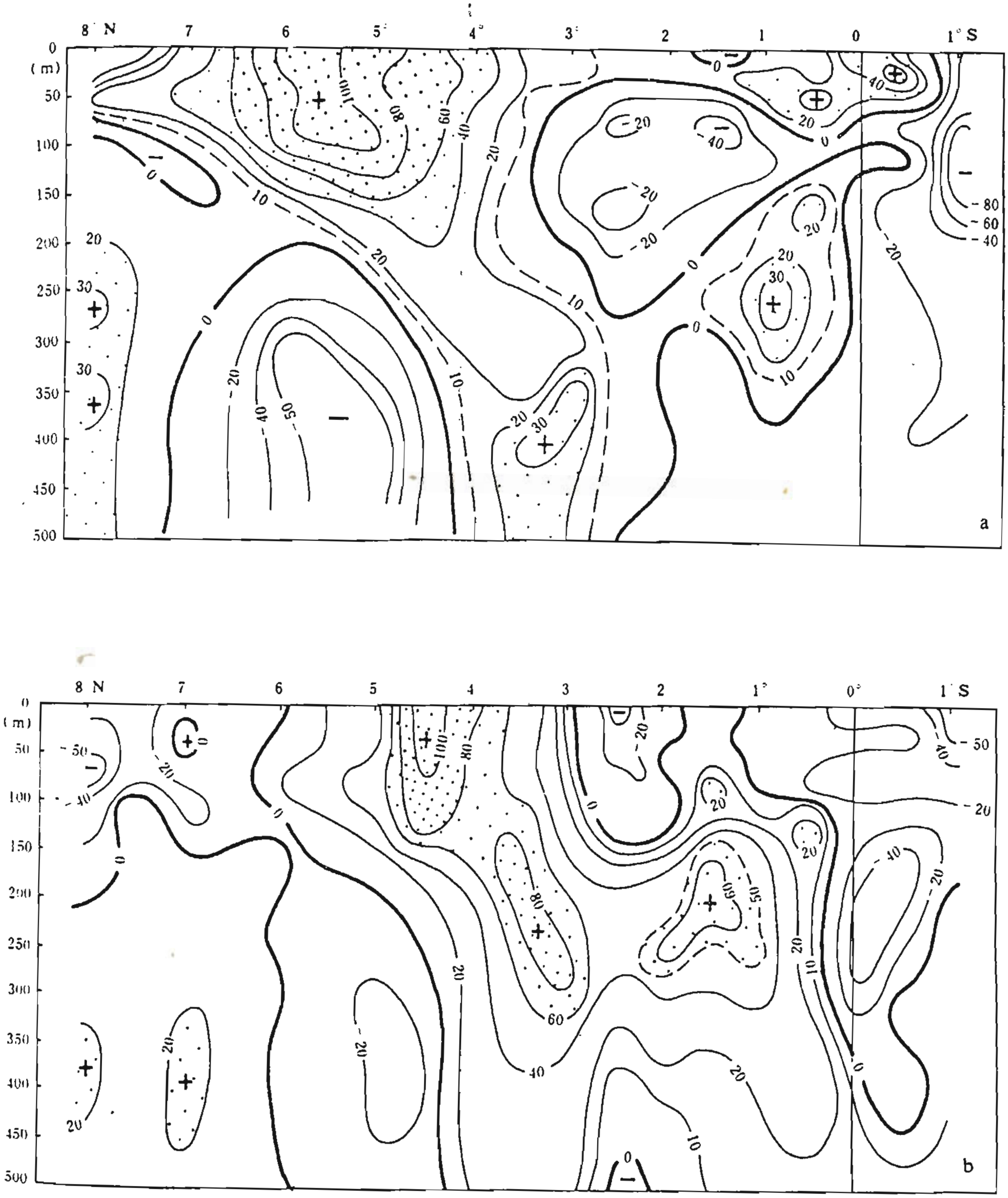

Fig. 9 Meridional distribution of zonal velocity components (cm . s^{-1}, positive eastward) at 137°E in winter (a, Jan 31—Feb 1) and summer (b, June 30—July 2), 1981.

Therefore, in the 1982—83 El Niño event, the ocean current anomalies that appeared from the far western equatorial Pacific to the eastern Pacific were comparable to the corresponding atmospheric anomalies. Both included reversals in the normal direction of flow. The phenomenon of ocean current anomalies also propagated from west to east, with an average speed ca. $1.0 \sim 0.5\ m \cdot s^{-1}$. In addition, the average speeds of an eastward travelling wave from the far western equatorial Pacific to the eastern equatorial Pacific are reconcilable each other.

NORTH EQUATORIAL COUNTERCURRENT AND ITS VARIATIONS

In the winters and summers of 1980—83, the NECC was the most powerful current in the area of 8°—0°N. It had the highest speed, widest width and deepest penetration. Fig. 9 shows the meridional distribution of zonal velocity components at 137°E in winter (a) and summer (b), 1981. Generally, it has only one current core (nucleus) in the horizontal direction. Sometimes double cores appeared with a some weak region in between. But in the vertical direction, there are two eastward current cores, one deeper and the other shallower. Underneath the NECC, and on the southern side, the deep eastward current core with its centre around 3°N , is the Northern Subsurface Countercurrent (NSCC, Tsuchiya, 1975). On the northern side of and underneath the NECC (200—500 m), the other core with its centre around 5°—6°N, on the contrary, is a westward current which was first recognized by Tsuchiya (1961) on the temperature and dynamic sections.

On both sides of the NECC are the North Equatorial Current (NEC) and SEC. The upper layer current north of the NECC is generally a westward flow, i.e., NEC. But at greater depth, especially around 8°N, a relatively strong and deep penetrating eastward current often appeared as in 1981 (Fig. 9a, b). Sometimes, it was still dominated with westward current as in 1982 and 1983 (figure not shown).

Therefore, the current structure in the Equatorial area of the western North Pacific has some outstanding feastures. Though similar in general with that in the central and eastern Pacific, and chiefly in line with the traditional idea, it is more complicated. With the location, depth and strength of the maximum velocity of the zonal component (i.e. the current core) as indexes, the seasonal and interannual variations of the NECC at 137°E in 1972—83 are shown in fig.10.

1. In the great majority of cases, the current core shifted northward (the average location was ca. 5.3° N) in winter and southward (ca. 3.8° N) in summer, quite regularly oscillated in the range 6°—3°N, The maximum speed of the N-S oscillation of the NECC axis may reach 55 km/mon, or 2 km/day.

2. The average depth of the current core is about 90 m, it deepens as its strength weakens, and vice versa.

3. On an average, the velocity of the current core was higher in summer (ca. 111.8 $cm \cdot s^{-1}$) than in winter (ca. 105.4 $cm \cdot s^{-1}$). The maximum (188.7 $cm \cdot s^{-1}$) appeared in summer, 1980. The second-maximum appeared in summer, 1976 (144.6 $cm \cdot s^{-1}$) and in winter, 1977 (135.0 $cm \cdot s^{-1}$). It is worth noting that, in the period 1972—83, there appeared three El Niño events, i.e., the 1972—73, 1976—77, and 1982—83 events. Except for the summer of 1976 and the winter of 1977, the core velocity of the NECC was not so strong.Especially, since the core velocity reached the peak value in summer, 1980, the velocity continued to decrease and remained at a low-level till the end of the obser-

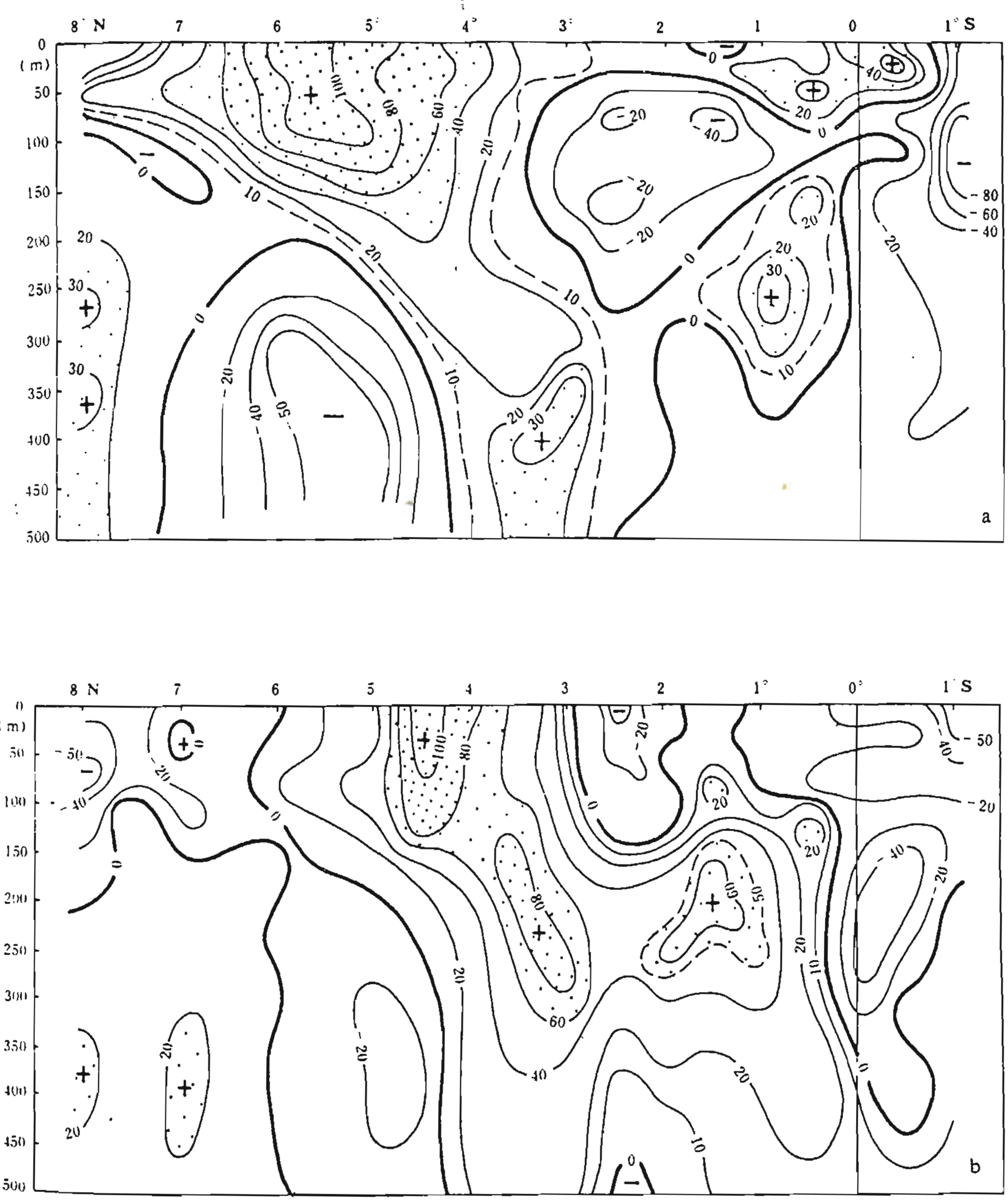

Fig. 9 Meridional distribution of zonal velocity components (cm . s^{-1}, positive eastward) at 137°E in winter (a, Jan 31—Feb 1) and summer (b, June 30—July 2), 1981.

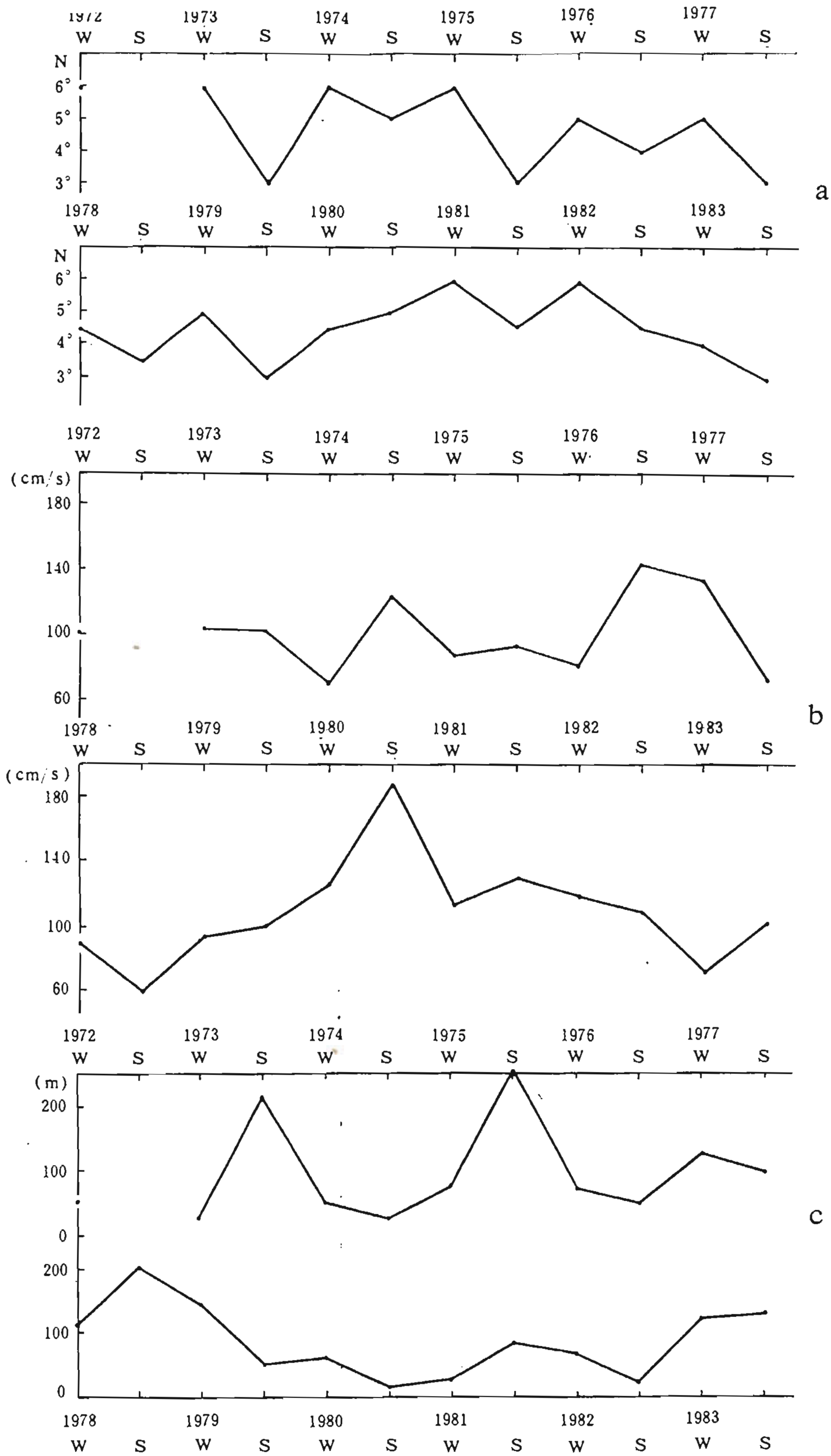

Fig. 10 Fluctuations of the velocity core of the NECC at 137°E in winter and summer, 1972—83. (a) Location, (b) Strength, (c) Depth

vation period. Therefore, the contribution of the NECC to the eastward transportation of water in the 1982—83 El Niño event seems to be not so great as usually conjectured, so far as the variation of its core velocity is concerned.

But the situation was quite different to the east, for example, at 160°E. The eastward surface flow of the NECC was stronger than normal from June to December, 1982. At approximately the same time, an enhanced eastward flow was observed in the central and eastern Pacific. Thereafter, the NECC diminished to an extremely weak level by March 1983 and remained weak until June 1983 (Meyers & Donguy, 1984). The above mentioned different tendencies of the interannual variation of the NECC at 137°E from 1979 to 1983 suggest that the variability of the currents in the western most part of the equatorial North Pacific Ocean has some peculiar features.

4. Fig. 11 shows the time series (1950—75) of the sea level difference across the NEC (a), NECC (b) and the wind stress curl over the sea region 2°—10°N, 160°E—150°W(c). Curves a and b (after Wyrtki, 1979) depict the fluctuations of the velocities of the NEC and NECC, respectively. Comparison shows that the fluctuations of the NECC and NEC (they fluctuate synchronously, Wyrtki, 1974) approach to be coincident with those of the wind stress curl over the sea region 2°—10°N. Except the initial parts (1950—53),

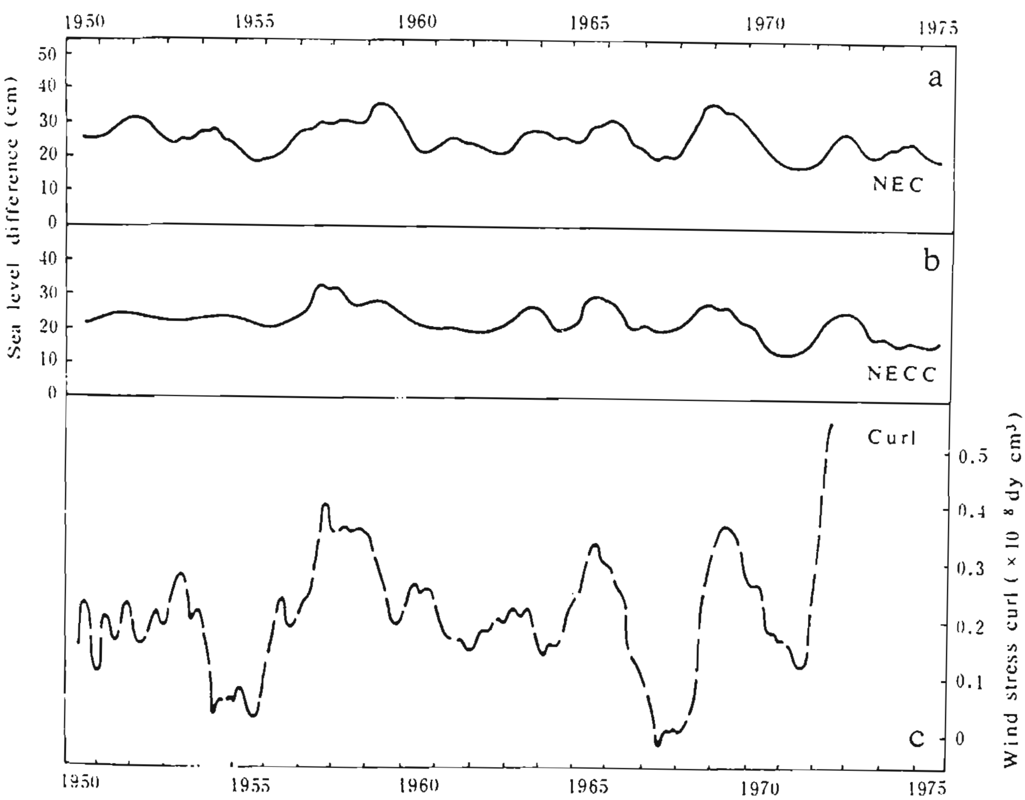

Fig. 11 Time series (1950—75) of sea level difference across the NEC (a), NECC (b) and the wind stress curl (c) over the sea region 2°—10°N, 160°E—150°W. Curves give the 12-month running mean (Curves a and b after Wyrtki, 1979).

significant peaks and troughs of these three curves nearly approach coincide one another. Therefore, in the period 1953—1972, the fluctuations of equatorial currents of the North Pacific Ocean were controlled mainly by the fluctuations of the wind stress curl field over the sea region north of the equator.

References

[1] Akamatsu, H. and T. Sawara, 1969. The preliminary report of the third cruise for CSK, January to March, 1969. *Oceanogr. Mag.*, 21:83—96.

[2] Chaen, M., 1982. About the fluctuations of the North Equatorial Current and Equatorial Countercurrent in the western Pacific Ocean. *In*: Abstracts of Lectures in Spring Assembly of Oceanographic Society of Japan 1982, p. 73—74. (in Japanese)

[3] Colin, C., F. Jarrige, F. Rougerie and P. Rual, 1973. Equatorial Current system north of the New Guinea. *In*: The kuroshio III-Proceedings of the Third CSK Symposium, p. 150—160.

[4] Donguy. J. R. &. C. Henin, 1983. Fluctuations of the Equatorial Currents system connected with the hydroclimatic conditions in the western Pacific. *Océanogr. trop.*, 18(1):17—24.

[5] Donguy,J., R. G. Eldin, A Morlière, J. P. Rébert and G. Meyers, 1984. A thermal interpretation of a change in equatorial western Pacific circulation. *Trop. Ocean-Atmos. Newslett.*, 24:9—11.

[6] Firing, E., R. Lukas, J. Sadler and K. Wyrtki, 1983. Equatorial Undercurrent disappears during 1982—1983 El Niño *Science*, 222:1121—1123.

[7] Gill, A. E., 1982. "Atmosphere-Ocean Dynamics", Academic Press, 482—483.

[8] Halpern, D., 1983. Variability of the Cromwell Current at 110°W before and during the 1982—83 warm event. *Trop. Ocean-Atmos. Newslett.*, 21:31—34.

[9] Hisard, P. & P. Rual. 1970. Courant equatorial intermediaire de l'ocean Pacifique et contre-courants adjacents. *Cah. Oceanogr.*, 8(1):21—45.

[10] Japan Meteorological Agency, 1973—84. The Results of Marine Meteorological and Oceanographical Observations No. 51—74.

[11] Masuzawa, J., 1967. An oceanographic section from Japan to New Guinea at 137°E in January 1967. *Oceanogr. Mag.*, 19:95—118.

[12] Masuzawa, J. and K. Nagasaka, 1975. The 137°E oceanographic section. *Journal of Marine Research, Supplement.*, 33:109—116.

[13] Meyers, G, & J. R. Donguy, 1984. The North Equatorial Counter current and heat storage in the western Pacific Ocean during 1982—83. *Nature*, 312(5591):258—260.

[14] Nagasaka, K., 1980. The oceanographic section along 137°E. *In:* The Kuroshio IV-proceedings of the 4th CSK Symposium, p. 313—320.

[15] Nagasaka, K., 1983. El Niño and the current system in the equatorial area of the western Pacific Ocean. *In:* Abstracts of Lectures in Spring Assembly of Oceanographic Society of Japan 1983, p. 35. (in Japanese)

[16] Nagasaka, K. & T. Sawara, 1972. A preliminary report of the cruise of the R/V Ryofu-Maru in January—March 1971. *Oceanogr. Mag.*, 24:25—38.

[17] Rasmusson, E. M., P. A. Arkin, A. F. Krueger, R. S. Quiroz and R. W. Reynolds, 1983. The equatorial Pacific atmospheric climate during 1982—83. *Trop. Ocean-Atmos. Newslett.*, 21:2—3.

[18] Tsuchiya, M., 1961. An oceanographic description of the equatorial current system of the western Pacific. *Oceanogr. Mag.*, 13:1—30.

[19] Tsuchiya, M., 1975. Subsurface countercurrents in the eastern equatorial Pacific Ocean. *J. Mar. Res.*,

Supplement, p. 145—175.

[20] Wyrtki, K., 1974. Equatorial currents in the Pacific 1950 to 1970 and their relations to the trade winds. *J. Phys. Oceanogr.* 4(3): 372—380.

[21] Wyrtki, K.,1979. Sea level variations: monitoring the breath of the Pacific. *Trans. Amer. Geophys. Union,* 60(3):25—27.

EVIDENCE FOR A COUNTER-WIND CURRENT IN WINTER OFF THE SOUTHEAST COAST OF CHINA*

Guan Bingxian (管秉贤)

(*Institute of Oceanology, Academia Sinica, Qingdao*)

Received June 5, 1986

Abstract

Regarding the current pattern in winter in the near-sea region of Zhejiang, Fujian and Guangdong (including the western and central parts of the Taiwan Strait), oceanographers both at home and abroad had considered unanimously that under the intense influence of the northerly monsoon, the current (not only at the surface but also in the deep and near-bottom layers) flows southwestward with the wind. It was not until the end of the fifties that scientists began to question such a traditional concept.

In this paper, based on the results of more than 20 years' studies on the current patterns of the East China and South China Seas, all kinds of current data available are reanalysed comprehensively. These data include: 1) current measurements at day-night anchored stations, and with mooring buoys, collected mostly from 1959 to 1982 by many Chinese oceanographic and fisheries organizations; 2) current vectors derived from the ship-drift of Japanese naval vessels in the period from 1910 to 1921; and 3) geostrophic current velocities deduced from hydrographic observations in the periods of the CSK and 1975—1976 conducted by the Fisheries Research Station, Hong Kong, and the SOA. A combination of all the evidences revealed in the above data suggests and confirms that, besides the China Coastal Current flowing southwestward at a shallow layer of a zone closely adjacent to the coast, there also exists a northeastward counter-wind current in winter off the southeast coast of China (though its surface current may be weakened or even covered up by the drift current when the northerly monsoon strengthens). Furthermore, the two parts of the winter counter-wind current in the South China Sea and the East China Sea are connected through the Taiwan Strait. This suggestion now has been confirmed by the recent observations in the Taiwan Strait, i.e., 1) with sea-bed drifters released in 1984 (Zhang, 1985) and 2) with current meter moorings deployed in 1983 (Chuang, 1985).

It is suggested that detailed field investigation in winter for filling the gap of observations should be needed to give further confirmation of this important new finding. At the same time, dynamical, numerical and experimental studies should also be carried out for a better understanding of the mechanism of this counter-wind current, and its variations and correlation with the adjacent currents, such as the southward flowing coastal current and the northward flowing Kuroshio Branch.

I. INTRODUCTION

Regarding the current pattern in winter in the offshore region of Zhejiang, Fujian and Guangdong (including the western and central parts of the Taiwan Strait), oceanographers both at home and abroad have considered unanimously that under the intense influence of the northerly monsoon, the current (not only at the surface but also in the deep and near-bottom layers) flows with the wind from northeast to southwest. In addition, the northern part of the current may have originated from the Chinese offshore area of the East China Sea and the Huanghai Sea, and the southern part may extend even

* The paper was presented at the symposium sponsored by the Chinese Society of Oceanology and Limnology in November, 1978, Qingdao. Some recent contents were supplemented before publication. Contribution No. 1364

to the coastal area off the Indo-China Peninsula. The two parts constitute the China Coastal "Cold" Current flowing first from north to south and then from northeast to southwest. To the best of the author's knowledge, no one has ever reported that besides the current flowing with the wind there still exists a current flowing against the wind in this region in winter.

It was not until the end of the fifties that scientists began to question such a traditional concept.

More than 20 years ago, while the Chinese national comprehensive oceanographic survey (1958—1960) was conducted, a more systematic survey was made in the offshore area of the western East China Sea and the northern South China Sea. Besides monthly hydrographic observations at oceanographic stations, day-night current measurements from the surface to the deep and near-bottom layers at many anchored stations were also made. A set of better quality residual current data was thus obtained. Some new and important findings concerning the winter current pattern which had not been discovered in the past foreign investigations in this area were revealed, such as:

1. In the offshore region off eastern Zhejiang, besides the East China Sea Coastal Current flowing with the wind in the area closer to the coast, there existed a current flowing northeastward and against the wind from the near-surface layer (~ 5 m) down to the bottom in the area a little farther away from the coast. This flow has been known as the "Taiwan Warm Current" (Guan and Chen, 1964)

2. In the nearshore region off Shantou (east of 116°E), there also existed a current flowing northeastward and against the wind. Its velocity was so strong that the tidal current there was no longer the predominant component of the overall current (Guan & Chen, 1964).

3. In the coastal area northeast of Hainan Island, the counter-wind current was also observed. At that time, the northeastward flowing currents observed in the nearshore regions off Shantou and northeast of Hainan Island were considered to be connected with each other and were known as the "Nanhai (South China Sea) Warm Current" (Guan & Chen, 1964).

After the completion of the Chinese national comprehensive oceanographic survey, current measurents by the departments concerned (especially those carried out in the northern South China Sea in the early seventies by the South China Sea Division of the State Oceanic Administration (SOA)) provided further evidences for the existence of the Nanhai Warm Current (Guan, 1978 b). Furthermore, through an analytical study of the CSK (Cooperative Study of the Kuroshio and Adjacent Waters) data collected by the R/V Cape St. Mary of the Fisheries Research Station of Hong Kong during the winter of the years 1966—1968, a strong, narrow and band-like northeastward current was discovered on the geostrophic current field south of the Tropic of Cancer, 19—22°N, i.e. in the open sea off Guangdong (Guan, 1978 a). It was considered that this current was the main stream of the Nanhai Warm Current, while that discovered at the end of the fifties was only a weaker left flank of the Nanhai Warm Current in comparison with this (Guan, 1978 a, b).

In the early sixties, based upon the preliminary observation results of the two above mentioned counter-wind currents, i.e. the Taiwan Warm Current and the Nanhai Warm Current, the author considered such problems, as "where is the end of the China Coastal

Current which flows with the wind in winter ?", "is the direction of the deep and near-bottom currents in the Taiwan Strait consistent with that of the surface current?", and so on. At that time, the author conceived that there might also exist in the deep and near-bottom layers of the western part of the Taiwan Strait a northeastward counter-wind current. And it was further considered that should this suggestion be confirmed by the future observations, then off the southeast coast of China, besides the large amounts of cold water flowing southward with the wind in winter there should exist at the same time a part of warm water flowing northward against the wind from the coastal area east of Hainan Island, passing through the near-sea region of eastern Guangdong and the western part of the Taiwan Strait, and reaching the near-sea region of Fujian and Zhejiang, It suggests that , at least a part of the water of the Nanhai Warm Current flowing against the wind in winter might be connected with the northeastward current in the offshore region of eastern Zhejiang through the Taiwan Strait (Guan et al., 1964, MS)*.

Regarding the idea of a counter-wind current in winter off the southeast coast of China suggested about 20 years ago, the author is still imbued with confidence, especially so in view of the new information of the winter current condition collected in the western part of the Taiwan Strait (Chen, 1978; Guan, 1980) and the recent data from the sea-bed drifters released by the Institute of Oceanology, Academia Sinica, Qingdao, in the middle and northern parts of the Taiwan Strait (Zhang, 1985) and from the current meter moorings deployed by Institute of Oceanography, Taiwan University, Taibei, China in the eastern Taiwan Strait(Chuang, 1985).

Based on the results (obtained since the end of the fifties) of investigations on the offshore current patterns of the East and South China Seas, this paper presents a comprehensive reanalysis of the data of the current measurements and seawater mass distribution collected during a period of more than 20 years. Some evidences of the existence of a current flowing against the wind in winter off the southeast coast of China will be suggested and demonstrated in order to confirm preliminarily my idea conceived about 20 years ago of such a current (Guan, 1983, 1984).

II. EVIDENCES FROM THE CURRENT MEASUREMENT DATA

In this aspect, there are current observation data collected by the Chinese organizations concerned since the end of the fifties, and ship-drifts data collected by Japanese naval vessels during the early part of this century.

1. In Fig. 1, the solid vectors show the residual currents at the 10 m depth in winter (Nov., Dec. and Jan.—Mar.) in the offshore area of Guangdong, and off western Taiwan and eastern Zhejiang. Most of these current measurements were taken in the periods of 1959—1960, 1971—1973 and 1977—1978. The largest solid arrow located southeast of Shantou shows the resultant velocity of the current measurements taken at a mooring station in the deep water region($\sim$1000 m) in February, 1982 under very intense north-

* Guan Bingxian, Ding Wenlan and Mao Hanli, 1964. The winter surface current systems of the southern Huanghai Sea and the northern East China Sea and discussions of some related problems (MS, in Chinese).

east winds by the South China Sea Institute of Oceanology, Academia Sinica, Guangzhou (Guo et al., 1985).

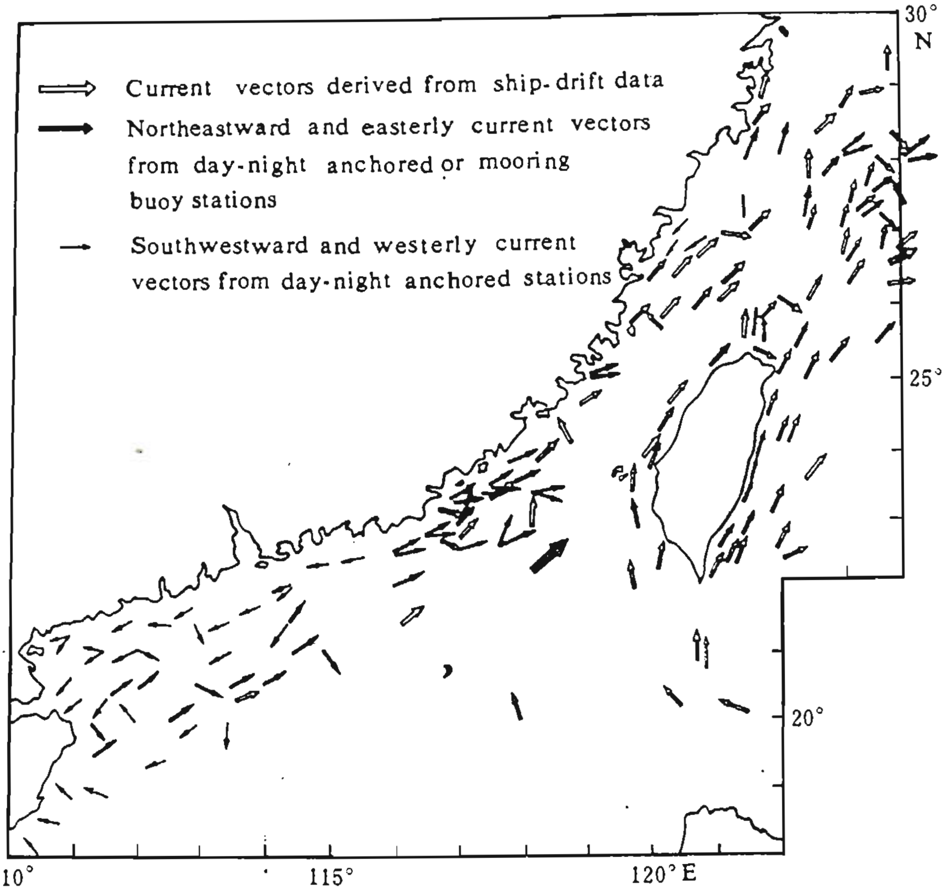

Fig. 1 Observation results of the current in winter off the southeast coast of China.

2. Concerning the winter current regime of the western side of the Taiwan Strait, observations since the late fifties showed that the current did not entirely flow southwestward; the southward East China Sea Coastal Current appeared only at a shallow layer (< 10 m) of a zone closely adjacent to the Zhejiang and Fujian coast (depth < 25 m). Its maximum velocity generally did not exceed 30 cm/s, and only during the strongest northeast wind did it reach to the neighbouring area off Quanzhou and the layer deeper than 10 m. And the current in the offshore region (depth > 25 m) and at a deeper layer (> 10 m) in the western part of the Strait still flowed against the wind, i.e. it flowed northeast ward or northward as in spring and summer (Chen, 1978; Guan, 1980).

3. Figs. 2 a, b were reproduced from the "Meteorological and Ocean Current Charts in the Adjacent Sea of Japan" (Figs. 20 and 23. JHO, 1925). The current vectors on these charts were compiled based on the observation reports of Japanese naval vessels in the period from 1910—1921. The current part consisting of four charts gives the surface

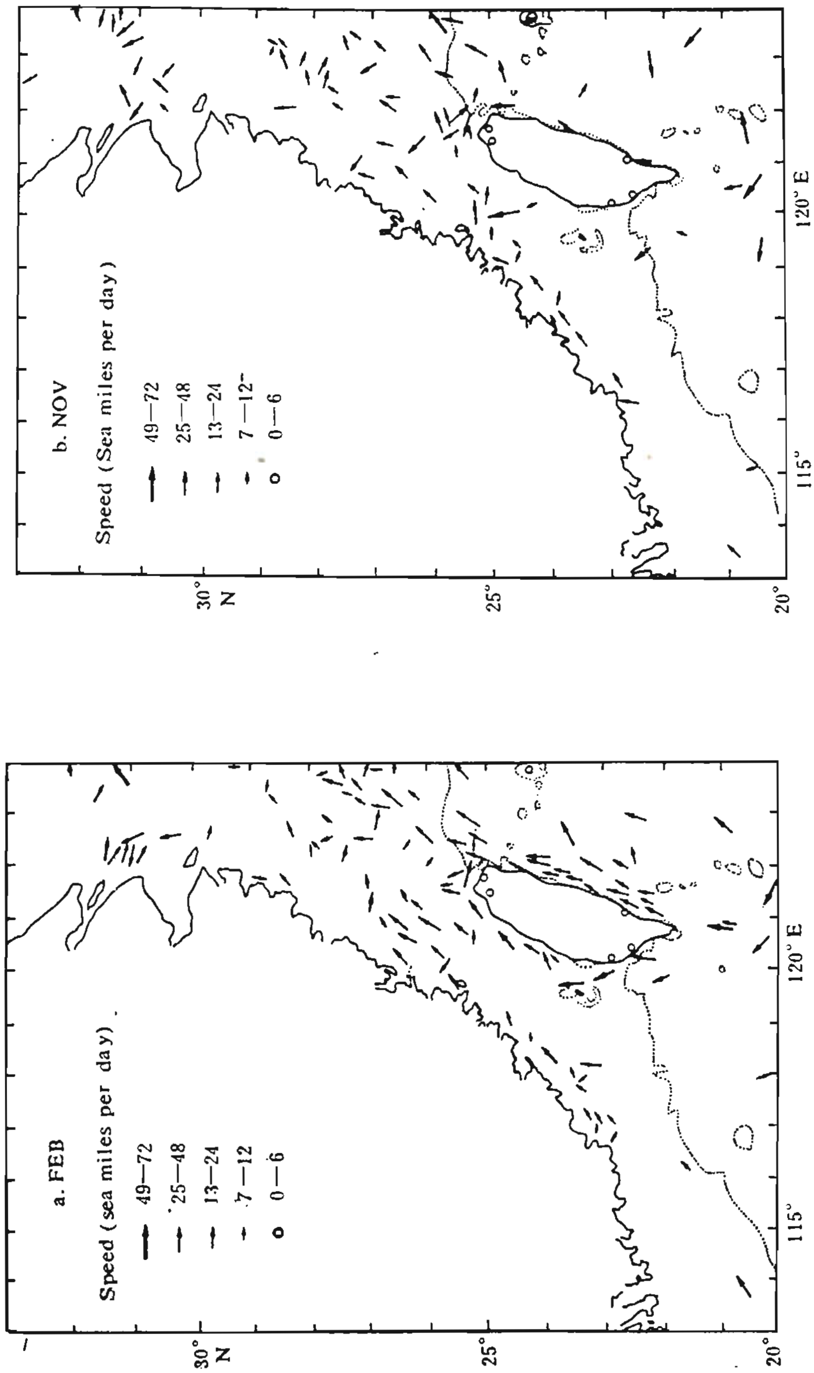

Fig. 2 Current vectors derived from ship-drift data(From JHO. 1925).

currents in winter (February), spring (May), summer (August) and autumn (November), respectively. Each vector on the charts represents one observation. The speed of the current is shown in 5 scales. The superiority of these charts is that they may be considered as original data sets indicating the current conditions that were actually happening then. On the other hand, the other prevalent current charts were compiled through a process of taking scalar or vector averages of vectors of currents observed in a longitude and latitude grid. Therefore, the fewer vectors of non-predominant currents are covered up by the more numerous vectors of predominant currents so that the non-predominant currents are not displayed on the charts. In order to make a special effort to analyse (besides the current flowing southward with the wind) whether or not there exists a counter-wind current in winter off the southeast coast of China, only the current vectors directing northward (along the Guangdong, Fujian, Zhejiang and Taiwan coasts) and eastward are reproduced in the Figs. 2 a, b; while the vectors directing southward along the coasts and westward are not reproduced.

It is evident from a comparison of the above mentioned figure that the information of the winter current conditions off Guangdong, Fujian and Zhejiang provided by these two sets of data collected more than half a century apart is quite similar. The current vectors derived from shipdrift (observed in 1910—1921) and those from current measurements at day-night anchored stations (observed in 1959—1982) all indicate that, off the eastern part of Hainan Island and Guangzhou, along the eastern Guangdong coast and the western coast of Taiwan, and off eastern Zhejiang, there really exists a counter-wind current flowing from southwest to northeast. It is in obvious contrast to the traditional concept that the current there totally flows from northeast to southwest. Judging from the density (dense or scarce) of the distribution of current vectors, these two sets of data supplemented each other. For example, the northeastward vectors derived from ship-drift are scarce in the area off Guangdong, but those from current measurement are relatively numerous. The current measurement data in the coastal area from Xiamen to Wenzhou are scarce, while the northeastward vectors derived from ship-drift are comparatively numerous there. In the coastal zone of eastern Guangdong and southern Fujian, both these kinds of data are sufficient. Because the ship-drift data from Japanese Current Charts are limited to the area north of 20°N, the current regime in the area east of Hainan Island can only be explored from the data of current measurements and geostrophic current deduced from the water mass distribution.

The autumn-winter current regime in the area off central Fujian shown by Chen (1978) also agrees with that deduced from the ship-drift data.

Therefore, the counter-wind current flowing northward in winter which has been observed for more than 20 years (since the late fifties) is not an accidental phenomenon as it was also observed about half a century ago. However, it was covered up by the majority of observation results of the predominant southward drift current and had not attracted people's attention.

In order to get a more eye-catching and continuous impression, the vectors derived from the ship-drift in Fig. 2 a (February) are overlapped in Fig. 1. In this figure, the northeastward vectors derived from day-night observations at anchored stations accounted for more than 36 in the period from November to March, and those derived from the ship-drift accounted for 31 in February. Hence, the northeastward currents were observed nearly 70 times in winter altogether. Therefore, the trend of counter-wind current originating from the area east of Hainan Island and flowing northeastward seems more apparent. At the same time, it is also shown that the Kuroshio branch entering the South China Sea through the Bashi Channel in winter flows northward mainly along the west coast of Taiwan, moving side by side with the above mentioned counter-wind current flowing northward along the coast of Guangdong, Fujian and Zhejiang.

It may be been from the current measurement data in Fig. 1 that the velocity of the counter-wind current was around 50 cm/s (~1 knot ——the strongest) off the eastern Guangdong coast, around 20 cm/s (~0.4 knot) immediately northeast of Hainan Island, around 15 cm/s (~0.3 knot ——the weakest) off eastern Zhejiang. The current velocity in Fig. 2 was deduced from ship-drift data. Though its accuracy is less than that of direct current measurement, the figure shows that the northward speed off eastern Guangdong

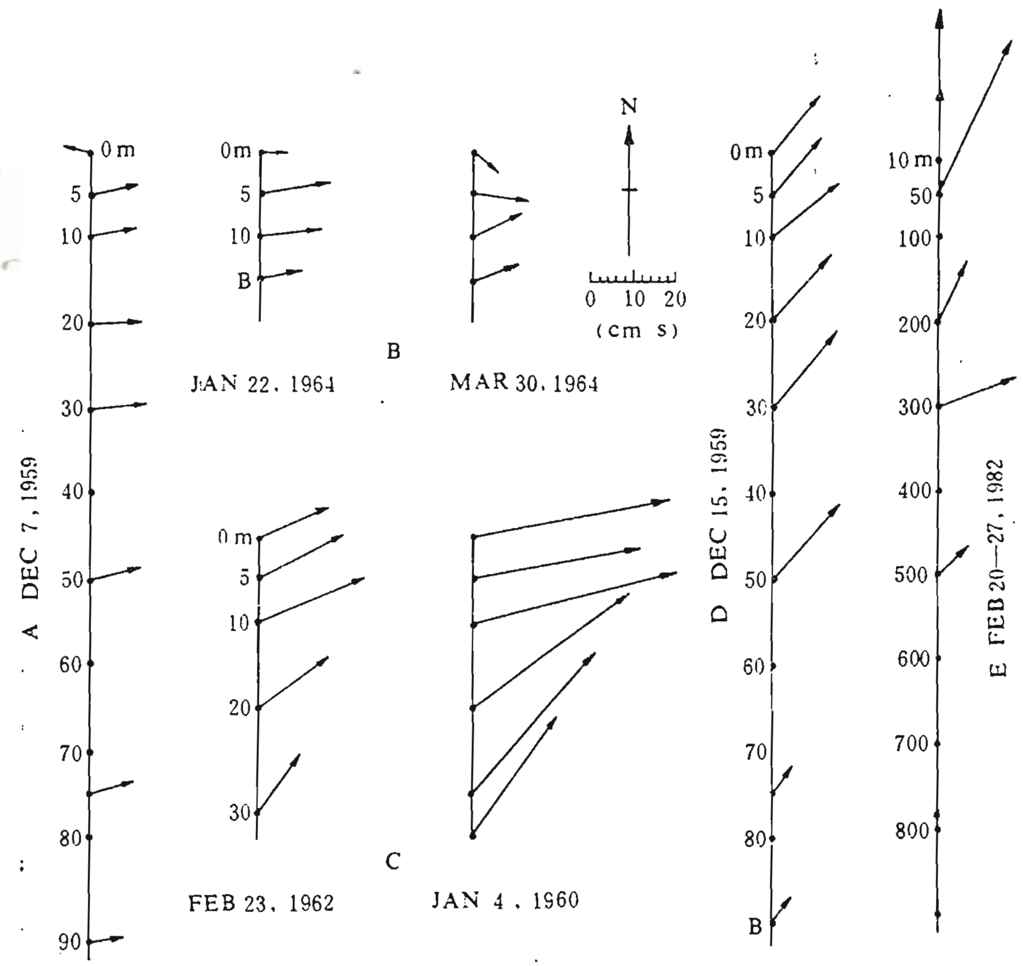

Fig. 3 Vertical structures of the residual current at some day-night anchored and mooring buoy stations in winter off the southeast coast of China.

and southern Fujian is still rather strong.

The author believes that the main stream of the Nanhai Warm Current may meet its left flank off eastern Guangdong, thereby strengthening the northeastward velocity of the current there and forcing a part of the Nanhai Warm Current to flow through the western side of the Taiwan Strait. And this part of water may extend farther to become the northeastward current off eastern Zhejiang. The author would like to point out that in the open sea off eastern Zhejiang in winter, the possibility of the existence of a Kuroshio branch (separated from the Kuroshio main stream northeast of Taiwan) at the subsurface layer is not excluded. But the northeastward current in the near-shore region of eastern Zhejiang should have originated mainly from the western side of the Strait.

Fig. 3 shows the vertical structures of the velocity at some day-night anchored and mooring buoy stations over which this counter-wind current flowed. Stations A,B,C,D and E are located in the offshore regions of eastern Zhejiang, Quanzhou, Shantou, east of Hainan Island and in the deep-water area southeast of Shantou, respectively.

Some characteristics may be seen from the vertial profiles of the current vectors at different levels in Fig.3.

1. Except for the surface layer of individual stations, current directions of the upper and lower layers are basically the same and the variation of the speeds is also not large. This suggests that except for the surface layer, this current is rather homogeneous vertically, or its barotropic nature (or barotropy) is relatively evident.

2. The maximum velocity appears at the 5—30 m layer in the offshore region of Quanzhou and Shantou where the water is shallow, and at the 30—50 m layer in the offshore or open sea region of eastern Zhejiang, Guangdong and east of Hainan Island where the water is deep.

3. The velocity of the near-bottom current is relatively small, and the nearer to the bottom, the closer the current direction approaches NNE or NE.

4. At some stations, the direction of the surface current is different from that of the current below, and the velocity is also smaller because of the counter-wind movement of this current. Therefore, when the northeast wind strengthens this current will very likely be covered up by the drift current and will disappear at the surface layer. However, the depth of the wind effect is not large.

It may be seen from the above-stated characteristics that the distribution of the residual currents at the 10 m depth in Fig. 1 is more representative of the current condition there.

III. EVIDENCES FROM THE WATER MASS FIELD DATA

To make up for the fewer current measurements and lack of ship-drift data in the offshore region east of Hainan Island, the water mass field, that is the geostrophic current data of two sections southeast of Hainan Island, was used to demonstrate the existence there of a northeastward current almost all the year round.

In the period of 1975—1976, systematic hydrographic observations on two parallelly spaced sections between Hainan Island and the Xisha and Zhongsha Islands were conducted by the South China Sea Division of the SOA and time series data covering 20 months were obtained. The respective month by month fluctuations of the maximum surface velocity of the northeastward component of the geostrophic current at the two sections are shown in Figs. 4 a, b. The maximum differences of the dynamic height (ΔD, 0/500 db, dyn. m.) between two adjacent stations of the section are used as the index of the current velocity. The differences were calculated from the dynamic height of the right station Dr (in the down-stream direction) minus that of the left one De, with the positive values indicating northeastward current (Guan, 1981).

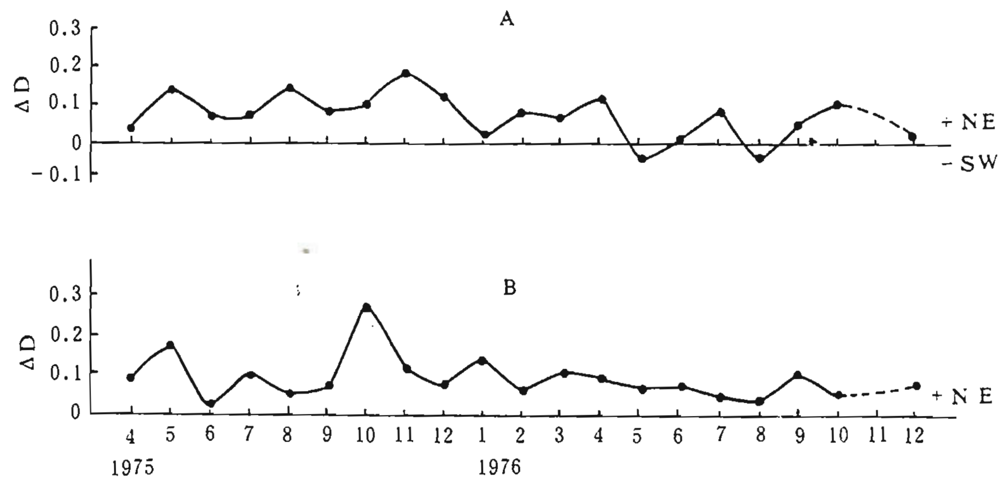

Fig. 4. Maximum surface velocity of the northeastward component of the geostrophic current (ΔD, dyn. m., 0/500 db) at two sections southeast of Hainan Island (Guan, 1981).

It is evident from Fig. 4 that except for the cases in May and August, 1976, the northeastward current appeared at these two sections all the year round. In addition, the velocity in the winter half of the year (October—March) was generally higher than that in the summer half of the year (April—September). For example, the maximum of the northeastward current at two sections appeared in October and November, respectively. The respective ΔD of two stations 42 nautical miles apart reached 0.28 and 0.18 dyn.m, (equivalent to velocities of 84 and 55 cm/s around 15°—18°N). Therefore, the northeastward counter-wind current is rather strong. The location of the maximum velocity is also relatively stable. It generally appears around the central part of the sections.

Therefore, there is no doubt that in the area between Hainan Island and the Xisha and Zhongsha Islands there exists a northeastward counter-wind current in the winter half of the year on the geostrophic current field. Of course, on both sides of the northeastward current there also exist the southwestward currents flowing with the wind.

The hydrographic data obtained during the CSK (No. 72) by the R/V Cape St. Mary of the Fisheries Research Station of Hong Kong in the south part of the Taiwan Strait from January 9—10, 1966, also provided evidences of the existence of a northward current in the western part of the Taiwan Strait. From the density (σ_t) and geostrophic current distributions of the W-E section Hong Kong—Heng Chun, as shown in Fig. 5 a, b, it is evident that the northward current on the left side of the section (between St. 2—3) corresponds to the northeastward current observed in the open sea south east of Shantou, while the northward current on the right side (between St. 4—5) may be the Kuroshio branch entering the South China Sea flowing northward along the west coast of Taiwan; or it may be the same as that between St. 2—3, this needs to be further identified. The geostrophic current velocity in Fig. 5 b is calculated with reference to a level which is the maximum observation depth common to the neighbouring station pair.

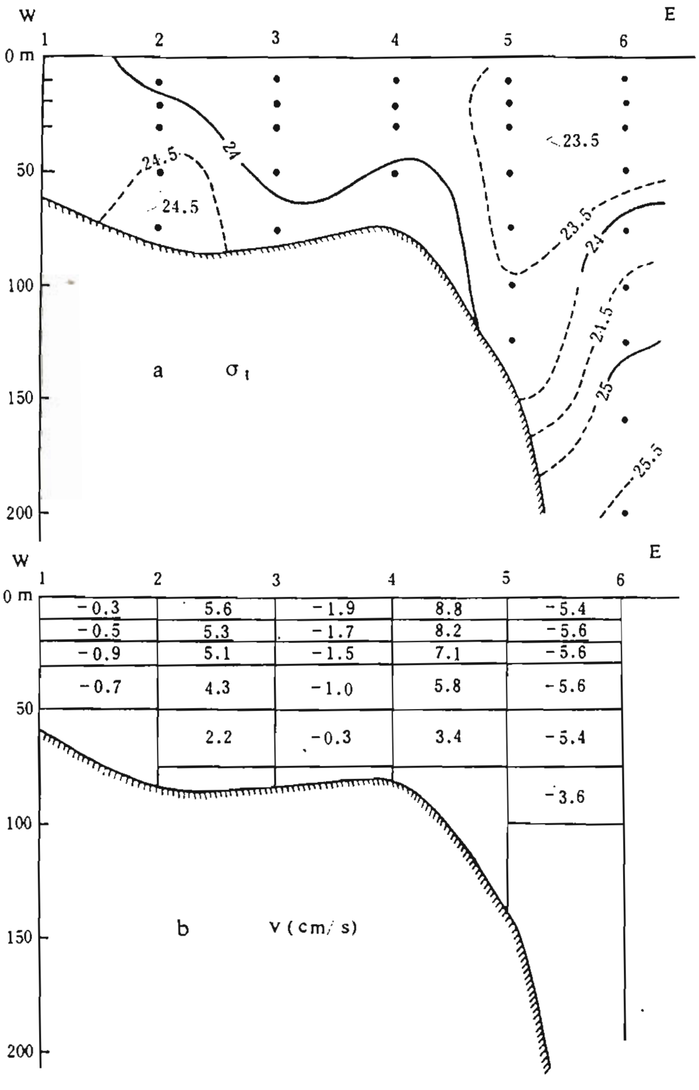

Fig. 5 Density (a, σ_t) and geostrophic current velocity (b, cm/s, positive northward) of the W–E section Hong Kong—Heng Chun, in Jan., 1966.

IV. EVIDENCES FROM THE RECENT INFORMATION

The above two northward currents revealed in the geostrophic current section on both sides of the Taiwan Strait agree with the recent information obtained from the data of sea-bed drifters and current meter moorings in the Strait during the northerly wind period.

1. Results from sea-bed drifters.

In the period of February—August, 1984, 3,050 sea-bed drifters were released in the area of the Taiwan Strait and north of Taiwan Province by the Institute of Oceanology, Academia Sinica in cooperation with the Fujian Fisheries Research and Fujian Oceanography Institutes. The recovery percentage of the sea-bed drifters attained 4%. Most of the drifters were recovered after 30 days of drifting in the sea, so their representation of the current condition may be considered acceptable. Preliminary analysis of the data of sea-bed drifters indicates that the drifters released in winter (February—March) all moved northward; especially those released in the northern Strait, the drifting direction was even more consistently northeastward, their drifting speed was around 1—4 nautical miles per day. The velocity of the drifters released in March was evidently higher than that in February. The drifters released in spring (April—June) also moved in a northerly direction.

The above-mentioned drifting direction of sea-bed drifters suggests that, in winter and spring (February—June), the deep and near-bottom water in the Taiwan Strait moves northward, that is to say, there exists a northeastward current flowing from southwest to northeast along the direction of the Strait. The northernmost part of this current may reach the area near the estuary of the Oujiang River. In the deep and near-bottom layer of the sea area north of Taiwan there also exists a northwestward current which may reach the area near Zhoushan Islands (Zhang Yiken, 1985).

2. Results of the current meter mooring observations.

Two current meter moorings were deployed in the Taiwan Strait from April 3 to May 5, 1983, by the Institute of Oceanography, Taiwan University, Taibei, China. One (St. B) was located in the northern part of the Strait and the other (St. C) at the head of the trough between Taiwan and Penghu Island. Their respective depths were about 55 m and 100 m. A current meter (Aanderaa RCM-4) was attached to each mooring at 14 m and 20 m above bottom at these stations. The average wind stress (0.07 dy/cm], corresponding to a wind speed of only about 4 knots) during the study period was toward the southwest, though it was in the transition period from NE to SW monsoon wind.

Analysis shows that the mean currents at St. B and C are strongly affected by local geographic conditions. The mean current flows northward at St. C (2°, 24, 2 cm/s) and northeastuard at St. B(51°, 28.6 cm/s). The magnitude of the speed is about 20% greater at St. B where the water is shallower. As the wind and the mean along-strait current are in opposite directions, they do not appear to be directly related. The observed persistent, up-Strait drift (at 25 cm/s, and the accompan-ying large volume transport to the East China Sea) must be induced by some forcing mechanism other than the wind (Chuang WenSi, 1985). The observation results confirm that there also exists a significant counter—

wind current in the deep and near-bottom layers of the eastern part of the Taiwan Strait under the northeast wind in spring.

V. DISCUSSION AND REMARKS

In conclusion, two problems will be discussed briefly in the following paragraphs.

1. Why has this northeastward cunter-wind current in winter been overlooked for such a long time in the past?

In the sea area studied in the paper, especially for the surface layer, southwestward currents were observed to flow with the prevailing wind in winter. The northeastward current flowing against the wind is relatively strong in some local regions but rather narrow in width and flanked by southwestward currents on either side just as mentioned in the paper entitled "The Warm Current in the South China Sea" (Guan, 1978 a, b). Therefore, under the action of the intense northeast wind, this counter-wind current is likely covered up by the surface drift current, and can not appear in the near-surface layer temporarily.

The knowledge of the current system is derived mostly from the data of ship-drift and current bottle-drift to this day, As mentioned above, through a process of taking scalar and vector averages of current vectors observed in a grid region, the predominant current sticks out while the non-predominant current is covered up. The data of current bottle-drift mainly reflect the direction of the predominant drift current at the surface layer, and could hardly reflect the narrow counter-wind current which sometimes may be covered up. In addition, the drifting path of the current bottles is still unavoidablely influenced more or less by the wind effect. Therefore, this counter-wind current in winter has not been reflected in these two kinds of data for a long time. But, as a matter of fact, indications of this non-predominant and counter-wind current can be seen, though indistinctly, on the current charts attached with current scale and stability(vector resultant velocity/scalar resultant velocity) or current roses. For example, on the chart of "Oceanographic and Meteorological Observations in the China Seas and in the Western Part of the North Pacific Ocean" (Royal Netherlands Meteorological Institute, 1935), the stability of resultant velocity in grids of the above-stated sea area in winter is relatively small. At the same time, its current roses also consist of northward or northeastward components.

2. How should we assess the quality of the current data derived from ship-drifts?

There is no doubt that the current data derived from ship-drifts are less accurate than that of current measurements. Hence, data sets of northeastward vectors in Fig. 2 a,b might be suspected to be random phenomena that do not reflect real conditions. A rough statistical analysis of the current data in autumn and winter in the above Japanese current charts has been made in order to check their quality. In the near-sea area along the Guangdong coast west of 116°E, (except for the left flank of the counter-wind Nanhai Warm Current appearing farther away from the coast) the currents obsorved with current meters since the end of the fifties almost all flowed southwestward with the wind. In addition, on the Japanese current charts, in the corresponding area west of 116°E, about

40 current vectors derived from ship-drift data in February and November (except for one to two vectors directing northeastward) are almost all directed southwestward, too (JHO, 1925). Furthermore, on either side of Taiwan, current data derived from ship-drift depict nearly without exception the patterns of the intense Kuroshio flowing northward along the coasts of Taiwan. Therefore, in this area the current conditions depicted by the ship-drift data agree with what were actually happening.

Let us consider the current situation in the sea area east of 116°E and northward along the coast of Guangdong, Fujian and Zhejiang. There are nearly 90 current vectors derived from ship-drift data in February and November, respectively. Among these, there are about 30 current vectors (ca. one third) directed northeastward, depicting the counter-wind current. The other vectors depict southwest current flowing with the wind. At the same time, it may be seen from Figs. 2 a, b that in general, the geographic distribution of such counter-wind current vectors is apparently continuous and not isolated. Therefore, regarding again the situation in the sea area west of 116°E and on both sides of Taiwan, in spite of the less accurate quality of the current vectors derived from ship-drift data, the reality of current characteristics depicted by the vectors in the area east of 116°E and northward along the coast of Guangdong, Fujian and Zhejiang is also beyond doubt; to say nothing of the fact that the current conditions depicted by these vectors agree too with the observed in the neighbouring area.

Current measurement results reveal that in the above-described area, when the northeast wind becomes stronger and stronger, the surface current flows southwestward with the wind, but the sub-surface current below the 5 m depth still flows northeastward. During the period of weak northeast winds, this counter-wind current even appears on the surface layer. It is speculated that the northeastward current vectors in Figs. 2 a, b were likely for the most part observed under conditions of weak northerly winds. These northeastward current vectors provided valuable information for our research on the existence of this counter-wind current which was not noticed for more than half a century.

On the basis of a combination of all the data mentioned above, it may be confirmed that there exists a northeastward and northward counter-wind current in winter in the offshore region of the South and East China Seas. Furthermore, the two parts of the winter counter-wind current in the South China Sea and the East China Sea are connected together through the Taiwan Strait. This hypothesis has been affirmed by the results of current meter mooring observations in the Taiwan Strait entitled "EXIST" (Experiment in the Strait of Taiwan) conducted recently by the Institute of Oceanography Taiwan University, Taibei, China (Wang, D.P. 1985, Personal communication).

Notwithstanding the facts stated above, the data collected in this paper are still not very sufficient and comprehensive: especially as current measurement data are still lacking for some local regions.

It is suggested that further field investigations in winter with CTD, with current meters and/or mooring buoys are needed for filling the gaps of observation in order to further confirm this important and new finding. Besides these, dynamical, numerical and experimental studies should also be carried out for a better understanding of the mechanism of this counter-wind current and its variations and correlations with the other currents in the surrounding area, such as the southward flowing coastal current and the northward flowing Kuroshio Branch.

It is considered that the finding and the confirmation of the existence of this counter-wind current would, in a greater dagree change the traditional concept of the current system, especially the coastal current system of the China Seas. A joint study (i. e. field work plus dynamic investigation) of the mechanism of this current would help much in raising our country's research level in shallow water oceanography.

References

[1] Chen Jiliang, 1978. Some viewpoints concerning the method and accuracy of the observations of temperature and salinity of sea water. *Oceanic Instrumentation* 1:59—61 (in Chinese).

[2] Chuang Wensi, 1985. Dynamics of subtidal flow in the Taiwan Strait. *J. Oceangr. Soc. Japan* 41:65—72.

[3] Guan Bingxian, 1978a. The Warm Current in the South China Sea——a current flowing against the wind in winter in the open sea off Guangdong Province. *Oceanologia et Limnologia Sinica* 9:117—127 (in Chinese with English abstract).

[4] Guan Bingxian, 1978b. New evidences for the South China Sea Warm Current. *Marine Sciences* (Supplement): 100—103 (In Chinese).

[5] Guan Bingxian, 1980. Current pattern in the southwestern part of the Taiwan Strait. *In*: Reports on the Fishery Resources of the Fishing Ground Southern Fujian-Taiwan Shallows". 1: 118—122 (in Chinese).

[6] Guan Bingxian, 1981. An important feature of the winter vertical thermal structure in the northern South China Sea. *Oceanologia et Limnologia Sinica* 12:311—320 (in Chinese with English abstract).

[7] Guan Bingxian, 1983. A sketch of the current structures and eddy characteristics in the East China Sea. *In*: "Proceedings of International Symposium on Sedimentation on the Continental Shelf, with Special References to the East China Sea" (April, 1983, Hangzhou). China Ocean Press. 1: 52—73.

[8] Guan Bingxian, 1984. Major features of the shallow water hydrography in the East China Sea and Huanghai Sea. *In:*"Ocean Hydrodynamics of the Japan and East China Seas" (Edited by T. Ichiye). Elsevier Oceanography Series, 39. Amsterdan. pp. 1—13.

[9] Guan Bingxian and Chen Shangji, 1964, The current systems in the near-sea area of China Seas. 1—85 pp. (in Chinese).

[10] Guo Zhongxin, Yang Tianhong and Qiu Dezhong, 1985. The South China Sea Warm Current and the southwestward current on its right side in winter. *Tropic Oceanology* 4: 1—9(in Chinese with English abstract).

[11] JHO (The Hydrographic Office of Japan), 1925. The Current and Meteorological Charts of the Sea near Japan (No. 6042). *Charts* 20—23 (in Japanese).

[12] Royal Netherlands Meteorological Institute, 1935. Oceanographic and Meteorological Observations in the China Seas and in the Western Part of the North Pacific Ocean (No. 115). *Charts*, 1—36, Government Printing Office, The Hague.

[13] Zhang Yiken, 1985. Bottom current measurements with releasing sea bed drifters in the Taiwan Warm Current region. *Marine Sciences* 9(2): 64 (in Chinese).

PRELIMINARY STUDY OF RELATION BETWEEN THE KUROSHIO MEANDER AND THE EL NINO EVENT

LIU JUPING (刘举平) AND GUAN BINGXIAN (管秉贤)

(Institute of Oceanology, Academia Sinica, Qingdao)

ABSTRACT

On the basis of the data of the trade wind field in the Pacific Ocean (1950–1972) it is shown that the Kuroshio meander and the El Nino event are not separate phenomena but related with the same air-sea system. It is found from analysis of the data that the cyclonic curl of the tropical wind stress is highly correlated with the anticyclonic curl of the subtropical wind stress. When the intertropical convergence zone (ITCZ) migrates towards the equator from its mean location and reaches its climax, both the cyclonic and anticyclonic curls of trade wind stress reach their maximums while the El Nino is prevailing. When the ITCZ runs rapidly northward against the equator or reaches an extreme point, both the cyclonic and anticyclonic curls of trade wind stress decrease sharply and then the Kuroshio meander occurs.

INTRODUCTION

The El Nino west of Peru and the Kuroshio meander south of Japan are two remarkable oceanic phenomena in the Pacific Ocean. Anomalous warm water in a large area of the coastal region of Peru induced by the El Nino and anomalous cold water along the coast of Honshu of Japan induced by the Kuroshio meander have caused the reduction of rice and the decline of fishery. At present it is generally accepted that the El Nino is not an event in local region but a phenomenon all over the tropical Pacific Ocean.

There are many papers describing the El Nino and the Kuroshio meander respectively. Attention of the present article is concentrated to the relation of the two phenomena.

The maps of the bimonthly trade wind stress vector compiled by Wyrtki and Meyers[1] are very helpful for this study. They cover ca 5 million wind observations from the merchant ships, which were averaged over the grids of 2° latitude and 10° longitude and last about one fourth of a century (1950–1972). The results of the article are based on this data with a calculation of the wind stress field.

For the cause of the El Nino events and the Kuroshio meander, it s generally accepted that the former is correlated with the collapse of strong southeast trade wind[2] while the latter is a consequence of the variation of the subtropical wind stress curl[3]. The problem

Received March 11, 1985. Accepted December 25, 1985.

about the mechanism of both phenomena, however, is still open. The relation between them will be explored in the following sections through an analysis of the relation between tropical and subtropical wind stress curls and, of course, this is merely one of elements that affects the mechanism of the El Nino events and the Kuroshio meander.

I. THE KUROSHIO MEANDER

Among the studies of causes of the Kuroshio meander, one is on the influence of the variation in the subtropical wind stress curl, as suggested by Guan Bingxian. He holds that, when the sea surface wind stress curl over the region of 22°–28°N and 175°E–165°W is continuously increased for several years or sharply increased to a peak, the volume transport of the Kuroshio in the East China Sea would likewise reach a peak before long; meanwhile, the Kuroshio menader would occur to the south of Japan[3].

The results of calculation of the trade wind stress curl all over the northern Pacific Ocean help us find out that the variation of the Kuroshio is governed, in fact, by the wind stress curl over the whole subtropical ocean. The region discussed by Guan Bingxian is merely a central area. When enlarged by 1.5 times towards the east and the west, the larger region (22°–28°N, 160°E–150°W) covers an area greater than one third of the latitudinal belt of 22°–28°N (Fig. 1). Curve(a) in Fig. 2 shows the annual mean wind stress curl over the large region, whose fluctuation is in agreement with that over the smaller region calculated by Guan Bingxian. By contrasting the Kuroshio meander period (thick, black line with M in Fig. 2) with curve (a), we can also see that the Kuroshio meander occurs soon after the wind stress curls have increased continuously or increase sharply to a peak value.

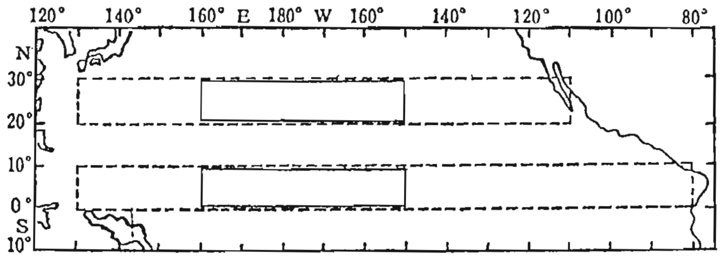

Fig. 1. The regions for calculating mean wind stress curls.

There are two main systems of mean wind stress curl over the northern Pacific Ocean from the equator to 30°N. One is the cyclonic wind stress curl from the equator to 10°N (hereinafter called "tropical cyclonic curl" for short), and the other is the anticyclonic from 15°N to 30°N (hereinafter called "subtropical anticyclonic curl" for short). Curve (b) in Fig. 2 is the counterpart of curve (a) in the corresponding tropical region (2°–10°N, 160°E–150°W, see Fig. 1). It is found from Fig. 2 that the variation of tropical cyclonic curl, curve (b), is correlated with that of subtropical anticyclonic curl, curve (a), and the correlation coefficient 0.57 is remarkable on the level 0.01.

For further examination, the 6-bimonthly running mean values of wind stress curl are calculated over the belt of 2°–10°N and of 22°–28°N, respectively (Fig. 3). The running mean values represent the interannual fluctuations of the wind stress curl. It is shown from Figs. 3 and 2 that (i) the pattern of the variation of the mean wind stress curl over the whole latitudinal belt is similar to that over the larger region of the belt; (ii) like both the larger regions in the tropics and subtropics, the 6–bimonthly running mean values of cyclonic wind stress curl over the whole 2°–10°N belt are positively related to those of anticyclonic wind stress curl over the whole 22°–28°N belt. The tropical cyclonic curl, (b), leads to the subtropical anticyclonic curl, (a) in Fig. 3. The maximum coefficient remarkable on the 0.01 level has a phase lag of less than 2 months.

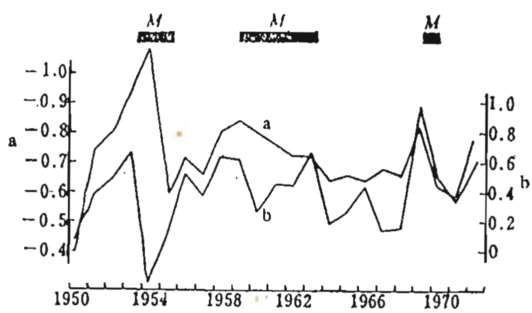

Fig. 2. Annual mean wind stress curl (10^{-8} dyn/cm^3).
a. the region of 22°–28°N, 160°E–150°W,
b. the region of 2°–10°N, 160°E–150°W.

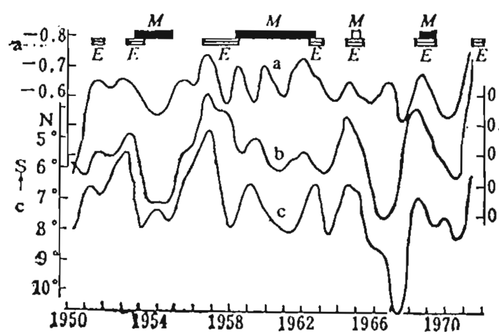

Fig. 3. a. Running mean wind stress curl over 22°–28°N belt (10^{-8} dyn/cm^3);
b. Running mean wind stress curl over 2°–10°N belt (10^{-8} dyn/cm^3);
c. Position of the ITCZ;
M. The period of the Kuroshio meander; *E*. The period of the El Nino.

The curves (a) and (b) in Fig. 3 show that the wind stress curl in tropical region is coherent with that in subtropical region. As the tropical cyclonic curl increases, the increase of the subtropical anticyclonic curl follows, and *vice versa*.

According to the previous description, it might well be said that the tropical cyclonic curl in the northern Pacific Ocean would strongly increase while the subtropical anticyclonic curl is also strongly increasing; shortly after both wind stress curls reach their maximums, the Kuroshio meander is likely to occur.

II. THE EL NINO EVENT

There are also many descriptions about the El Nino events. Wyrtki[4] has developed a well-known mechanism of the El Nino event in the point of view of air-sea interaction. The mechanism as given by him is, in brief, that the occurrence of the El Nino is a consequence of the collapse of the strong Walker circulation. During such a strong circulation, a large gradient between the subtropical high pressure centered at Easter Island and the Indonesia low pressure (*i.e.* the strong southern oscillation) makes the equatorial easterlies strong, inducing the divergence of the equator warm water and the upwelling of the cold water.

Warm water accumulates in the western part of the west Pacific Ocean. Meanwhile, the weakness of air ascent results in a weak Hadley circulation[5], inducing the weaker equatorial convergence of atmosphere. During this period, it is cold and dry in the tropics, especially in the eastern part of the dateline. Once the Walker circulation collapses the equatorial easterlies get weaker, the equatorial warm water converges, and the accumulated warm water in the western Pacific Ocean flows to the west of Peru mounding. Intense air ascent in the equatorial region results in a strong Hadley circulation, strengthening the equatorial convergence of atmosphere. During this period it is hot and wet and thus the El Nino occurs.

Both the tropical cyclonic curl and the position of the ITCZ calculated from the trade wind field can be made use of in monitoring the occurrence of the El Nino events. The two elements, as will be seen later, are helpful for explaining the Wyrtki's mechanism.

There is an obvious narrow belt at about 7°N in the vector maps of interannual mean wind stress over the northern Pacific Ocean. Along the belt the meridional components of wind stress are zero. This belt is the so-called intertropical convergence zone[6]. The curve (c) in Fig. 3 shows the 6-bimonthly running mean position of the ITCZ. Comparing curve (c) with curve (b), we can find out that the fluctuation of the tropical cyclonic curl is intimately linked to the north-south migration of ITCZ. As the ITCZ migrates southward the tropical cyclonic curl strengthens, and *vice versa.* We can see from Fig. 3 that the seven El Nino periods from 1950 to 1972 totally correspond to the maximum of the tropical cyclonic curl and the peaks of the southern position of ITCZ; in other words, all the peaks of the southern position of ITCZ and the maximums of the tropical cyclonic curl, except the case of 1959, correspond to the periods of the El Nino. It is concluded, therefore, that the maximum of the tropical cyclonic curl and the maximum of the southern position of the ITCZ are good indexes of occurrence of the El Nino.

The ITCZ migration towards the south, which surely increases the equatorial atmosphere convergence, is the symbol of strengthening of the Hadley circulation. The idea that the maximum of the southern position of ITCZ serves as an index of occurrence of the El Nino is, therefore, in agreement with Wyrtki's mechanism.

The fact that the maximum of the tropical cyclonic curl corresponds to the period of the El Nino can be regarded as the effect of the extra equatorial warm water. Reiter (1978) showed that the increase of the cyclonic wind stress curl in tropical region is a way to transport extra equatorial warm water towards the subtropical region[7].

The 23-year sequence of mean sea surface temperature in the region sensitive to the El Nino (5°S–5°N, 175°–165°W) and that of mean wind stress curl in the tropical region (1°–9°N, 175°–125°W) are given in Fig. 4. The contribution of annual variation of the mean values is filtered. Shown in Fig. 5 is the correlation coefficients, with which the sea surface temperature leads to the wind stress curl. The maximum of the coefficients remarkable over the 0.01 level corresponds to 2–3 months of the phase difference. Figures 4 and 5 show that increasing of the sea surface temperature in tropical area east of the dateline can induce the strengthening of wind stress curl over the region, and *vice versa*.

With the tropical cyclonic curl and the position of ITCZ as indexes, the Wyrtki's mechanism can be modified as follows: as the Walker circulation collapses, the equatorial easterlies become weak and ITCZ moves quickly towards the equator so that the warm water converges in the central and eastern part of the equatorial region. Following the warm-water convergence, the tropical cyclonic curl strengthens to make the warm water diverge. When the convergence overwhelms the divergence, the El Nino occurs.

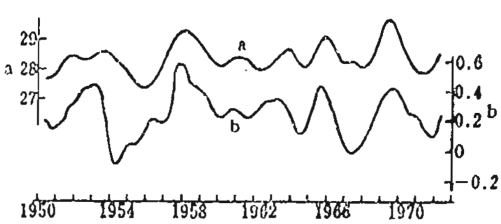

Fig. 4. a. Mean sea surface temperature in tropical region 5°S–5°N, 175°–165°W(°C); b. Sea surface wind stress curl in tropical region 1°–9°N, 175°–125°W (10^{-8}dyn/cm^3).

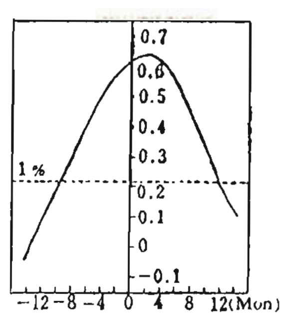

Fig. 5. Correlation coefficients with which the sea surface temperature leads to wind stress curl.

III. RELATION BETWEEN THE KUROSHIO MEANDER AND THE EL NINO

The tropical cyclonic curl and the subtropical anticyclonic curl, as well as ITCZ, belong to one system—the trade wind field in the northern Pacific Ocean. We can see from Fig. 3 that the variations of the three elements are almost synchronous. The occurrence of the El Nino and the Kuroshio meander, on the other hand, is coherent to the three elements. It is reasonable, therefore, that both the El Nino event and the Kuroshio meander are dominated by the same large-scale air-sea system in the northern Pacific Ocean.

In the respect of occurrence time, the Kuroshio meander always follows the El Nino; on the other hand, there is no El Nino occurring in the duration of the Kuroshio meander. Seven times of the El Nino corresponded to the southern maximum position of the ITCZ, but the two times of the Kuroshio meanders (1953, 1959) and a quasi-meander (1969) and a short-time meander (1965) appeared in the traveling way of the ITCZ rapidly running northward from its southern maximum position.

In the respect of mechanism, the relation between the El Nino and the Kuroshio meander can be described as follows: during the strong Walker circulation, equatorial easterlies are strong; tropical cyclonic curl and subtropical anticyclonic curl are moderate; warm water is mounded in the west Pacific Ocean; and colder water occupies in the central and eastern equatorial region. At the same time, the El Nino does not occur, nor does the Kuroshio meander. Once the strong Walker circulation collapses, the equatorial easterlies weaken; ITCZ moves towards the equator; and warm water converges in the central and eastern parts of the equatorial region, then the El Nino occurs. The tropical cyclonic curl and subtropical anticyclonic curl, meanwhile, rapidly increase and reach their maximum. Then, if tropical cyclonic and subtropical anticyclonic curl sharply decrease with ITCZ moving northward by a big margin, the Kuroshio meander is likely to occur.

A descriptive model is suggested, consisting of the three elements –the tropical cyclonic curl, the subtropical anticyclonic curl and the southern position of the ITCZ, *i.e.*, their maximum corresponds to the period of the El Nino; the sharp decrease from the maximum corresponds to the period of the Kuroshio meander.

According to the statistical relation mentioned in the last section, the decrease of both tropical cyclonic curl and subtropical anticyclonic curl seems to be dependent on the equatorial extra warm water. After the extra warm water is transported towards the subtropical region, the tropical cyclonic curl also rapidly decreases itself. The transport of the equatorial extra warm water off the equator, which implies the weakening of the El Nino, induces the decrease of the tropical cyclonic and subtropical anticyclonic curl and, furthermore, induces the Kuroshio meander. So, a conclusion can be derived that the Kuroshio meander may be due to the weakening of the El Nino.

IV. DISCUSSION

Generally speaking, the wind stress field in the northern Pacific Ocean should be affected by many other natural elements. The three elements of the wind stress field are not exactly synchronous because of various disturbances. The relation between each of the three elements and the Kuroshio meander mentioned in the last section, therefore, is not corresponding one to one. For example, after the El Nino in 1965, the ITCZ rapidly moved northward and the tropical cyclonic curl sharply decreased from the maximum but the Kuroshio meander was observed only for a few months; then, disappeared[8]. This meander, as merely a short-time one, should not be formally called the Kuroshio meander. The cause may be as follows: (i) the ITCZ peak was shorter at that time and it corresponded to the weaker El Nino in 1965; (ii) the peak of the subtropical anticyclonic curl was also smaller than others and its following decrease from the peak was rather small. Another example is the case in 1969. The Kuroshio meander then lasted less than a year, and thus it is called the Kuroshio quasi-meander. Although the tropical cyclonic curl and the subtropical anticyclonic curl at that time decreased sharply from the maximum, the ITCZ did not move rapidly northward–it moved in this direction for a short distance, and then turned its head and rapidly ran southward so that the strong El Nino in 1972 followed. In the light of the cases in 1954 and 1959, the favourable condition for the occurrence of the Kuroshio meander is the synchronous decrease from the peak of tropical cyclonic curl and the subtropical anticyclonic curl as well as from the southern maximum position of the ITCZ.

The present relation between the El Nino and the Kuroshio meander is only suggested from analysis of the wind stress field. Further studies, especially the studies of the phase relation of various links are needed with shorter time interval observations of wind, current, sea water temperature and sea level.

REFERENCES

[1] Wyrtki, K. and G. Meyers, *The Trade Wind Field Over the Pacific Ocean, Part II: Bimonthly Field of Wind Stress* 1950–1972, HIG-75-2, Hawaii Inst. Geophy., 1975, 1–152.

[2] Wyrtki, K., El Nino—the dynamic response of the equatorial Pacific Ocean to atmospheric forcing, *J. Phys. Oceanogr.*, 5(1975), 572–584.

[3] Guan Bingxian, Analysis of the variations of volume transports of the Kuroshio in the East China Sea, *Chin. J. Ocean. Limn.*, 1(1983), 2: 156–165.

[4] Wyrtki, K., The southern oscillation, ocean-atmosphere interaction and El Nino, *MTS Jour.*, 16 (1982), 3–10.

[5] Bjerknes, J., A possible response of the atmospheric Hadley circulation to equatorial anomalies of ocean temperature, *Tellus*, 18 (1966), 820–828.

[6] Wyrtki, K. and G. Meyers, *The Trade Wind Field Over the Pacific Ocean, Part I: The Mean Field and the Mean Annual Variation*, HIG-75-1, Hawaii Inst. Geophy., 1975, 1–51.

[7] Reiter, E.R., Long-term wind variability in the tropical Pacific, its possible causes and effects, *Mon. Wea. Rev.*, 160(1978), 324–330.

[8] Shoji, D., The Kuroshio south of Japan in 1965, *Researches in Hydrography and Oceanography Commemoration Publication of the Centenary of the Hydrographic Department of Japan*, 1972, 113–149.

MAJOR FEATURES AND VARIABILITY OF THE KUROSHIO IN THE EAST CHINA SEA

Guan Bingxian (管秉贤)
(*Institute of Oceanology, Academia Sinica, Qingdao, China*)
Received May 5, 1987

Abstract

This is a brief introduction of the Kuroshio in the East China Sea (ECS). The main results of the study for this part of the Kuroshio system in recent years are reviewed and presented with emphases placed on the major features of the current structure, annual and inter-annual variations of the velocity and volume transport of the Kuroshio in ECS, and the relation between the variation of the Kuroshio in ECS and that of the Kuroshio south of Japan. And finally, an indirect relation between the variation of the Kuroshio in ECS and that of the North Equatorial Current system is suggested. It is shown that the fluctuation of the Kuroshio in ECS is also correlated with that of the North Equatorial Current and North Equatorial Counter-current. Ties of the above relation are the wind stress curl field over the tropical and subtropical belts.

Kuroshio, a western boundary current, is not only the most important link of the whole subtropical circulation system of the North Pacific, but also the leading component of the current pattern of the East China Sea (ECS) (Fig. 1). In addition, it may exert some influences on the Yellow, Bohai and South China Seas. Therefore, it may be considered as one of the key points of the WEPACICS study.

The Kuroshio referred to here is the section of the Kuroshio System between Suao–Yonakunijima Island in the south and the Tokara Strait in the north, and is called "Kuroshio in ECS".

I. MAJOR FEATURES OF THE CURRENT STRUCTURE OF THE KUROSHIO

The results of GEK observations and geopotential topography at the sea surface (0/1200 dbar) in the CSK period in summer, 1965 are shown in Fig. 2 (Nitani, 1972). It is evident from the comparison of the figures that the maximum observed velocity is located at the western boundary of the maximum geopotential gradient zone. This suggests that the Kuroshio movement is essentially of a geostrophic or quasi-geostrophic nature.

There are some high velocity areas in the path of the Kuroshio in ECS. For example, at its entrance (somewhere northeast of Taiwan) to and exit (somewhere southwest of Yakushima Island) from ECS, and at the in-between region (somewhere northwest of Okinoerabujima Island), the maximum velocity of the Kuroshio reaches 3.3–3.8, 3.3–3.4 and 3.0–3.6 kt, respectively.

So far as the "climatological" condition of the Kuroshio is concerned, the measurements in the area northwest of Okinoerabujima Island, i.e., on section G (PN) since 1956 may be taken as a typical example. The distribution of the surface current of the Kuroshio and that of its counter-current in ECS, are quite stable. The maximum velocity (i.e., current axis) is located near the place where the bottom slope is steepest, that is, near the inflection point of the profile of the bottom as shown in Fig.

3. The current axis frequently varied within a range of 20 nautical miles. Its width was usually maintained at 40—60 nautical miles. Its direction generally varied within 40°—60°. It is, therefore, justifiable to say that the Kuroshio in ECS appears to be a western boundary current with relatively stable direction and narrow width. This phenomenon is closely related to the submarine topography of ECS (Guan, 1964, 1979).

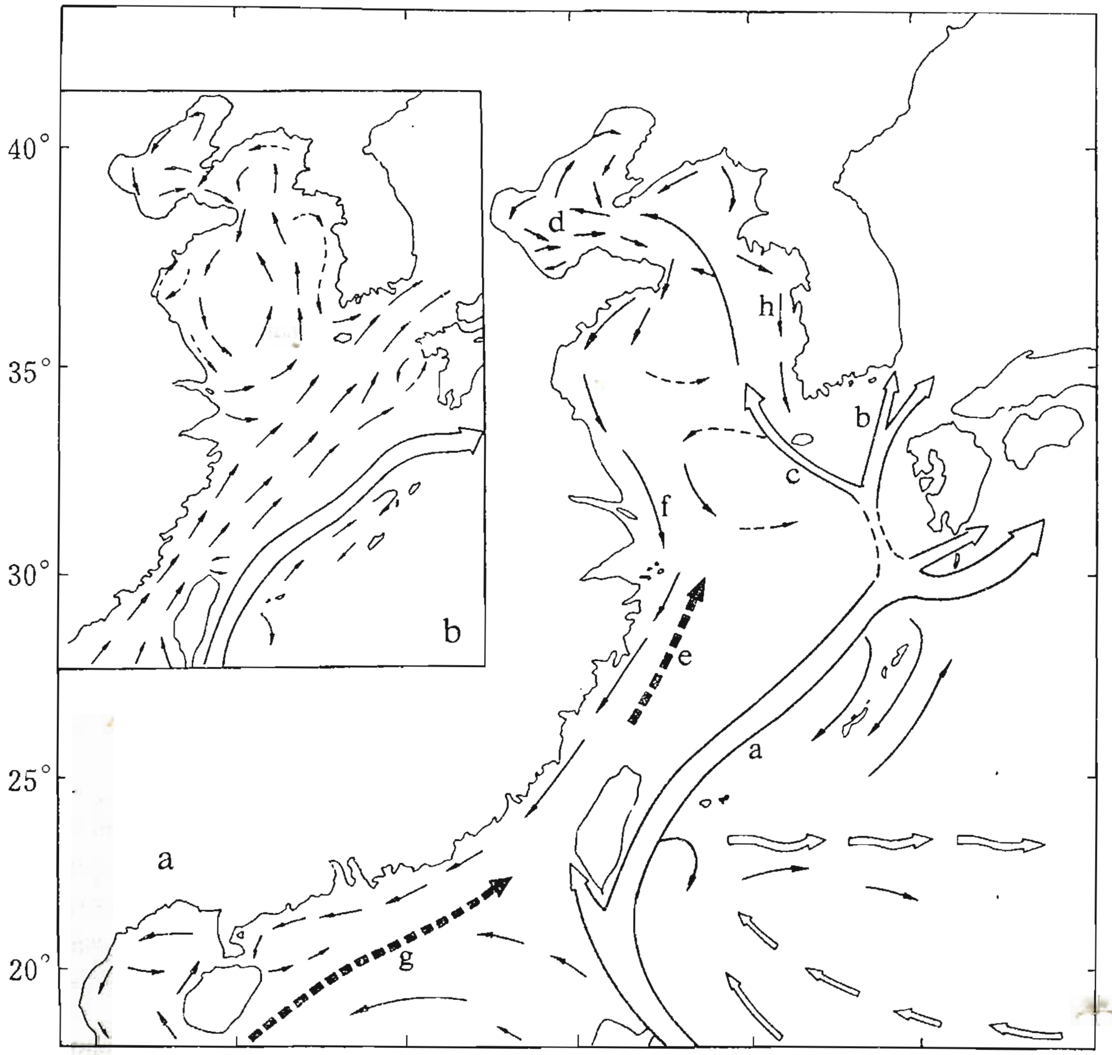

Fig. 1 Schematic representations of (a) the major current systems in the Bohai, Yellow, and East China Seas and the adjacent area in winter and (b) the surface current systems in summer

The vertical current structure of the Kuroshio in the central part of ECS along 125°E is shown in Fig. 4. The upper panel shows the E–W component of the calculated geostrophic current (referred to 1200 m) in the summer of 1967 and the lower panel shows the relative current (referred to 1000 m) measured directly by means of two current meters at a few stations along this section in the same

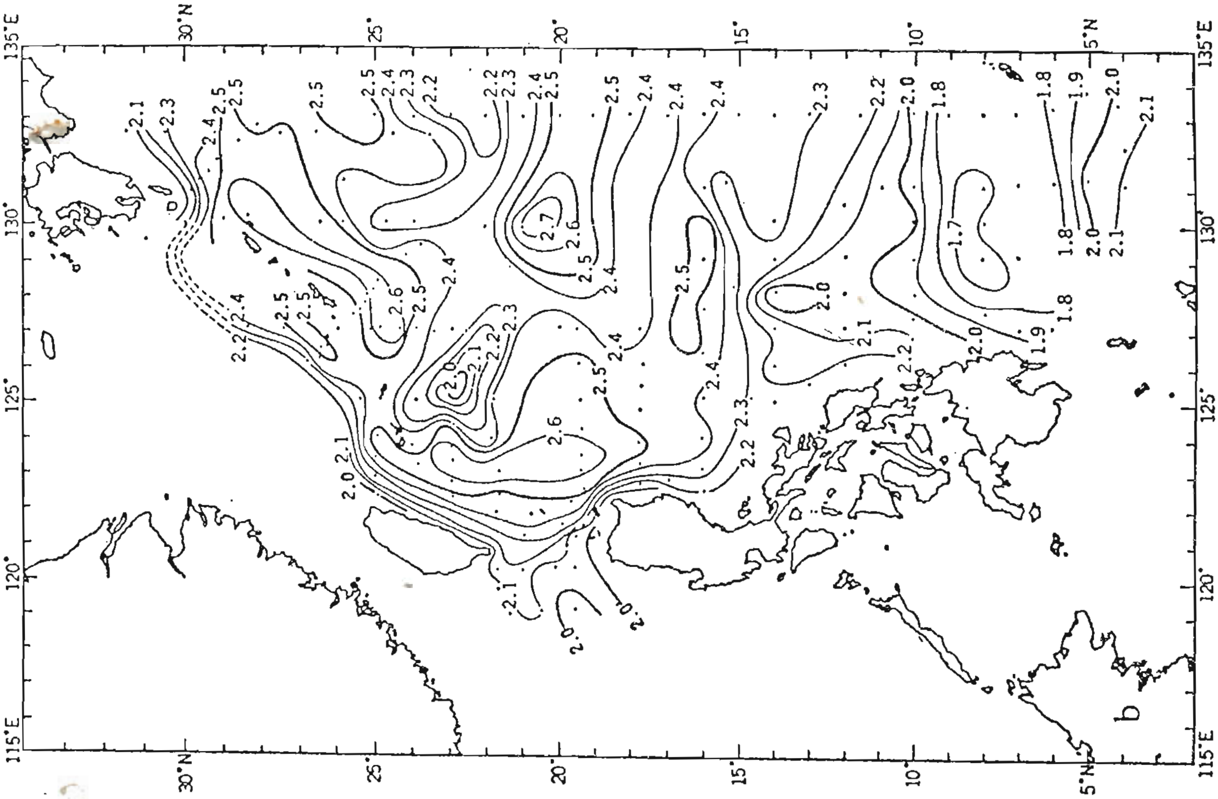

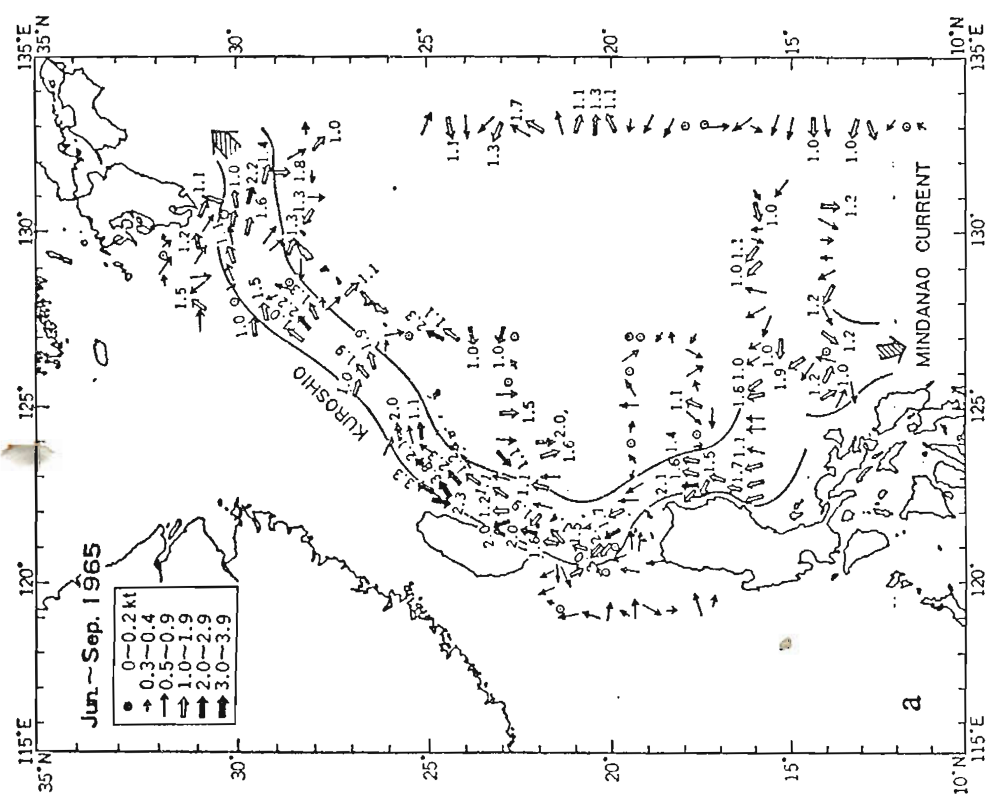

Fig. 2 Results of GEK observations (a) and geopotential topography (0/1200 dbar in dynamic meter) (b) in summer of 1965 (After Nitani, 1972)

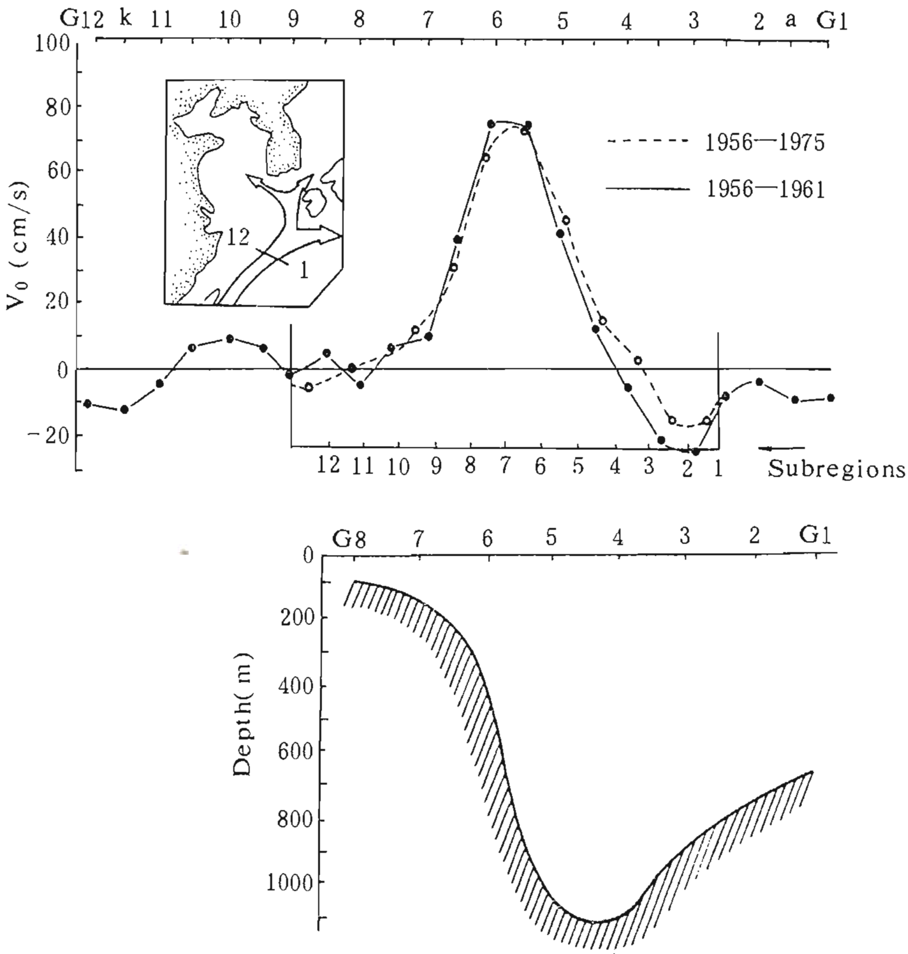

Fig. 3 Relationship of surface velocity distribution of the Kuroshio in ECS with submarine topography (After Guan, 1979)

period (Takahashi and Chaen, 1971). In general, the agreement between the calculated and observed results is satisfactory. In the upper 400 m, the velocity of the Kuroshio decreased slowly with increasing depth, but it still maintained a strong speed of about 1.5 kt (78 cm/s) at the bottom of this layer.

The results of deep–bottom current measurement in the area of the Okinawa trough (depth = 1060 m) in June–October, 1984 are shown in Fig. 5 and Table 1 (Yamashiro, Ichikawa, 1985). Even at a great depth and near–bottom layer, the current direction is still toward the northeast, that is, the same as that of the surface Kuroshio current. The average speed in a period of 100 days at a depth of nearly 600 m exceeds 20 cm/s. It is obvious that the Kuroshio in ECS extends through to a great depth. A counter–current in the near–bottom layer has not been observed to date.

As compared with the coastal and shelf water in China Seas, the Kuroshio water in ECS is characterized by higher temperature and salinity. Its surface temperature in sultry summer may reach to as high as 30°C. The highest salinity (~34.9 or more) is located in sub–surface water layer (~150–250 m) and lowest salinity (~34.3 or less) in intermediate water layer (~600 m). Because of its isolation from the Pacific by a submarine ridge, the temperature of the deep and bottom water of

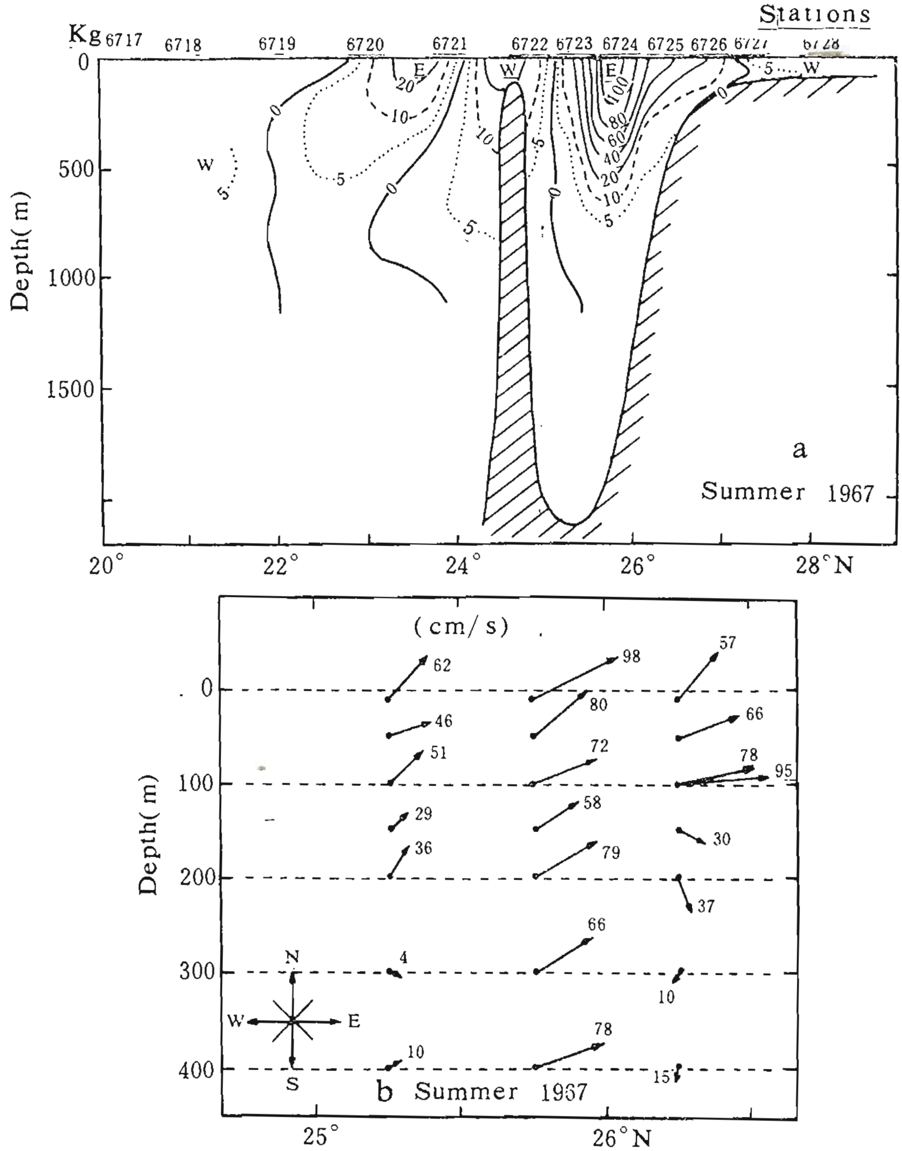

Fig. 4 Vertical current structure of the Kuroshio along 125°E in summer of 1967

a. E–W component ($cm.s^{-1}$) of the calculated geostrophic current referred to 1200 m

b. Relative current vector ($cm.s^{-1}$) referred to 1000 m measured directly by means of two current meters (After Takahashi and Chaen 1971)

Table 1 Results of deep–bottom current measurements (After Yamashiro and Ichikawa, 1985)

	KGIU	KGIM	KGIL
Set depth (m)	595	801	1007
Record duration (days)	100	15	89
$\bar{V}$ (cm/s)	23.6	2.9	4.1
Direction (degree)	37.7	16.6	30.3

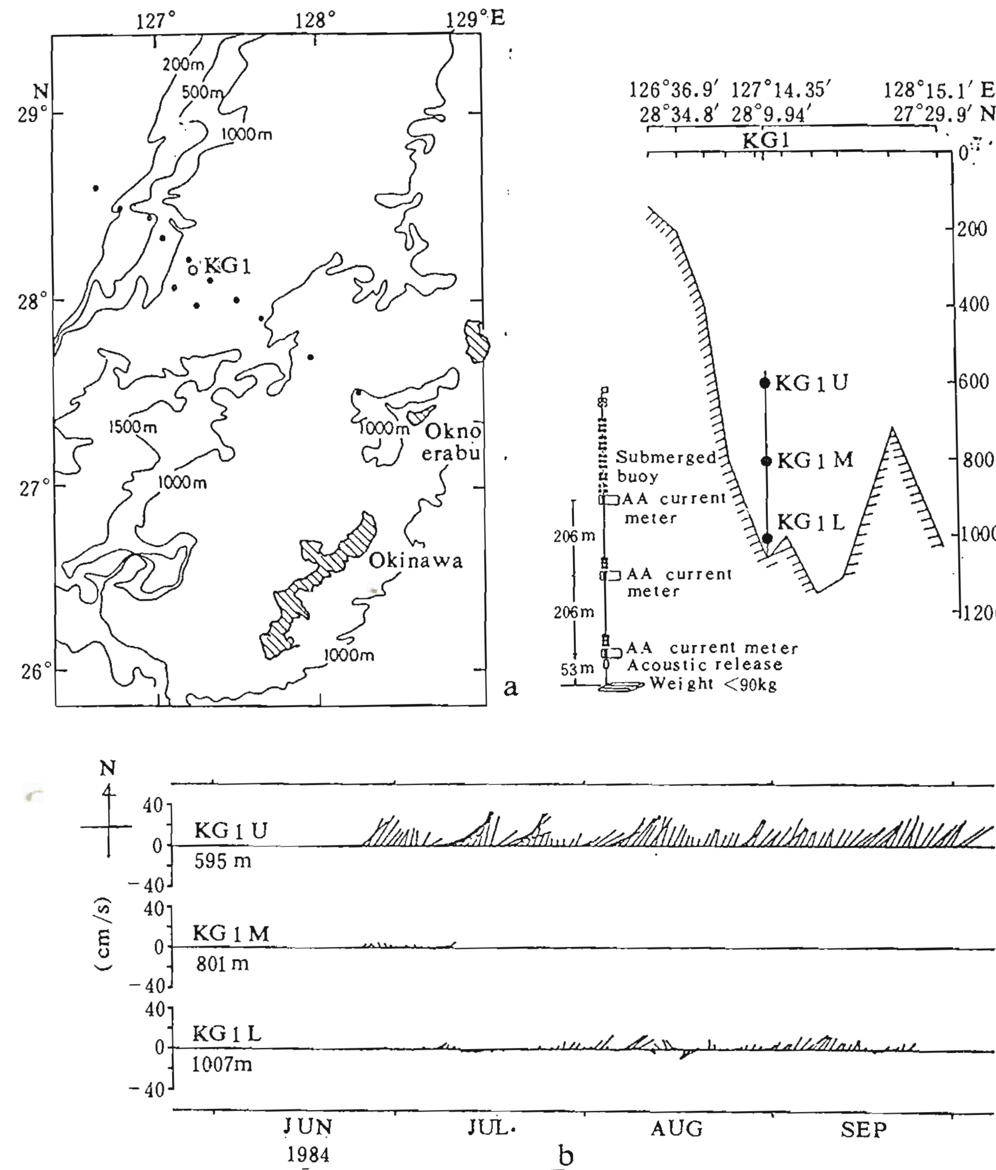

Fig. 5 Deep–bottom current measurements in the area of the Okinawa trough in June–October, 1984 (After Yamashiro and Ichikawa, 1985)

a. Observation location b. Observation results

the Okinawa trough is generally 1.5°C higher and the salinity is usually 0.1 lower than that of the Pacific water at corresponding depths below the sill. (Nitani, 1972).

Former observations from stations spaced at larger intervals showed that the Kuroshio axis had only a single current core. But recent temperature observations with XBT along section G(PN) at station intervals of less than 5 miles revealed that the Kuroshio in ECS usually has plural bands of strong current or multiple current cores (Akamatsu, 1979) as shown in Fig. 6.

Regular seasonal observations made in the past 25 years or so showed that the Kuroshio path in

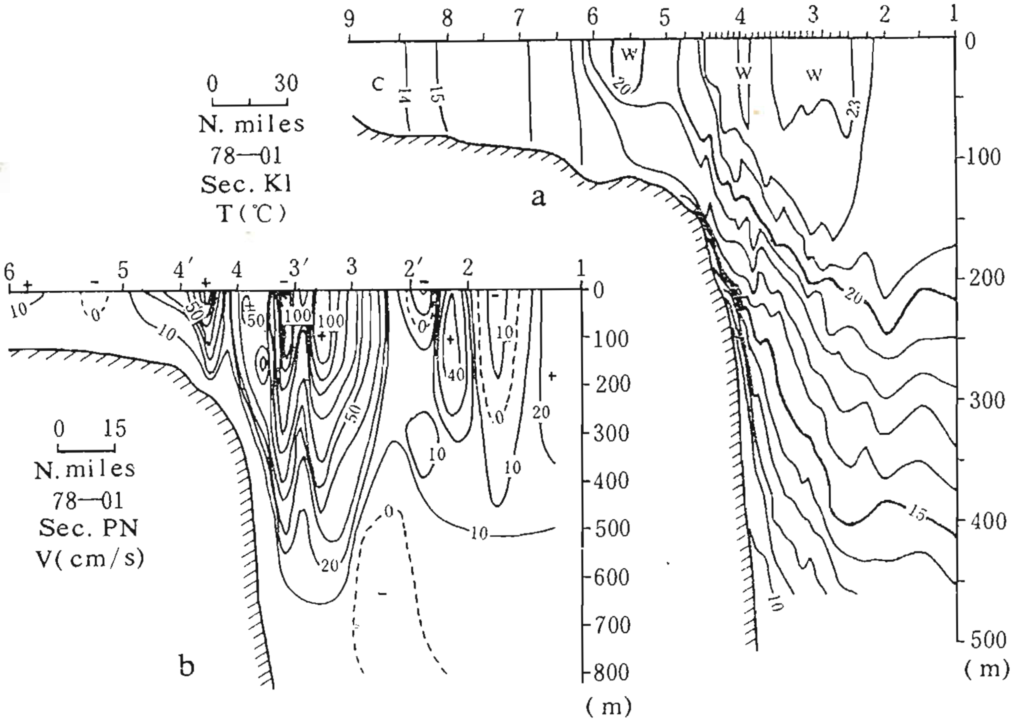

Fig. 6 Temperature (a) and geostrophic current (b) distributions along the section to the northwest of Okinoerabujima Island in Jan., 1978 (After Akamatsu, 1979)

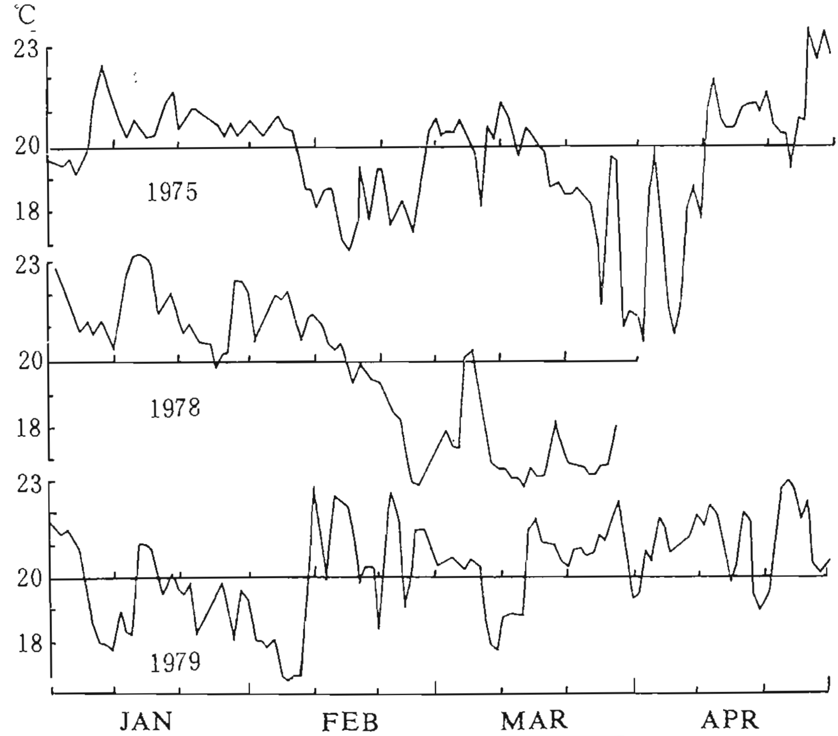

Fig. 7 Water temperatures at the Buoy Station No. 4 from January–April (1975, 1978, 1979) (After Shibata, 1983)

ECS did not change much and that there was no significant meander of considerable dimension such as the case south of Japan. But it was only recently that the meander of the Kuroshio along the edge of ECS continental shelf was revealed by the water temperature data of the marine meteorological Buoy Station No. 4 (28°20′N, 126°05′E) of JMA. The temperature fluctuated largely between 16° to 22°C from January to April every year, with a prominent period of about 20 days as shown in Fig. 7. The buoy was located in the frontal zone between the Kuroshio water and continental coastal or shelf water. As such a large and rapid temperature fluctuation cannot be explained by the normal seasonal variation, it is suggested that the meander of the Kuroshio caused this fluctuation of water temperature (Shibata, 1983).

II. ANNUAL AND INTER–ANNUAL VARIATIONS OF THE KUROSHIO

In the following, the time dependent phenomena of the Kuroshio in ECS will be treated with emphasis placed on the annual and inter–annual variations of its velocity and volume transport (VT).

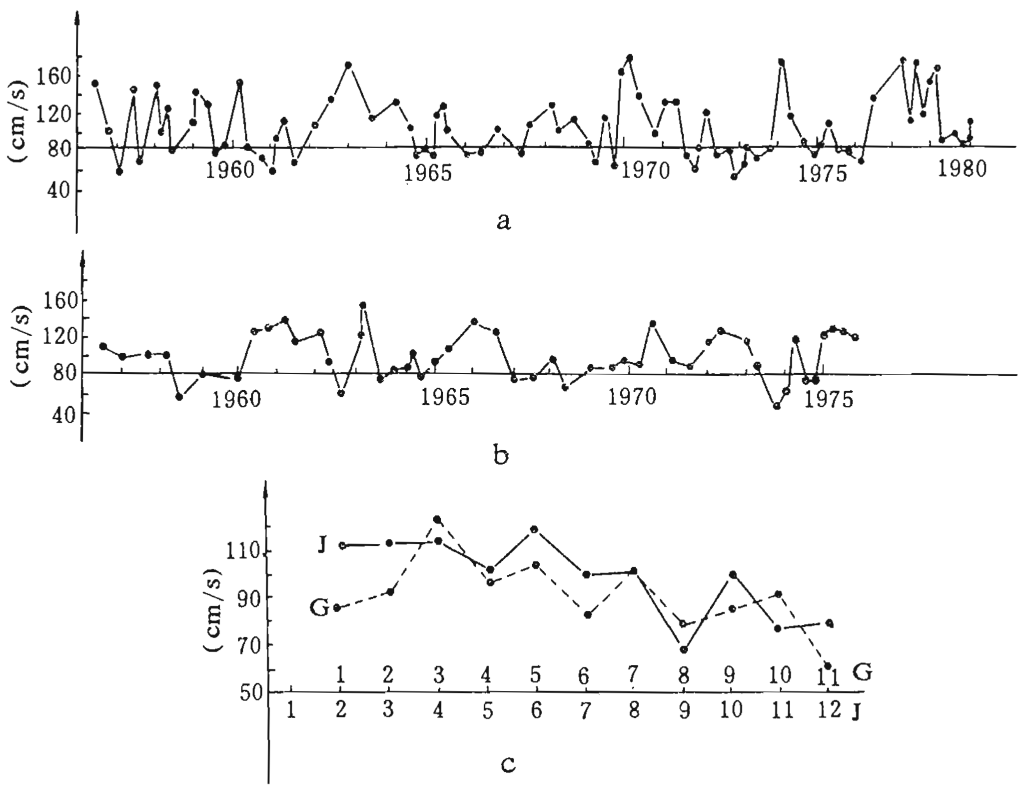

Fig. 8 Time series of the surface velocity component (cm.s^{-1}) at the Kuroshio axis on G(PN) (a) and J (b) sections, and their mean monthly variations (c) (After Lü, 1983)

1. Variations of the Velocity

Since the early fifties, surface current measurements with GEK have been made extensively by Japanese oceanographers in the Kuroshio area of ECS, especially along section G(PN) and section J (southwest of Yakushima Island). GEK measurements have continued for more than 20 years

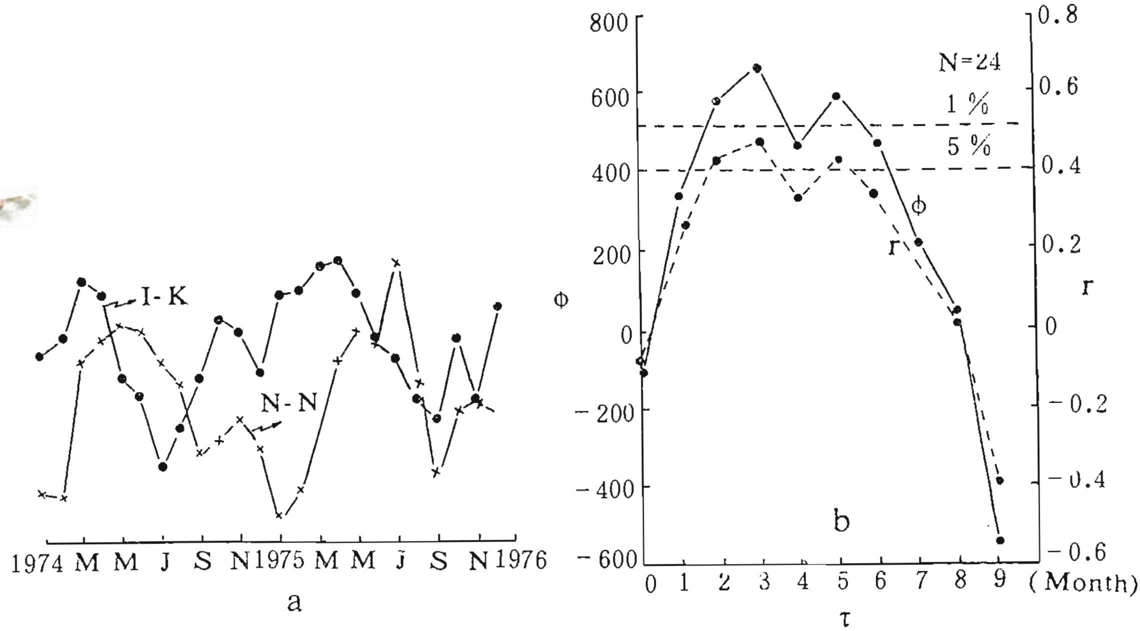

Fig. 9 Comparison of the differences of MMSL between the two sides across the Kuroshio east of Taiwan (I-K) and in Tokara Strait (N-N), 1974–75 (a), and their correlative functions (Φ) and coefficients (b) (After Guan, 1982)

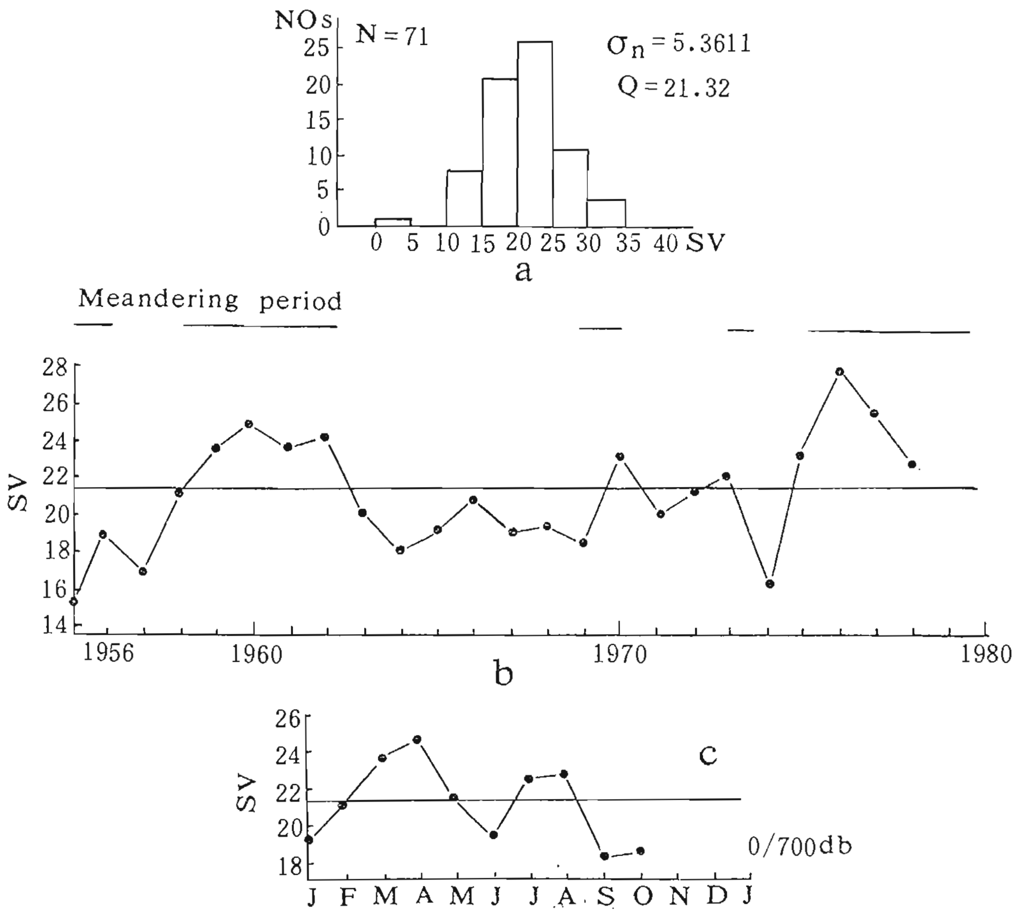

Fig. 10 Frequency distribution (a), annual values (b) and mean monthly values (c) of the Kuroshio VT through section G(PN) in period 1955—78 (After Guan, 1982)

(Guan, 1979; Lü, 1983).

Observation results show that the variations of the axial position, and the direction and width of the Kuroshio are indeed not large. On the other hand, variations of the velocity of the Kuroshio are quite large.

The fluctuation range of the surface velocity at the Kurashio axis on both sections is more than 2 kt, while the overall mean is about 1.9 kt, so that the amplitude of the fluctuation is equal to, or even exceeds the average velocity a little during this period (Guan, 1979).

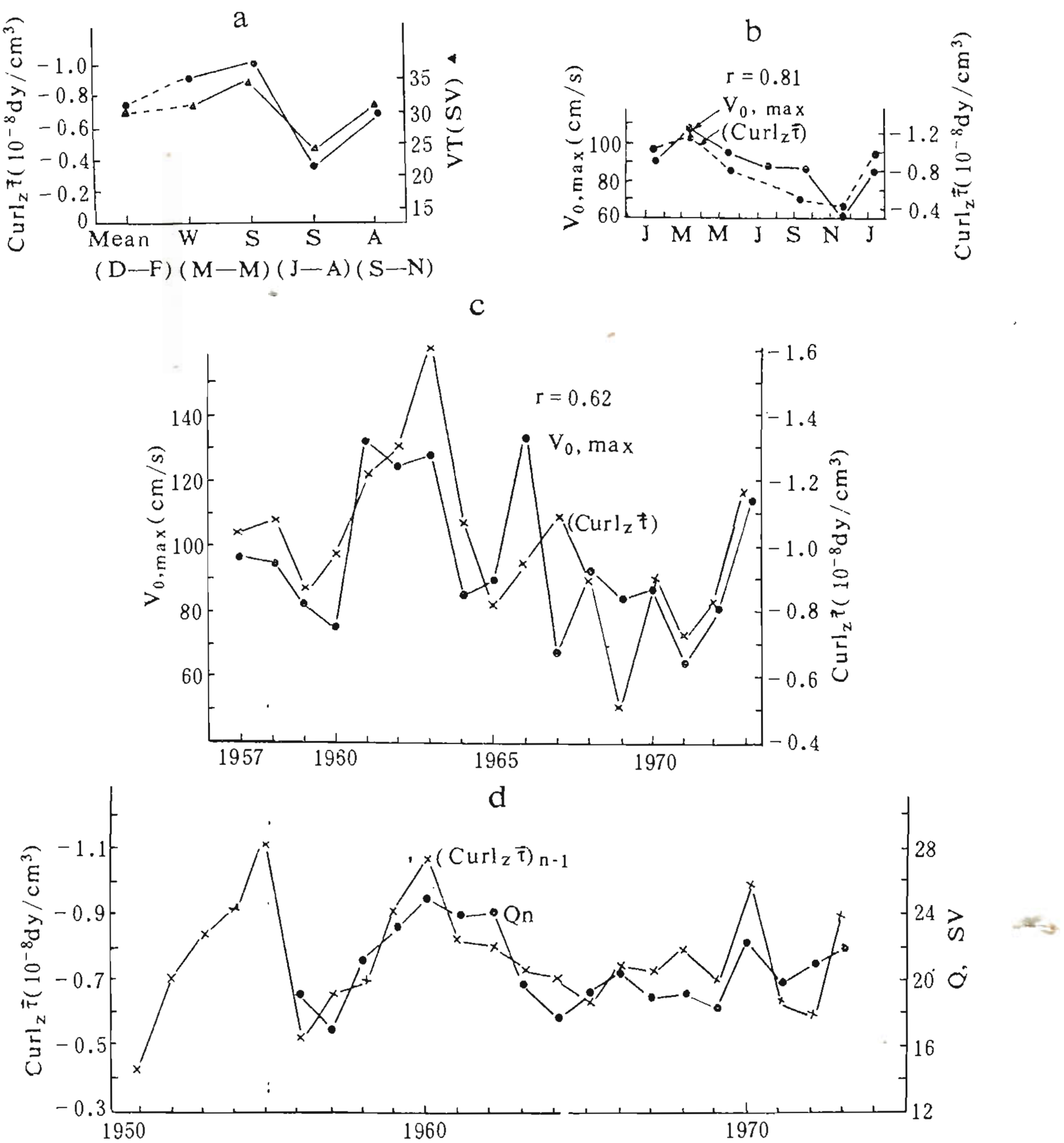

Fig. 11 Relation between the VT and surface velocity at the axis of the Kuroshio east of Taiwan and in ECS (a–c) and the surface wind–stress curl in the adjacent region of the Hawaiian Islands (d) (After Guan, 1982)

The time series of surface velocity (component perpendicular to the section) at the Kuroshio axis on G(PN) and J sections, and their respective mean monthly variations are shown in Fig. 8. It is evident from the figure that the fluctuations of the surface velocity at both sections had a similar tendency. Their mean monthly variations, with a lag of about a month, approached to coincide with each other. The general seasonal variation is strongest in spring, moderate in summer and winter, and weakest in autumn (Guan, 1979; Lü, 1983).

The time series of the differences of MMSL between two sides of the Kuroshio northeast of Taiwan and in Tokara Strait, 1974—75, and their relation are shown in Fig. 9. According to the geostrophic equation, the variations of such differences of MMSL represent those of surface velocity. Evidently, a significant linear correlation (with a time lag of some months) exists between the variations of the Kuroshio in Tokara Strait and those northeast of Taiwan (Guan, 1982).

The above mentioned relations clearly indicate that the velocities of the Kuroshio east of Taiwan, in ECS and Tokara Strait tend to fluctuate in unison but with a lag of a few months from one another (Guan, 1982).

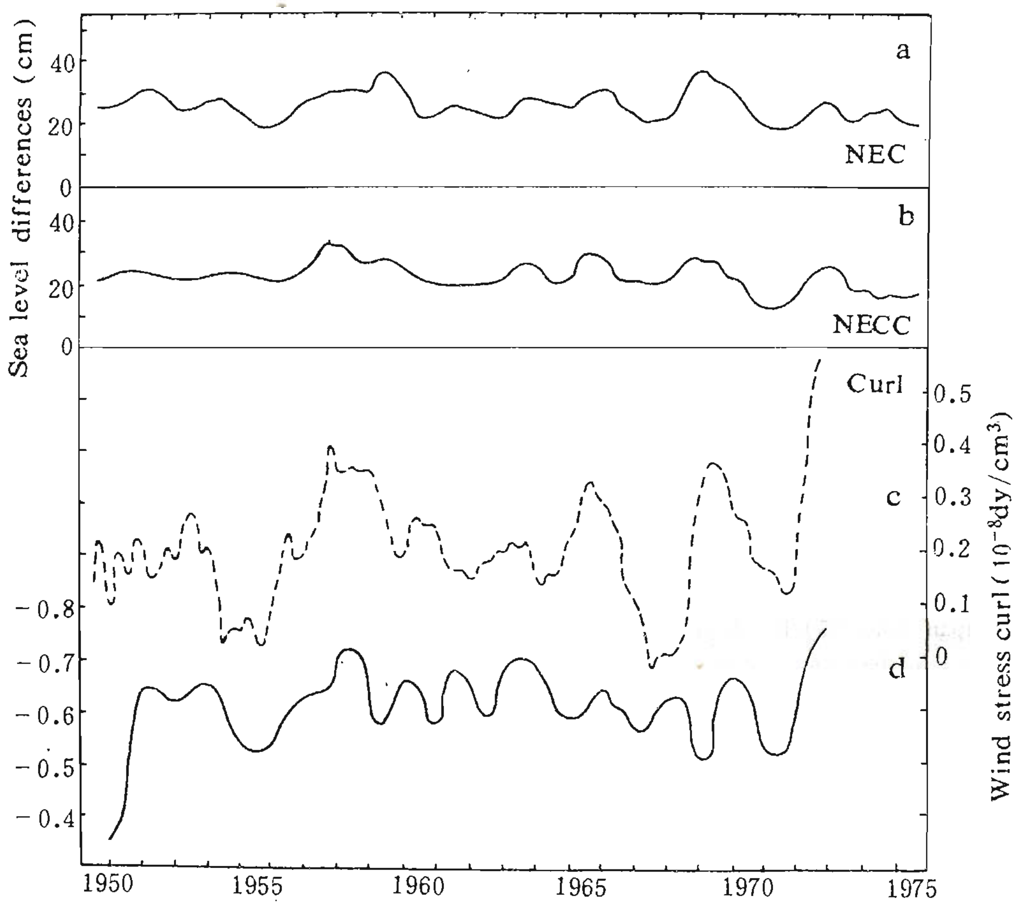

Fig. 12 Time series (1950—75) of the sea level differences (cm) across the North Equatorial Current (NEC) (a), North Equatorial Countercurrent (NECC) (b) (After Wyrtki, 1979), and time series (1950–72) of the wind stress curl (10^{-13}N/cm^3) over the sea region 2°–10°N(c), 22°–28°N (d) (After Liu and Guan, 1986)

2. Variations of VT

The magnitude of VT is one of the most important and evident indices characteristic of the variations of the Kuroshio. Since the sixties, the variation of VT of the Kuroshio in ECS and its relation to the appearance of the large meanders south of Japan have been studied by many authors. In the following, the general variation characteristics of VT, and its cause and relation to the appearance of the large meander south of Japan will be briefly discussed.

Hydrographic observations made on the section G(PN) from July, 1955 through September, 1978 reveal that the maximum VT (referred to 700 dbar) was 35 SV (April, 1977), and that the overall mean was 21.3 SV with $\sigma_t = 5.36$ SV. The frequency distribution of the occurrence of VT is almost a Gaussian type distribution. The annual and mean monthly values of VT of the Kuroshio for this period are shown in Fig. 10 (Guan, 1982).

Since the end of the seventies, in the studies on the annual and interannual variations of the Kuroshio, a significant teleconnection (with a time lag of about 2 months to 1 year) has been found between the variations of the surface axis velocity and VT of the Kuroshio east of Taiwan and in ECS, and the corresponding variations of the sea surface wind stress curl over the central subtropical region of the North Pacific (22°—28°N, i.e., the area adjacent to the Hawaiian Islands), as shown in Fig. 11 (Guan, 1979, 1981, 1982).

This important result suggests that it is the wind stress field between the northeast trade wind and the westerlies that chiefly governs the fluctuations of the Kuroshio east of Taiwan and in ECS, and this relation may serve as a clue for the prediction of the variation tendency of the Kuroshio in this region (Guan, 1979).

Seasonal observations in a decade (1972–81) show that the average VT of the Kuroshio through section G(PN) is 25.5 $\pm$ 2.75 SV (referred to 700 dbar, Fujiwara et al., 1982), that both mean seasonal variations of the surface velocity and VT of the Kuroshio are stronger in spring and summer, and weaker in winter and fall, and that they appear to be of the two peaks type.

Conerning the inter–annual variation of VT, there were four periods (i.e., 1959–62, 1970, 1973 and 1975–78) in 24 years (1955–78) when the annual value of VT of the Kuroshio was greater than the average. The maximum was observed in 1976, the minimum in 1955 and 1974. On the whole, VT of the Kuroshio in ECS remained at a low level from 1963 through 1974. The VT peak periods of the Kuroshio in ECS coincided with the periods of the occurrence of large or quasi–large meanders of the Kuroshio south of Japan. The two periods (1959–62, and 1975–78), when VT of the Kuroshio remained greater than the average for several years, coincided respectively with the periods of large meanders of No. 2 and No. 3 after World War II. A meander of medium degree occurred south of Japan about 1970 (Fig. 10b). As revealed by the above relations, the large meanders of the Kuroshio south of Japan were often accompanied by a peak value VT of the Kuroshio in ECS, and hence, accompanied by a peak value of wind–stress curl over the central subtropical region of the North Pacific. This relation may be a significant clue for studying the mechanism of the large meanser of the Kuroshio south of Japan (Guan, 1982).

III. RELATION BETWEEN THE VARIATION OF THE KUROSHIO IN ECS AND THAT OF THE NORTH EQUATORIAL CURRENT SYSTEM

The Kuroshio is generally considered to be a continuation of the North Equatorial Current (NEC) and to have originated from an area southeast of Taiwan Island and east of Bashi Strait and

Luzon Island. Therefore, a close relation between them may be expected to exist certainly. But up-to-date, adequate data sets are not available to analyse their direct relation. In the following, an indirect relation through the wind stress curl is suggested.

Figure 12 shows the time series (1950–75) of the sea level differences (cm) across NEC (a), North Equatorial Counter-current (NECC, b), and the time series (1950–72) of the wind stress curl ($10^{-13}N/cm^3$) over the sea region 2°–10° N(c), 22°–28° N, respectively. Curves a and b give 12-month running means (after Wyrtki, 1979). Curves c and d give 6-bimonthly running means (Liu and Guan, 1986). The running means represent the inter-annual fluctuation. Therefore, curves a and b depict the inter-annual fluctuations of the velocities of NEC and NECC, and curves c and d the inter-annual fluctuations of the wind stress curl over the tropical and subtropical regions, respectively.

NEC and NECC are two major ocean currents in the equatorial North Pacific, and are located north and south of the counter-current trough (~10°N), respectively. Comparison shows that the fluctuations of NEC and NECC are not only synchronous (Wyrtki, 1974), but also approach to be coincident with those of the wind stress curl over the tropical sea region (2°–10°N). Besides the initial part (1950–53), significant peaks and troughs of these three curves (a,b and c) nearly approach to coincide with one another. Therefore, in the period 1953–72, the fluctuations of NEC and NECC were closely related to the fluctuations of the cyclonic wind stress curl field over the sea region to the north of the equator (Guan, 1986).

Comparison also shows that the tropical cyclonic wind stress curl (c) is positively correlated with the subtropical anticyclonic wind stress curl (d), and leads the latter. The maximum coefficient remarkable on 0.01 level has a phase lag of less than 2 months. Therefore, the wind stress curl in tropical region is coherent with that in subtropical region, that is, as the tropical cyclonic curl increases, the increase of the subtropical anticyclonic curl follows, and vice versa (Liu and Guan, 1986).

Combining the results mentioned above, that is, 1) the fluctuation of the Kuroshio in ECS is positively correlated with that of the subtropical anticyclonic wind stress curl, 2) the fluctuation of NEC (and NECC) is positively correlated with that of the tropical cyclonic wind stress curl, and 3) the tropical cyclonic wind stress curl is positively correlated with the subtropical anticyclonic wind stress curl, it follows that the fluctuation of the Kuroshio in ECS is also correlated with that of NEC and NECC. Ties of the above relations are the wind stress curl field over the tropical and subtropical belts.

These results (though they are preliminary and qualitative) strongly support the classical wind-driven ocean circulation theory and demonstrate statistically that water which goes west or east must then go north or south to close the gyre, and that the permanent ocean currents are related to the wind stress curl field over the ocean.

References

[1] Akamatsu, H., 1979. From the observations in the East China Sea—The Kuroshio in the region near the continental slope. *Marine Sciences Monthly* 11(3): 175–181. (in Japanese)

[2] Fujiwara, I. et al., 1982. Oceanic conditions on the PN Section in the East China Sea. *Reports of KER* 5: 61–70. (in Japanese)

[3] Guan Bingxian (Kwan Pinghsien), 1964. A preliminary study of the distribution and variation of the velocity and volume transport of the Kuroshio and their relation to the topography. *Oceanologia et Limnologia Sinica* 6(3): 229–

251. (in Chinese with English abstract)

[4] Guan Bingxian, 1979. Some results from the study of the variation of the Kuroshio in the East China Sea. *Oceanologia et Limnologia Sinica* **10**(4): 297–306. (in Chinese with English abstract). Also in: The Kuroshio IV-Proceedings of the 4th Symposium for CSK, Saikon Publishing Company, Ltd. Tokyo, pp. 897–911 (1980).

[5] Guan Bingxian, 1981. The characteristics of the velocity structure of the Kuroshio and its seasonal variation on the section Suao–Yonagunijima *Studia Marina Sinica* **18**: 1–18. (in Chinese with English abstract)

[6] Guan Bingxian, 1982. Analysis of the Variations of Volume Transport of the Kuroshio in the East China Sea. *In*: Proceedings of the Japan–China Ocean Study Symposium. Oct., 1981, Shimizu, p. 118–137. Also in: *Chin. J. Ocean. Limno.* **1**(2): 156–165 (1983).

[7] Guan Bingxian, 1986. Current structure and its variation in the Equatorial area of the western North Pacific Ocean. *Chin. J. Ocean. Limno.* **4**(3): 239–255.

[8] Liu Juping and Guan Bingxian, 1986. Preliminary study of relation between the Kuroshio meander and the El Nino. *Acta Oceanologica Sinica* **8**(5): 541–546. (in Chinese)

[9] Lü Caixia, 1983. A preliminary analysis of the variation of surface velocity of the Kuroshio on section J in the East China Sea. *Transactions of Oceanology and Limnology*, **1**: 7–12. (in Chinese with English abstract)

[10] Nitani, H., 1972. Beginning of the Kuroshio. *In*: "KuroshioIts Physical Aspects," edited by H. Stommel and K. Yoshida, University of Tokyo Press, pp. 129–163.

[11] Shibata, A., 1983. Meander of the Kuroshio along the edge of the continental shelf in the East China Sea. *Umi to Sora* **58**(4): 113–120. (in Japanese with English abstract)

[12] Takahashi, T. and M. Chaen, 1971. Oceanic conditions near the Ryukyu Islands–III. Oceanic conditions along 125°E in spring and summer of succesive four years, 1965–1968. *Mem. Fac. Fish., Kagoshima Univ.* **20**(1): 31–54.

[13] Wyrtki, K., 1974. Equatorial currents in the Pacific 1950 to 1970 and their relations to the trade winds. *J. Phys. Oceanogr.* **4**(3): 372–380.

[14] Wyrtki, K., 1979. Sea level variations: monitoring the breath of the Pacific. *Trans. Amer. Geophys. Union*, **60**(3): 25–27.

[15] Yamashiro, T. and N. Ichikawa, 1985. Currents in the Deep Layer of the Okinawa Trough. *In*: Abstracts of Lectures in Spring Assembly of Oceanographic Society of Japan pp. 109. (in Japanese)

第 20 卷 第 2 期
1989 年 3 月

海 洋 与 湖 沼
OCEANOLOGIA ET LIMNOLOGIA SINICA

Vol. 20, No. 2
Mar., 1989

棉兰老冷涡的变异及其与 El Niño 的关系*

管 秉 贤
（中国科学院海洋研究所，青岛）

提要 本文根据北太平洋西南部分 1965—1974 年冬季的水文资料及附近区域 1975—1983 年月平均水位资料，比较详细地探讨了棉兰老冷涡的变异及其是否与 El Niño 事件有关的问题。结果表明，棉兰老冷涡的变异与 El Niño 有着密切的关系，在 El Niño 期间，棉兰老冷涡变得较强；而在非 El Niño 期间，冷涡变得较弱。然而，冷涡强化的程度并非总与 El Niño 的强度相对应。这显然是由于 El Niño 仅是影响或控制冷涡变化的主要因素之一而已。

北赤道流自东向西流，在遇到菲律宾海岸前，有一部海水折向南流成为棉兰老海流 (Mindanao Current)，并又折向东流成为北赤道逆流，在转弯过程中右侧有一部分水体进入苏拉威西海，左侧形成棉兰老涡 (Mindanao Eddy)。这是棉兰老岛和新几内亚岛之间

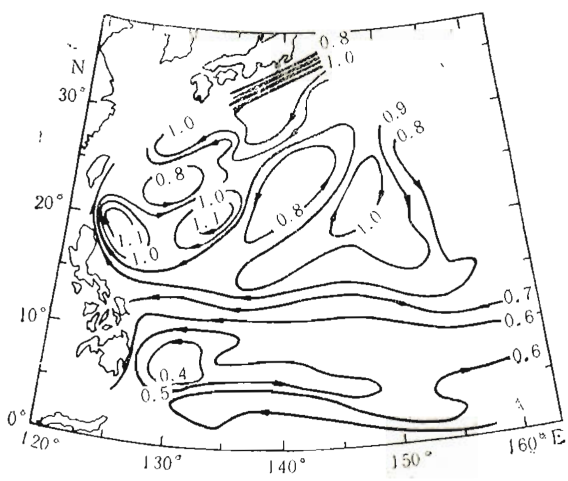

图 1 100m 层上的 ΔD 分布（根据 Koenuma, 1937）
（图上数字均应加上 680，例如，0.8 应读为 680.8）
Fig. 1 Distribution of ΔD at 100 m layer (After Koenuma, 1937) (680 should be added to the numerals in the figure, for example, 0.8 should be read as 680.8)

* 本文得到国家自然科学基金的资助。
中国科学院海洋研究所调查研究报告第 1692 号。
收稿日期：1988 年 5 月 30 日。

海域引人注目的一个较强大的冷涡。早在 30 年代，Koenuma[4] 在讨论北太平洋西南部的水文特征时，已根据动力高度偏差的分布指出这一海域存在着一个显著的气旋型涡旋(如图 1 所示)。冷涡中心约位于 7°N，130°E。60 年代初期，Wyrtki[8] 在 Naga 报告中曾引用 Snellius 号调查船（1929—1930）的调查资料，对这个冷涡的西南部分作过较详细的阐述。这个冷涡的海面动力高度（0/1250db）如图 2 所示。

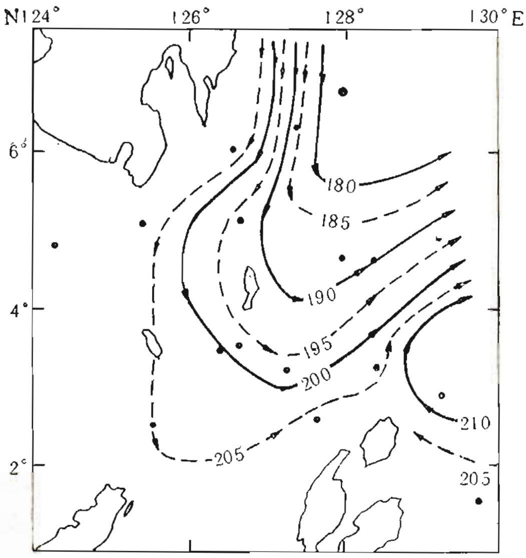

图 2 棉兰老冷涡的海面动力高度分布
（根据 Wyrtki，1961）

Fig. 2 Sea surface dynamic height topography of the Mindanao Cold Eddy (After Wyrtki, 1961)

本文主要引用冷涡及其毗邻区域 1965—1974 年间冬季的水文资料及 1975—1983 年间月平均水位资料，比较详细地来讨论这个冷涡的变化。同时，由于这个冷涡毗邻西太平洋的“热库”(Heat Pool)，后者被公认为是引发 El Niño 的关键性区域之一，故还拟讨论冷涡变异是否与 El Niño 有关的问题。

1. 棉兰老冷涡的水文特征

图 3 指出了棉兰老冷涡及其附近区域 200m 层的温、盐度分布[3]。这是一个中心为低温的气旋型涡旋。特异的是，它在 200m 层上下却显现为一个低盐的水体。例如，在 1968 及 1969 年冬季，该层上涡旋中心的低温、低盐分别为 <10℃ 及 <34.4‰。这种低盐特征与赤道以北(新几内亚北岸)的高盐水形成了十分明显的对比。这种出现在 200m 层上下的低盐水，在盐度垂直结构上表现为上层盐度极小值，与略深处的氧含量极小值同时出现。这一上层盐度极小值是北太平洋中间水所固有的，它随着棉兰老海流带入苏拉威西海，并遍布在棉兰老岛以东、4—5°N 以北的 200—300m 层水域中。最低盐度约为 34.4‰，也可低于此值[8]。低盐水体的存在，在某种程度上减弱了上层冷涡的强度。

2. 棉兰老冷涡的变异

菲律宾以东和新几内亚岛以北海域海面动力高度的分布如图 4 所示。从图上可以明显地看到，在北赤道流与北赤道逆流之间的最西端部分有一个有时趋于封闭的低值槽区，四个冬季都有。1965—1966 年冬季槽区向东扩展超过 140°E。1967 年冬季低槽向西大大收缩，因 130°E 以西无资料，故图上只呈现半个向西开口的槽区。1968 及 1969 年冬季低槽向西趋于封闭，分别呈近似的圆形及菱形。

如以 1.5 动力米线作为冷涡核心的界限，则其平均纬度约在 7°N 处。在 1965—1966 年冬季，涡核向东扩展呈一带状，其纬向长度约 12 个经度或以上，经向宽度约 2.5 个纬度。在 1967 年冬季，涡核大大缩小，图上几乎不见。1968 年冬季涡核重新出现并向西趋于封闭，纬向长度只有 3 个经度，经向宽度约 3 个纬度。1969 年冬季封闭涡核又向东扩展，纬向长度达到 6 个经度以上，经向宽度约 2 个纬度。如取 1.6 动力米线作为冷涡的边界，则

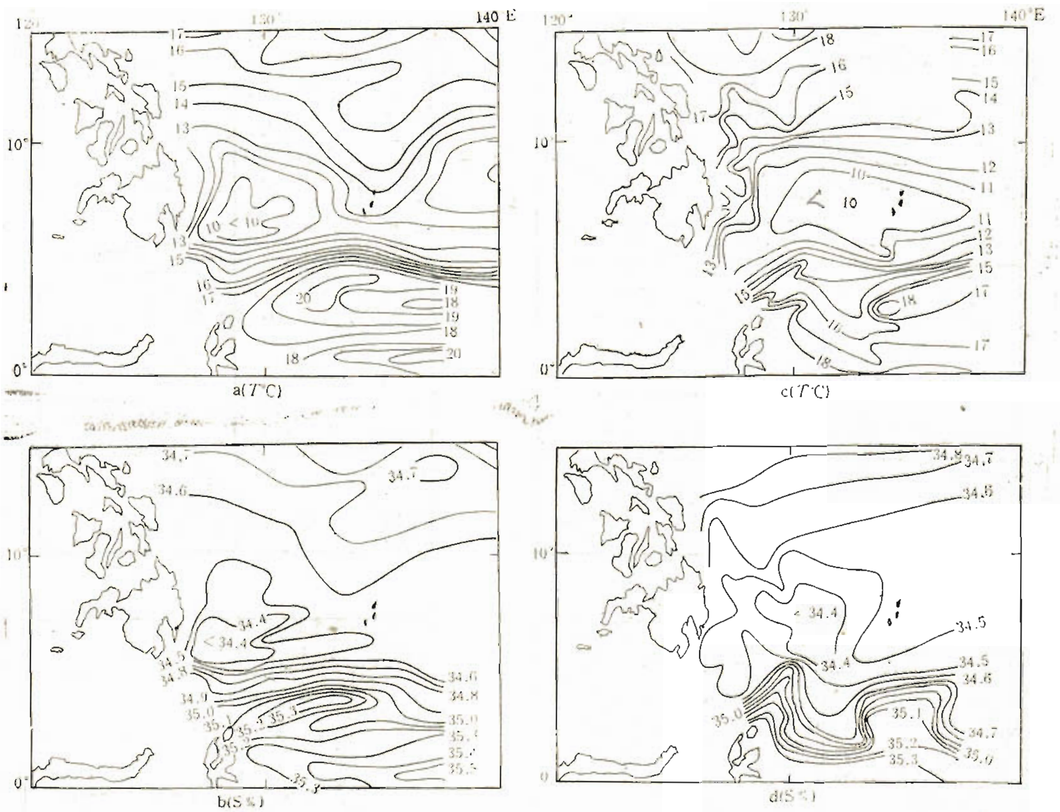

图 3　棉兰老冷涡及其附近 200m 层的温度(℃)及盐度(‰)分布

Fig. 3　Temperature (℃) and salinity (‰) distribution at 200m layer in the area adjacent to the Mindanao Cold Eddy

1968 年 (a—b) 及 1969 年 (c—d) 年 1—3 月(根据 C. S. K. Atlas[3]改画)

四个冬季冷涡最大经向宽度分别约为 6，2.5，4.5 及 5.5 个纬度。归纳起来，可以这样认为，在这四个冬季，棉兰老冷涡时而向东扩展，时而向西收缩，尺度有明显变异。1965—1966 年冬季向东扩展最甚，1969 年冬季其次。1968 年冬季向西收缩，1967 年冬季收缩最甚。

3. 冷涡变异与 El Niño 的关系

在 1965—1983 年期间，出现过多次强弱不等的 El Niño，即强型 (1972—1973)，中等型 (1965—1966 及 1976—1977)，弱型 (1969) 及甚弱型 (1975) El Niño[7]。并且有迹象表明，1979—1980 年也应视为一次弱型 El Niño[5]。当然，1982—1983 年是甚强型 El Niño。

上节所述 1965—1969 年四个冬季冷涡在水平尺度上的变异，显然与 El Niño 的出现与否及强弱有关。在非 El Niño 年 (1967, 1968)，冷涡在不同程度上向西收缩，并趋于封闭，1967 年冬季收缩最甚。在 El Niño 年 (1965—1966, 1969)，冷涡在不同程度上向东扩展。在 1965—1966 年的中等型 El Niño 期间，冬季冷涡向东扩展最远而呈带状。在 1969 年的弱型 El Niño 期间，冬季冷涡亦较非 El Niño (1968) 年为扩展。所以，从

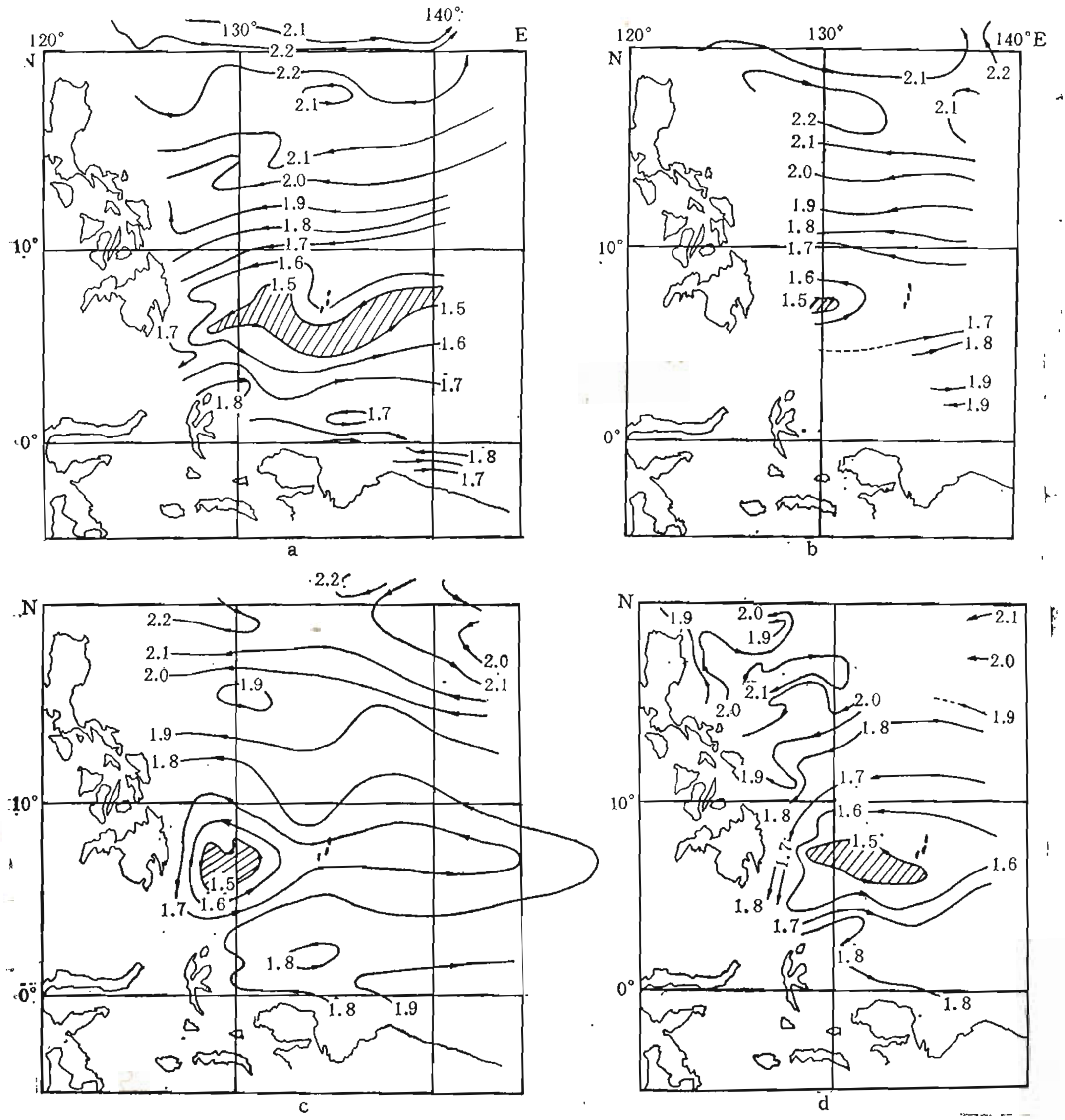

图 4　棉兰老涡旋及其附近区域海面动力高度（0/1000 db, dyn. m.）的分布[3]

Fig. 4　Sea surface dynamic height topography (referred to 1000db, dyn. m.) in the area adjacent to the Mindanao Cold Eddy[3]

a. 1965—1966 年冬季；　b. 1967 年冬季；

c. 1968 年冬季；　d. 1969 年冬季。

这四个冬季的情况来看，冷涡向东扩展或向西收缩的程度，是与这几年 El Niño 的强弱或出现与否相联系的。

检验一下这种关系在 70 年代及 80 年代早期的几次 El Niño 期间是否存在，是很有意义的。

在 1970—1974 年间，只有沿 137°E 断面的观测资料[2]可用以检验这一关系。137°E 断面位于帕劳群岛以东，有时冷涡向东扩展成带状低槽可跨越 137°E 线，如 1965—1966

年（中等型 El Niño）冬季。

137°E 断面（0—10°N）1970—1974 年冬季海面动力高度的分布（见图 5）表明，在此期间，只有两个冬季出现 1.5 及 1.6 动力米等高线。一次是在 1970 年冬季，于 7°N 附近出现 1.6 动力米线。这表明此时冷涡的边界向东扩展达到或跨越 137°E 线。这是 1969 年弱型 El Niño 残余影响的反映，与 1969 年冬季冷涡边界向东扩展的情形相一致的。另一次是在 1973 年冬季，于 5—10°N 范围内出现 1.5 及 1.6 动力米线。1.5 动力米线所围的冷涡核心位于 7—10°N 之间。这表明此时冷涡的核心及边界向东扩展达到或超过 137°E 线。这情况与 1965—1966 年冬季（中等型 El Niño）冷涡向东扩展的情况相类似。显然，这是 1972—1973 年强型 El Niño 显著影响的反映。

在 1975—1983 年期间，没有 60 年代后期那样测站密布的动力高度分布图可用以监测冷涡的变化。幸运的是，有月平均水位的系列资料[10,11]，可以检验上述关系。水位与比容水位（即动力高度）具有线性关系，而且水位包含斜压和正压两部分效应，能更全面地反映冷涡的变化。

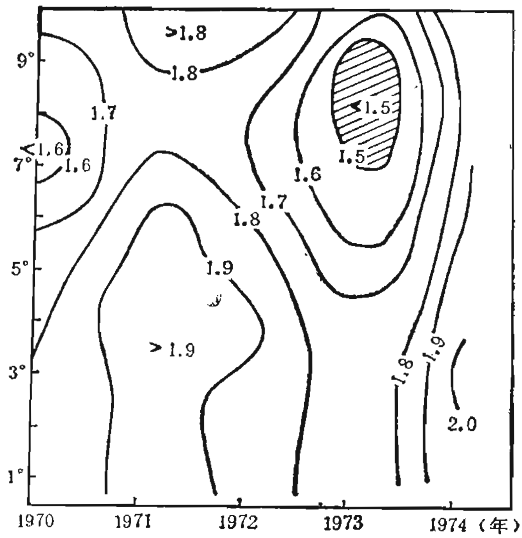

图 5　137°E 线上 1970—1974 年冬季（1 月）海面动力高度（0/1000 db, dyn. m.）的分布

Fig. 5　Sea surface dynamic height topography (0/1000db, dyn. m.) distribution at 137°E in the winters (JAN) from 1970 to 1974

本文选取位于帕劳群岛上的 Malakal（7°20′N，134°28′E）作为监测冷涡变化的参考站，它是最接近冷涡的一个海岛水位观测站，有时位于冷涡边界上。图 6 指出了 Malakal 站这 9 年（1975—1983）逐月平均水位相对于该站 1975—1981 年平均水位（MSL）的距平（cm）。

（1）1975 年 1 月至 1976 年 1 月出现一强正距平（高达 27.8cm）。紧接着，自 1976 年 3 月至 1977 年 3 月出现一显著的负距平（1976 年 3 月超过－20cm）。水位的这一涨落过程与 1976—1977 年的中等型 El Niño 有关。这表明，涡核毗邻区域的水位在 1976—1977 年 El Niño 期间下降（相对于 MSL，下同）超过 20cm。

（2）自 1977 年春至 1979 年底，Malakal 水位虽多波动，但总趋势偏高，最大正距平约 10cm。随后 1980 及 1981 年初出现一负距平（达－20cm）。水位的这一涨落过程与 1979—1980 年的弱型 El Niño 有关。虽然，此时在东太平洋未出现 El Niño，但在西太平洋却观测到通常由 El Niño 引起的许多现象[1]。这表明，在 1979—1980 年 El Niño 期间，涡核毗邻区域的水位下降约 20cm。

（3）1981 及 1982 年初 Malakal 水位出现一弱正距平。自 1982 年 4 月至 1983 年初出现一强达 20cm 的负距平。水位的这一涨落过程显然与 1982—1983 年的甚强型 El

Niño 有关。这表明，在 1982—1983 年 El Niño 期间，涡核毗邻处的水位下降约 20cm。

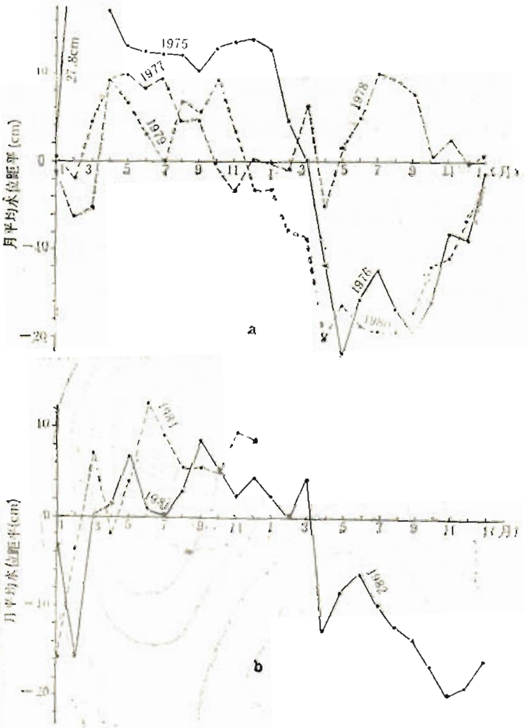

图 6 Malakal 站 1975—1983 年逐月平均水位距平 (cm)

Fig. 6 Monthly mean sea level deviations (cm) at Malakal from 1975 to 1983

a. 1975—1980; b. 1981—1983。

显而易见，冷涡低比容水位范围(即动力高度的槽区）的向东扩展与冷涡毗邻区域的水位比正常偏低，两者是互相一致的。因而，可以概括上述结果得出如下结论：即根据 60 年代后期（包括 1965—1966，1969 两次 El Niño）水文资料中得出的棉兰老冷涡的变异与 El Niño 的这种密切关系，在 70 年代及 80 年代初期的 El Niño 期间(包括 1972—1973，1976—1977，1979—1980 及 1982—1983 四次 El Niño）也存在。这就是说，在 El Niño 期间，冷涡低比容水位范围向东扩展和(或)冷涡毗邻区域的水位比正常偏低，因而冷涡变得较强。反之，在非 El Niño 年间，冷涡低比容水位的范围向西收缩和(或)冷涡毗邻区域的水位比一般偏高，因而冷涡变得较弱。然而，水位下降或低比容水位范围向东扩展的程度（也就是冷涡强化的程度）并非总与 El Niño 的强度相对应。这显然是由于 El Niño 仅是影响或控制冷涡变化的主要因素之一而已。

西太平洋赤道区域海水的低温、高盐、低比容水位特征是与中及东太平洋赤道区域的表面水高温特征即秘鲁外海的 El Niño 事件有关[6]。同时，上述关系的机制可用赤道太平洋热结构对大气扰动力（或风场变异)的响应来阐明。在一般的信风情况下(即非 El Niño 年)，水位向西上升，温跃层加深，亦即海面比容水位升高，低比容水位范围缩减。但当信风衰退时(即 El Niño 年)，海水向东倾泻，导致西太平洋(包括棉兰老岛以东及新几内亚岛以北海域)水位下降和温跃层上升[9]，亦即海面比容水位下降，低比容水位范围扩大，因西部受阻于棉兰老海岸，才向东展延。所以，本文的结论是：棉兰老冷涡的上述变化和 El Niño 之间的这种局部性的中尺度关系是与赤道太平洋海一气变异之间的总的大尺度关系相一致的。

参 考 文 献

[1] Donguy, J. R., C. Henin and G. Meyers, 1982. Appearances in the western Pacific of phenomena induced by El Niño in 1979—1980. *Trop. Ocean-Atmos. Newslett.* 10: 1—2.

[2] Japan Meteorological Agency, 1971—1975. The Results of Marine Meteorological and Oceanographic Observations. Nos. 47, 49, 51, 53, 55.

[3] Japanese Oceanographic Data Center, 1967—1977. CSK Atlas, Vol. 1—7.

[4] Koenuma, K. 1937. On the hydrography of the southwestern part of the North Pacific and the Kuroshio. Part I: General oceanographic features of the region. The Memoirs of the Imperial Marine Observatory Kobe, *Japan* 6(1): 279—332.

[5] Luther D. S., D. E. Harrison and R. A. Knox, 1983. Zonal winds in the central equatorial Pacific and El Niño. *Science* **222**: 327—330.

[6] Masuzawa, J. and K. Nagasaka, 1975. The 137°E oceanographic section. *Jour. Mar. Res.* (Supplement), **33**: 109—116.

[7] Quinn, W. H. D. O. Zopf and K. S. Short et al., 1978. Historical trends and statistics of the Southern Oscillation, El Niño, and Indonesian droughts. *Fish Bull.* **76**: 663—678.

[8] Wyrtki, K., 1961. Scientific results of marine investigation of the South China Sea and the Gulf of Thailand, 1959—1961. *Naga Report* **2**: 1—195.

[9] Wyrtki, K., 1982. The Southern Oscillation, Ocean-Atmosphere Interaction and El Niño. *Mar. Technol. Soc. J.* **16**(I): 3—10.

[10] Wyrtki, K., 1985. Monthly maps of sea level anomalies during the El Niño of 1982 and 1983. *In* Time series of ocean measurements. Vol. 2, 43—54. *I. O. C. Tech. Series.* No. 30.

[11] Wyrtki, K. and S. Nakahara, 1984. Monthly maps of sea level anomalies in the Pacific 1975—1981. Univ. Hawaii, Ref. HIG-84-3, pp. 1—8.

VARIATION OF THE MINDANAO EDDY AND ITS RELATION WITH EL NIÑO EVENT*

Guan Bingxian

(Institute of Oceanology, Academia Sinica, Qingdao)

ABSTRACT

Mindanao Cyclonic Eddy (MCE) is one of the most striking phenomena in the sea region between Mindanao and New Guinea.

Based on the hydrographic data in the southwestern part of the North Pacific Ocean in winters from 1965 to 1974 and monthly sea level data from 1975—1983 in the adjacent area, the variation of MCE and its relation with El Niño event are discussed in some detail in this paper.

Geopotential topography of the sea surface (relative to 1000db) in winters of late sixties in the area east of the Philippines and north of New Guinea shows that a trough was displayed between the westernmost parts of North Equatorial Current and North Equatorial Countercurrent in winters of 1965—1969. Judging from its horizontal extent, MCE was stronger (eastward expanding) in winter of 1965—1966, moderate in winter of 1969, weaker (westward reducing) in winter of 1968 and weakest in winter of 1967.

The above-mentioned variation of MCE is evidently consistent with the classification of El Niño events, that is, MCE became stronger in the moderate El Niño period (1965—1966), moderate in the weak El Niño period (1969), weaker or weakest in the non-El Niño period (1968, 1967).

This relation is further examined with hydrographic observations along 137°E in the period 1970—1974 and with time series of monthly sea level anomalies at Malakal for the period 1975—1983.

Results show that the relation between the variation of MCE and El Niño deduced from the hydrographic data of late sixties (including El Niño events of 1965—1966, and 1969) also holds for the periods of El Niño events in the seventies and early eighties (including El Niño of 1972—1973, 1976—1977, 1979—1980 and 1982—1983). That is to say, during the period of El Niño, the steric sea level of the core of MCE and/or the sea level in the adjacent area are lower than normal; and hence, MCE becomes more intense. On the contrary, during the period of non-El Niño, the steric sea level of the core of MCE and/or the sea level in the adjacent area are higher than normal; and hence, MCE becomes weaker. However, the degree of the sea level drop or of the steric sea level reduction (and hence, the degree of the intensification of MCE) does not always correspond to the strength of El Niño. It is due to the fact that El Niño is only one of the main factors controlling or influencing the variation of MCE.

Finally, the mechanism of this relation is briefly discussed and concluded that such a local and mesoscale relation between the variation of MCE and El Niño is consistent with the general and large scale relation between oceanographic and meteorological fluctuations in the equatorial Pacific.

* Contribution No. 1692 from the Institute of Oceanology, Academia Sinica.

第 20 卷 第 5 期　　海　洋　与　湖　沼　　Vol. 20, No. 5
1989 年 9 月　　OCEANOLOGIA ET LIMNOLOGIA SINICA　　Sept., 1989

台湾与菲律宾以东海域冬季的环流结构及其变异*

管秉贤
(中国科学院海洋研究所，青岛)

提要　本文主要根据 CSK 水文资料及图册，比较详细地探讨了台湾和菲律宾以东海域 1965～1968 年冬季的海流结构及其变异。指出副热带流涡的西端部分在 1965～1966 及 1967 年冬季其基本结构只含二脊一槽，而与吉田及城所(1967)的模式更为相似。本文还引用信风场应力资料，得出了本海域主要平均纬向海流的带状结构与海面上风应力的作用相一致的结果。这是海一气相互作用的一个好例。

台湾和菲律宾以东海域的海洋学调查研究，最近愈来愈受到人们的重视，这主要由于下列两个流系结构及其变异会对气候变异产生显著的影响所致：(1)纬向的赤道流系(特别是北赤道逆流及赤道潜流)对 El Niño 发展过程的作用和影响，西太平洋赤道区域已被公认为是引发 El Niño 的关键性区域；(2)经向的黑潮流系对热量自较低纬区向中纬区的传输作用，等等。当然，本海域流系结构本身也具有一些吸引人的新特征值得研究．其中之一是 20 年前日本学者[12,16]发现了东向副热带逆流的存在，从而引起人们不仅对副热带逆流本身机制的热烈探索，也深化了对副热带环流结构的认识。从这个意义上说，这一发现给经典的世界大洋环流理论提出了一个新课题：环流经典模式是否完善无缺?

黑潮及其邻域的合作调查（CSK，1965～1977）为研究这一海域的海流结构及其变异提供了迄今为止观测范围最大、测站最密和重复次数最多的宝贵资料。当然，要深入研究这一课题，现有资料仍然不足。

CSK 资料已为有关国家的许多海洋学者所广泛引用。但借此来系统地、大范围地探讨西北太平洋，特别是台湾和菲律宾以东海域的海况和环流的工作，还为数不多。值得提到的有，二谷颖男（Nitani)[11] 比较全面地探讨了菲律宾和吕宋海峡以东海域 1965 及 1966 年夏季的海况，重点是黑潮源地区域，及北赤道流和棉兰老海流等。增泽让太郎(Masuzawa)[5] 及其合作者[10]对 137°E 线断面的海流结构、水团、地转流量等多次作了细致的分析，还指出了 El Niño 对这一断面上温盐结构和海平面等的影响。

最近，作者[5]根据“凌风丸”在赤道区域 137°E 及 155°E 的双机测流资料，对赤道流系的纬向结构及其变异作了较系统的分析。王宗山等[1]也应用 137°E 线的海流观测资料分析了热带西太平洋海流(主要是流量)的变化。法国学者引用他们的调查资料研究了西

中国科学院海洋研究所调查研究报告第 1653 号。
* 本文得到国家自然科学基金的资助。本文摘要刊于第 19 届 IUGG 大会(1987 年 8 月，温哥华)论文摘要汇编。
收稿日期：1988 年 5 月 23 日。

太平洋赤道流系的变化[3,4]。苏联学者引用他们的调查资料分析研究了菲律宾海1980年夏季和北太平洋西部1982年夏季海水水平环流的主要特征[17,18]。本文主要根据CSK的水文资料及图集[6,7]较系统和详细地分析了台湾和菲律宾以东海域1965～1969年冬季的海流结构及其变异；并引用北太平洋信风场资料[15]探讨了本海域海流带状结构与风场的关系等。

1. 冬季流况基本特征

1965—1966年冬季是这四个冬季中测站最多的时期，故以此冬作为代表来阐明本海域冬季流况的基本特征。

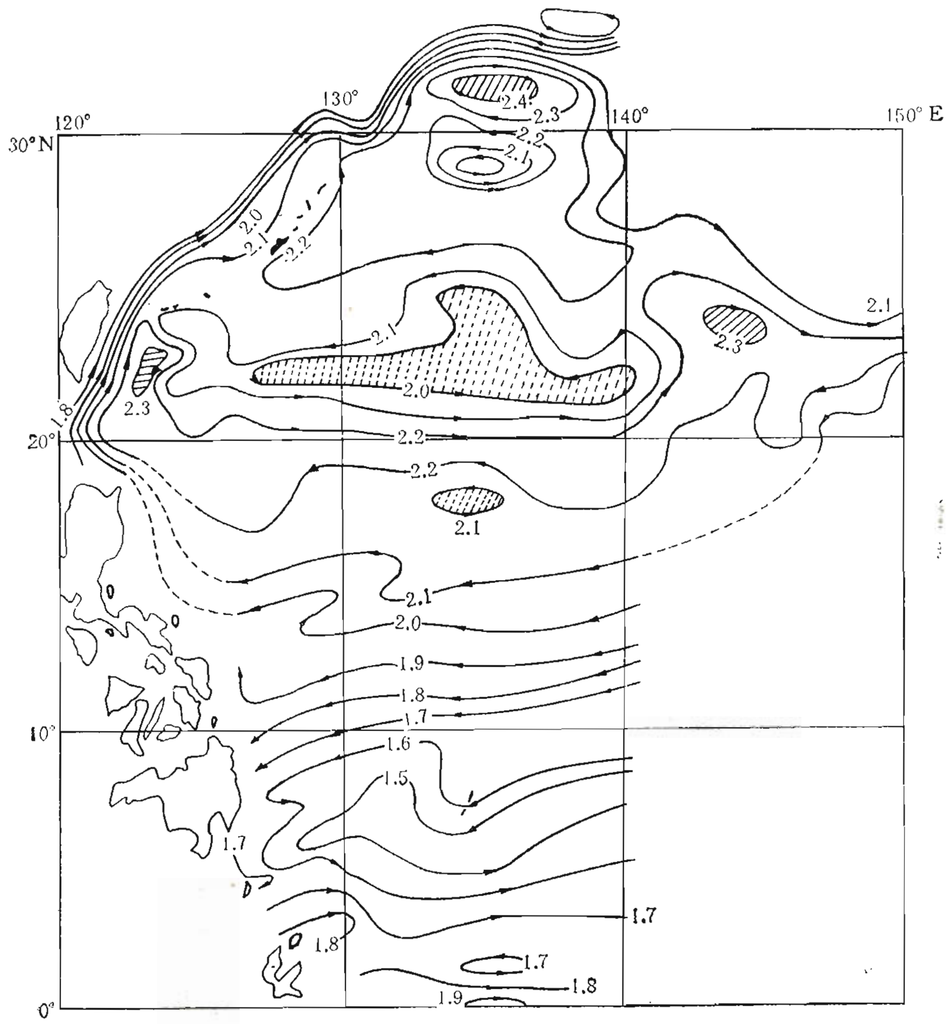

图1 1965～1966年冬季海面动力高度（0/1 000db,dyn.m）分布图
（根据CSK Atlas, Vol. 2,1968）
Fig. 1 Sea surface dynamical height topography (0/1 000db, dyn. m) in winter, 1965～1966 (From CSK Atlas, Vol. 2, 1968)

从1965～1966年冬季海面动力高度分布图（图1）上可以看出，北赤道流约在11～

12°N 处，南北分叉。1.9 动力米线由自东而西转向北，沿萨马岛（Sharma I.）东岸北上，成为北向西边界流的渊源。2.2 动力米线为西向流的北界。它位于源自台湾东岸的暖脊的南坡，是不同于北赤道流的另一支西向流，与副热带逆流组成这一暖脊[8]。但此脊强度不大，只有台湾以东的暖涡和 140°E 以东的暖涡脊高才达 2.3 动力米。在 18°N，135°E 附近出现一弱的以 2.1 动力米线封闭的槽。以南为一系列纬向西流，即北赤道流，其宽度约为 8 个纬度（15～7°N），南界达到帕劳群岛（Palau Is.）以南（2.1～1.5dyn.m）。如将 2.2 动力米线的西向流亦视为北赤道流，则其宽度增至 12 个纬度（19～7°N）。1.8 动力米线在 11°N，130°E 附近开始由向西转向西南，延伸为棉兰老海流。1.5～1.7 动力米线在棉兰老岛以东呈反时针旋转，形成向东流动的北赤道逆流的渊源。在帕劳群岛以南附近出现纬向的气旋型涡旋，有些年份，如 1968，1969 年冬季，它趋于封闭状。这就是棉兰老涡旋。

在新几内亚北岸流况比较复杂，在 130～140°E 附近，赤道偏北处为东向流，即新几内亚沿岸流；在 140～150°E 附近，赤道偏南处为西向流，即南赤道流；还出现一些顺时针或反时针旋转的涡旋（图略）。

在巴士海峡及台湾以东，以密集的 1.8～2.1 动力米线为标帜的黑潮沿台湾东岸进入东海，出吐噶喇海峡流向日本南岸。在 135°～140°E 附近黑潮离岸（只南达 32° N）作反时针弯曲，在伊豆诸岛以西、纪伊半岛以南出现气旋式涡旋，在 100m 及 200m 层上均有相应的冷水团存在，但强度不大。

2. 副热带流涡的结构

副热带流涡的西端部分（WSG）的海流结构是本海域最显著的特征之一。测站最密的 1965～1966 年冬季海面动力高度（图 1，0/1 000db）分布表明：在 140°E 以西及 15°N 以北海域，WSG 确实不象传统概念所描述的是单一流涡，而是分裂为两个或多个次级流涡。但其结构与莲沼和吉田（Hasunuma and Yoshida）[8] 所揭示的并非完全相同。两者在天气式的“细”结构上有一些差异，特别是在副热带流涡的南部。莲沼和吉田（1978）根据长期平均资料及 1974 年 2～3 月调查资料所揭示的 WSG 都含有三脊和两槽，即黑潮脊（KR）、热带脊（TR）、北赤道脊（NER）和副热带槽（STT）、热带槽（TT），并且三脊在其西端相联结。但 1965～1966 及 1967 年冬季的 WSG 的基本结构只含二脊和一槽，即黑潮脊，副热带槽和另一从台湾以东的暖涡先向南后向东延伸出来的脊。此脊在 1965～1966 年冬季位置偏北，而在 1967 年冬季位置稍偏南。按莲沼和吉田的命名，前者似以称为“热带脊”为宜，后者则可称为“北赤道脊”。为方便计，本文中均称为北赤道脊。副热带槽向西伸展很深，故黑潮脊及北赤道脊在西边界附近并不互相联结．热带脊及热带槽甚弱，或竟不明确。这两冬 WSG 的结构，与其说与莲沼和吉田的模式[8] 相似，不如说，与吉田和城所（Youshida and Kidokoro）[16] 的模式（二脊一槽）更为相似．所以，WSG 虽分裂为若干次级流涡，但其天气式“细”结构并非固定或规则，而随季节和年际而变。1965～1966 年冬季是“二脊一槽”模式发展最典型的时期。

和 1965 年夏季的情况[11]相比，1965～1966 年冬季在台湾以东出现的涡旋个数较少，强度亦较弱。在 120°～150°E 范围内，明显的涡旋只有 3 个。即自西向东，分别为暖涡—冷涡—暖涡。一个大而长的气旋型冷涡（纬向长度约 17 个经度，经向宽度约 5 个纬度）构

成副热带槽。北赤道脊(纬向长度约 30 个经度)呈一“U”字形，在西、东两端各有一峰.台湾以东暖涡冬季所出现的峰值(>2.3 动力米)较夏季(>2.5 动力米)为弱，峰的尺度亦较小。黑潮脊构成极向次级流涡。值得指出的是在黑潮脊之内却有气旋型涡出现。

冬季，副热带逆流明显地出现在副热带较低纬度区域。它由副热带槽的南坡和北赤道脊的北坡所组成。从这样看，副热带逆流的起源部分只是与黑潮邻接。但如将北赤道脊的西边界看成是黑潮东边界的一部分，则可以看到在 24°N 附近，黑潮东边界的流线开始从其主体分离出来，绕台湾以东的暖涡作反气旋式转动，然后在 124°E 附近大致沿

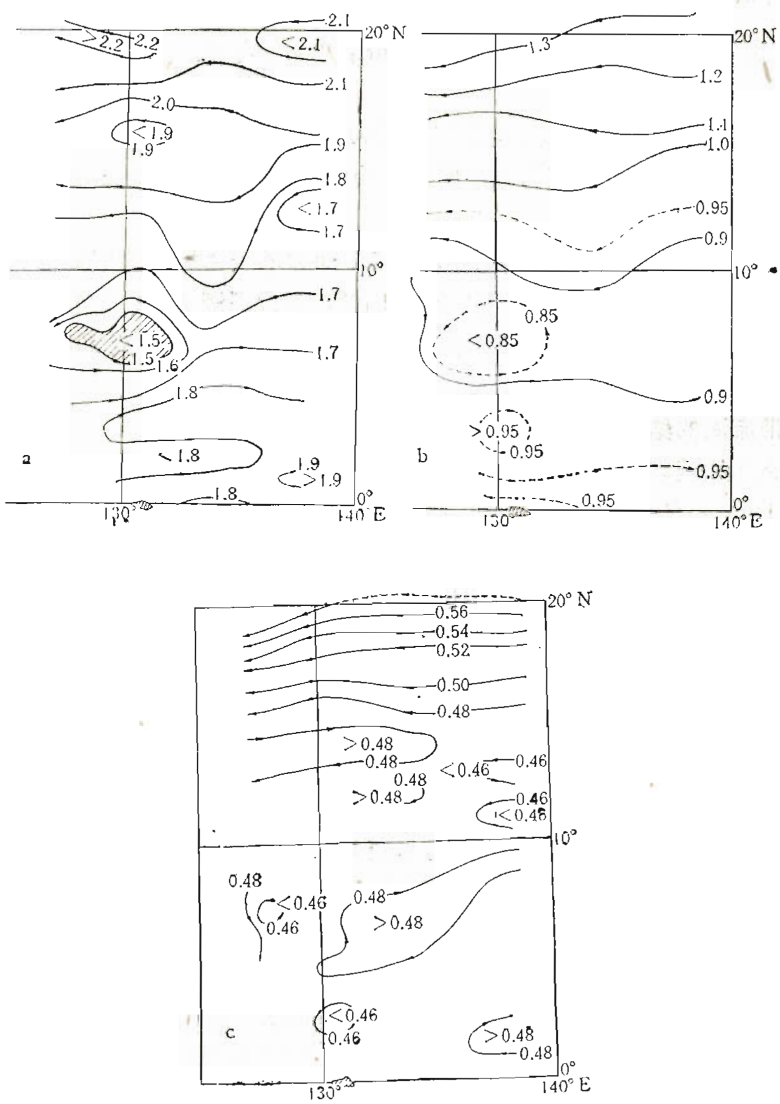

图 2　1968 年 1～3 月海面 (a)，200db(b) 及 500db(c) 面动力高度
(相对于 1 000 分巴面，动力米)分布图

Fig. 2 Dynamical height topographies (referenced to 1 000db surface, dyn. m.) at sea surface (a), 200db surface (b) and 500db(c) surface in Jan.~Mar., 1968

20°N 纬线向东延伸，并与副热带槽南坡的流线平行流动，一起形成副热带逆流。从这样看，副热带逆流部分地是从台湾以东的黑潮东边界分离出来的一个分支。其流径在冬季(1965～1966,1967)较夏季(1965)更为连续。1965～1966 年冬季副热带槽很发展，且位置偏西，故副热带逆流的较强部分出现在 140°E 以西及 20°N 以北海域。而在 1967 年冬季副热带槽的位置偏东，故副热带逆流的较强部分出现在 142°E 以东及 24°N 以北海域。

3. 棉兰老冷涡

在棉兰老岛以东及帕劳群岛以西海域，在这四期冬季都存在着一个气旋型涡旋。它位于北赤道流、棉兰老流和北赤道逆流之间(见图 1)。1965～1966 年冬季这涡向东延伸越过 140°E，形成一条纬向长度在 12 个经度以上，中心动力高度小于 1.5 动力米的带状结构。1967 年冬季，因 130°E 以西无资料，这涡在图上只呈向西开口的半椭圆形，中心 1.5 动力米高度线的范围大大缩小。1968 及 1969 年冬季这涡更趋于封闭，中心呈圆形或菱形。这涡是中心部分具有低温特征的水体，但伸展不深。研究发现，棉兰老冷涡的变化与 El Niño 密切相关。在 El Niño 年期间，冷涡低比容水位的范围向东扩展和(或)冷涡毗邻区域的水位比正常偏低，因而冷涡变得较强，范围亦较大。反之，在非 El Niño 年期间，冷涡低比容水位的范围向西收

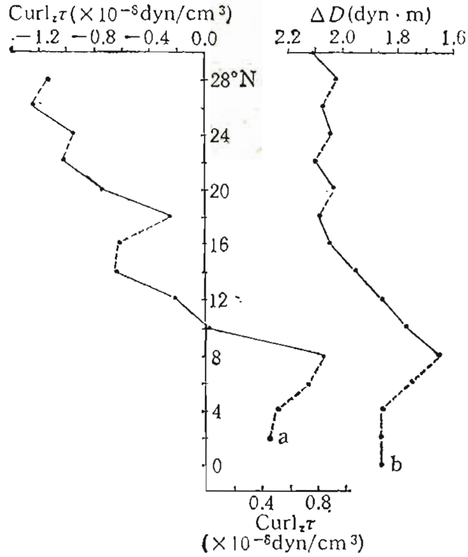

图 3　风应力涡度 (a,Curlzτ) 及海面动力高度 (b, ΔD) 的经向分布

Fig. 3 Meridional distributions of wind stress curl(a, Curlzτ) and sea surface dynamical height (b, ΔD)

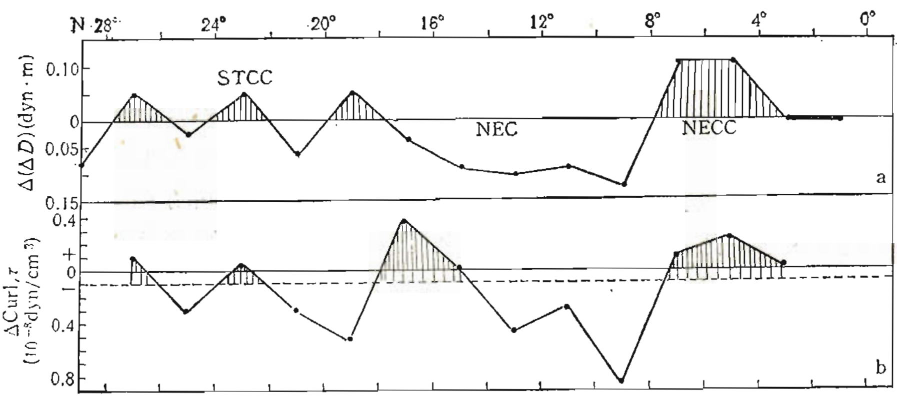

图 4　$\Delta(\Delta D)$(a) 及 ΔCurlzτ(b) 的经向分布

Fig. 4 Meridional distributions of $\Delta(\Delta D)$ (a) and ΔCurlzτ (b)

STCC　为副热带逆流；NEC　为北赤道流；NECC　为北赤道逆流。

缩和(或)冷涡毗邻区域的水位比一般偏高,因而冷涡变得较弱,范围亦较小。详情已在文献[2]中专题讨论。

4. 地转流的带状结构

本海域的主要纬向地转流,边界分明,且呈明显的带状结构。这不仅表层流如此,次表层流及深层流也是这样。这一特征显示在 1968 年冬季(1～3 月)0～20°N 海域的海面、200m 层及 500m 层的动力高度分布图(相对于 1 000 分巴面,见图 2)上。除深层的若干局部区域可能出现流向迥异或相反的微弱海流外(例如,在 500m 层上 5～10N 及 130～140°E 区域内出现很弱的反气旋型流),虽流速随深度减弱,但流场的带状结构保持基本不变。同时,北太平洋西部海流的带状结构具有准稳定性[13]。

判明这种带状结构是否与其上空的风场作用相一致,是很有意义的。

在吉田和城所[16]早年试图用 Sverdrup (1947) 理论来解释东向的副热带逆流的成因时,由于当时风应力涡度资料的分辨度太粗(经向为 5 个纬度),未能很好地来阐明宽度只有 1～2 个纬度的带状结构。为了进一步探索东向流带状结构的原因,一定要构作分辨度更高的长期平均的风应力涡度场。

Wyrtki 及 Meyers[15] 的太平洋信风场资料(经向分辨度为 2 个纬度)及日本凌风丸调查船(R/V Ryofu Maru)自 1967 年开始的 137°E 断面定期观测水文资料[6]为检验这种带状结构与风应力场的关系提供了良好的条件。

137°E 断面的水文测站间距,除靠近日本南岸及新几内亚岛北岸的为半个纬度外,其余在 2～30°N 范围内均为 1 个纬度。Wyrtki 及 Meyers[15] 的太平洋风应力场资料的经向间距为 2 个纬度。为了便于两者相互比较,本文选取了自 0～30°N 每隔 2 个纬度的测站计算了海面动力高度(ΔD, 0/1 000db, dyn. m.)及风应力涡度($\mathrm{Curl}_z\boldsymbol{\tau}$, $10^{-8}\mathrm{dyn/cm^3}$),如图 3 所示。在此基础上又计算了动力高度和风应力涡度的经向梯度 [$\Delta(\Delta D)$, $\Delta\mathrm{Curl}_z\boldsymbol{\tau}$] 如图 4 所示。$\Delta D$ 是沿 137°E 断面上六个冬季(1967～1972 年 1～2 月)观测的平均值。$\Delta(\Delta D)$ 由低纬测站的 ΔD 中减去高纬测站的 ΔD 而得,正值表示东向流,负值表示西向流。$\mathrm{Curl}_z\boldsymbol{\tau}$ 是沿纬圈七个冬季(1966～1972 年 1～2 月)的平均值. $\Delta\mathrm{Curl}_z\boldsymbol{\tau}$ 由高纬平均值中减去低纬平均值而得。由于前期的风可能也有影响,所以风应力涡度资料自 1966 年取起。又由于风应力资料限于 1950～1972 年期间,故动力高度资料相应地只取到 1972 年。图 3 两条曲线比较表明,风应力涡度和海面动力高度两者的经向分布几乎相互平行。即当风应力涡度向北增加时,相应地,动力高度向北减少。这是东向流的情况。反之,则是西向流的情况。由图 4 可知,两相邻测站动力高度差值与风应力涡度差值的关系也十分密切。自赤道向北相继出现:(1)东向的北赤道逆流(3～8°N),与 $\mathrm{Curl}_z\boldsymbol{\tau}$ 的正梯度带(3～7.5°N)相对应;(2)西向的赤道流(8～18°N),与 $\mathrm{Curl}_z\boldsymbol{\tau}$ 的负梯度带(7.5～15°N)相对应;(3)三支宽度为两个纬度的东向流(中心分别位于 19°N, 23°N 及 27°N 附近),与 $\mathrm{Curl}_z\boldsymbol{\tau}$ 的三个正梯度带(中心分别位于 17°N, 23°N 及 27° N)相对应。这三支东向流组成副热带逆流。在两支相邻东向流之间,有一西向流区,它与 $\mathrm{Curl}_z\boldsymbol{\tau}$ 的负梯度带相对应。除了 19°N 附近的东向流与以 17°N 为中心的风应力涡度正梯度带位置略有偏移外,两者的关系确实十分紧密。

东向副热带逆流的带状结构是北太平洋西部环流结构中最引人注目的现象之一。莲

沼和吉田[8]根据长期平均资料得出的海面动力高度图指出，在130～160°E 区域内，副热带逆流是由三个东向流组成，其中心分别位于 19°N，23°N 及 27°N 附近。White 及 Walker[14] 最近利用分辨度更好的(0.5° 纬距)资料分析结果表明，副热带逆流至少由三个半永久性的东向地转流所组成，其中心分别位于 20°N，24°N 及 26°N 附近。本文所得出的 1967～1972 年 137°E 断面上的副热带逆流的分布是与上述两项结果颇为一致的。

更值得指出的是，本文所得上述结果也为判明迄今仍在争论中的副热带逆流的成因问题，提供了有力的佐证。东向副热带逆流的存在及其带状结构(分辨度为两个纬度)与风应力涡度的经向梯度(分辨度为两个纬度)颇为一致，这一事实明确地表明，反气旋涡度沿经向分布上的“槽”结构是副热带逆流的一个重要驱动力，至少也是重要动力之一。

本文所得出的台湾及菲律宾以东海域冬季的海流结构充分表明，本海域主要平均纬向海流的带状结构是与海面上风应力场的作用相一致的。这项定性结果是海-气相互作用的一个好例。

参　考　文　献

[1] 王宗山、邹娥梅，1987。热带西太平洋海流的变化。黄渤海海洋 **5**(4)：15—20。

[2] 管秉贤，1989。棉兰老冷涡的变异及其与 El Niño 的关系。海洋与湖沼 **20**(2)：131—138。

[3] Donguy, J. R. and C. Henin, 1983. Fluctuations of the equatorial current system connected with the hydroclimatic conditions in the western Pacific. *Océanogr. trop.* **18**(1): 17—24.

[4] Donguy, J. R., G. Eldin and A. Morlière et al., 1984. A thermal interpretation of a change in equatorial western Pacific circulation. *Trop. Ocean-Atmos. Newslett.* **24**: 9—11.

[5] Guan Bingxian, 1986. Current structure and its variation in the equatorial area of the western North Pacific Ocean. *Chin J. Oceanol. Limnol.* **4**(3): 239—255.

[6] Japan Meteorological Agency, 1968—1973. The Results of Marine Meteorological and Oceanographic Observations. No. **41—51.**

[7] Japanese Oceanographic Data Center, 1967—1977. CSK Atlas. Vol. 1—7.

[8] Hasunuma, K. and K. Yoshida, 1978. Splitting of the Subtropical Gyre in the western North Pacific. *Jour. Oceanogr. Soc. Japan.* **34**(4): 160—172.

[9] Masuzawa, J., 1967. An oceanographic section from Japan to New Guinea at 137°E in January 1967. *Oceanogr. Mag.* **19**: 95—118.

[10] Masuzawa, J. and K. Nagasaka, 1975. The 137°E oceanographic section. *Jour. Mar. Res.*, Supp. **33**: 109—116.

[11] Nitani, H., 1970. Oceanographic conditions in the sea east of the Philippines and Luzon Strait in summers of 1965 and 1966. *In* The Kuroshio-A Symposium on the Japan Current, Edited by John C. Marr. East-West Center Press. Honolulu, pp. 213—232.

[12] Uda, M. and K. Hasunuma, 1969. The eastward Subtropical Countercurrent in the western North Pacific Ocean. *Jour. Oceanogr. Soc. Japan* **25**(4): 201—210.

[13] White, W. B. and K. Hasunuma, 1982. Quasi-stationary banded structure in the mean zonal geostrophic current regimes of the western North Pacific. *Jour. Mar. Res.* **40**(4): 1035—1046.

[14] White, W. B. and A. E. Walker, 1985. The influence of the Hawaiian Archipelago upon the wind-driven Subtropical Gyre in the western North Pacific. *J. Geophys. Res.* **90**(C4): 7061—7074.

[15] Wyrtki, K. and G. Meyers, 1975. The trade wind field over the Pacific Ocean, Part II, Bimonthly fields of wind stress: 1950—1972. Rep. HIG-75-2. Hawaii Inst. Geophys. University of Hawaii, 16pp.

[16] Yoshida, K. and T. Kidokoro, 1967. A Subtropical Countercurrent (II)-A prediction of eastward flows at lower subtropical latitudes. *Jour. Oceanogr. Soc. Japan* **23**(5): 231—246.

[17] Ластовецкий, Е. И. и А. Д. Нелезин, 1984. Осовенности горизонтальной циркуяции вод север-западной части Тихого Осеана летом 1982г. Результаты Экпедиций КЗТИ-82, стр. 233～248.

[18] Яричин, В. Г. и Е. И. Ластовецкий, 1981. Основые черты горизонталыной циркуяции вод

в Филиппинском море летом 1980г. Результаты Экпедиции КИСЗ-80, Часть 1～2, стр. 65～76.

CURRENT STRUCTURE AND ITS VARIABILITY IN THE AREA EAST OF TAIWAN AND PHILIPPINES IN WINTER

Guan Bingxian

(Institute of Oceanology, Academia Sinica, Qingdao)

ABSTRACT

In this paper, based on CSK hydrographic data and atlas (JODC, 1967～1977) the current structure and its variations in the area east of Taiwan and Philippines in winters of 1965～1969 are systematically analyzed in some detail.

In the area west of 140°E and north of 15°N the Western Subtropical Gyre (WSG) in indeed not a single one as traditionally described, it splits into two or more subgyres. But its structure is not totally alike as that shown by Hasunuma and Yoshida (1978). The Subtropical Gyre shown by them reveals three major ridges and two troughs, and the three ridges come in contact at their western end. But the basic structure of WSG in winters of 1965～1966 and 1967 reveals only two major ridges and one trough, and the two ridges are not joined together near the western boundary. Therefore, though WSG splits into subgyres, its synoptic "fine" structure is not fixed or regular, but changes seasonally and yearly. The winter of 1965～1966 is the period during which the model of two ridges and one trough well developed.

The Subtropical Countercurrent (STCC) is evidently displayed at lower subtropical latitudes in winter. Its path is more continuous in winters (1965～1966, 1967) than in summer (1965). It is evident from the pattern of stream-lines that STTC seems to be a branch separated from eastern boundary of the Kuroshio east of Taiwan.

In the area east of Mindanao Island and west of Palau Islands, a cyclonic eddy existed among the North Equatorial Current (NEC), Mindanao Current and North Equatorial Countercurrent (NECC) throughout the period. The variation of the Mindanao Cyclonic Eddy is closely related with the El Niño event, which has been discussed in a separate paper.

The major zonal geostrophic currents of this area are well defined in their boundaries and display a pronounced banded structure of quasi-stationary nature. The relation of the current banded structure with the overlying wind fields is analyzed by using the trade wind stress data (Wyrtki and Meyers, 1975). Results show that, qualitatively speaking, banded structure of the major mean zonal currents along 137°E from Equator to 28°N (including NECC, NEC and STCC) is closely related to the meridional distribution of the zonally averaged wind stress curl. This is a good example of air-sea connection.

A NOTE ON THE DEEP CIRCULATION IN THE AREA EAST OF TAIWAN AND THE PHILIPPINES*

Guan Bingxian (管秉贤)
(*Institute of Oceanology, Academia Sinica, Qingdao*)
Received Feb. 23, 1989

Abstract

The deep water (1000 – 3000 m) circulation in the area east of Taiwan and the Philippines has been little studied. Moriyasu (1972) and Reid (1981) discussed the 3000 db surface (3000/1200 db) and 2000 db surface (2000/3500 db) circulations of the Philippine Sea Basin, respectively. They both showed that there may be a northward current close to the western margin of the Sea Basin. Recent analyses of two sets of deep sea hydrographic data yielded quite different results, i. e., at deep waters in the area east of Taiwan and the Philippines southward countercurrents flow under the upper northward currents.

The possible causative mechanism of these southward deep countercurrents is the blocking effects of the submarine ridge east of Suao and of the Ryukyu Islands Shelf on the northward flowing upper currents.

The above-mentioned preliminary deductions were wholely based on consideration of the relative geostrophic current and calculation, though the reference surface (3500 db) was very deep. It is suggested that direct measurements of the deep currents in the study area are needed to verify these results.

In this short report, the mid-depth circulation or current pattern in the area east of Taiwan and the Philippines is briefly discussed. According to the working definition suggested by Reid (1981), mid-depth waters are those found between about 1 and 3 km in middle and low latitudes. But the mid-depth waters are called deep waters for short in this paper.

Moriyasu (1972), in the study of "deep waters in the western North Pacific", discussed the 3000 db surface circulation of the Philippine Sea Basin and showed that there might be a northward current close to the western margin which might have been regarded by us as western boundary current as in the Stommel and Arons (1960) model (Fig. 1).

Reid (1981), in the study of "the mid-depth circulation of the world ocean", discussed the 2000 db surface circulation of the Philippine Sea Basin and presented the steric height topography at 2000 db relative to 3500 db as shown in Fig. 2. Evidently, the 0.7 dyn. m. contour also exhibits a northward current close to the western boundary.

Recent analyses of two sets of data from deep sea hydrographic observations yielded quite different results.

The station chart of the first set of data is shown in Fig. 3. There were 14

* Contribution No. 1750 from the Institute of Oceanology, Academia Sinica. This paper was presented at the PRC/USA Symposium on Western Pacific Air-Sea Interaction (Nov., 1988, Beijing). This project was supported by the National Natural Science Foundation of China.

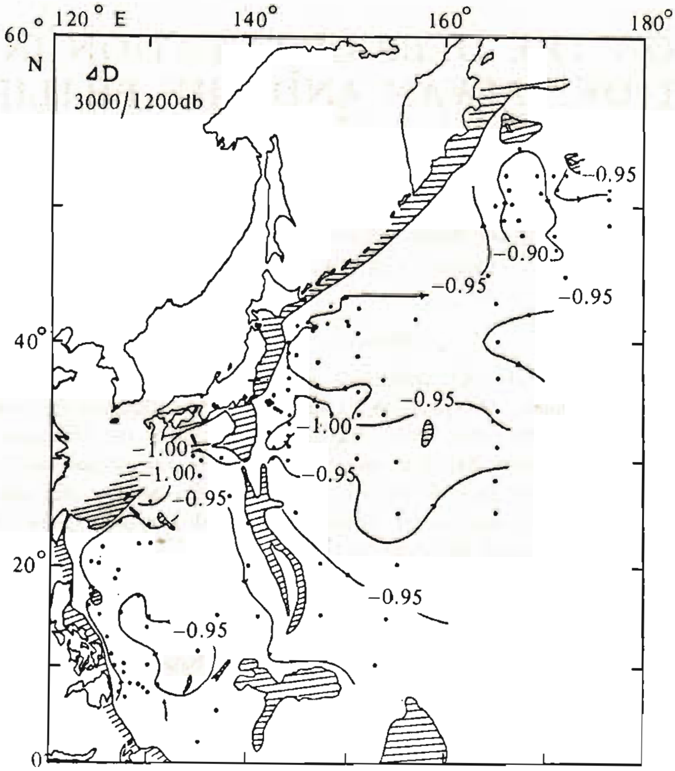

Fig. 1 Geopotential topographic chart (referred to 1200 db) of the 3000 db surface (After Moriyasu, 1972, in dyn. m)

Fig. 2 Steric height topography (2000 / 3500 db) (After Reid, 1981, in dyn. m.)

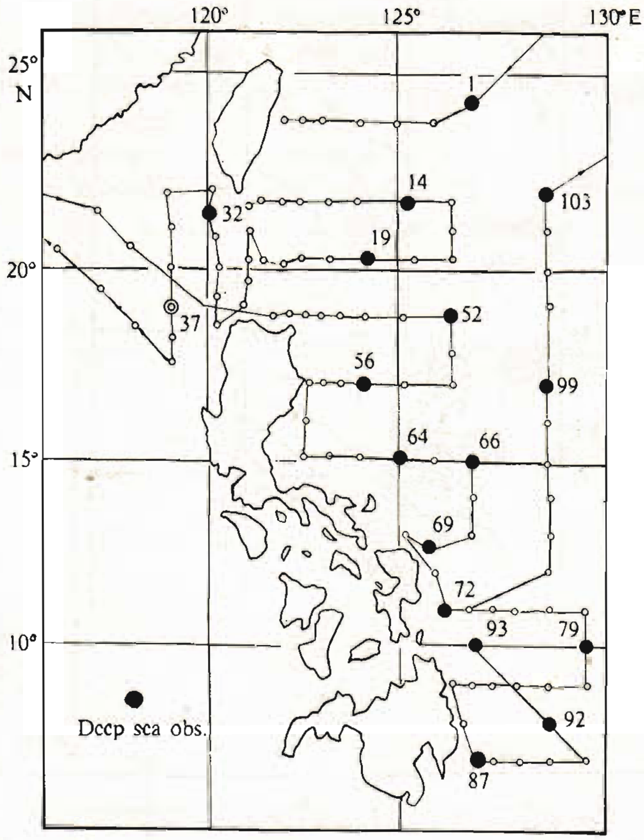

Fig. 3 Station map of the *R/V Takuyo Maru* (July 1 – Sept. 13, 1966)

deep water stations between 124 °E and 130 °E from which observations were taken in July-September, 1966, by the *R/V Takuyo Maru*. The deepest observed levels of these stations all reached 3500 m or more. The dynamic height topographies of the sea surface and the 1500 db and 2000 db surfaces (referenced to 3500 db surface) are shown in Fig. 4a – c.

The reasons for selection of the 3500 db surface as the reference level are as follows. First of all, just as shown by Reid (1981), the shear field is weak over the area in this depth range and it seems useful to consider it a thick layer. Second, it is the deepest common level of the observations of these 14 stations. Third, we hope to compare the results with those of Reid (1981), who also selected the 3500 db surface as the surface level of no motion.

What a contrast between the flow pattern of the sea surface and that at the 1500 db and 2000 db levels! The most striking difference between them is that on the sea surface topography, there is a strong anticyclonic and mainly northeastward flow in the area north of 13 °N and a southwestward flow to the south (Fig. 4a), while on the 1500 db and 2000 db level topographies, there is a cyclonic and mainly southward flow in the area north of 13 °N and an eastward flow to the south (Fig. 4b, c).

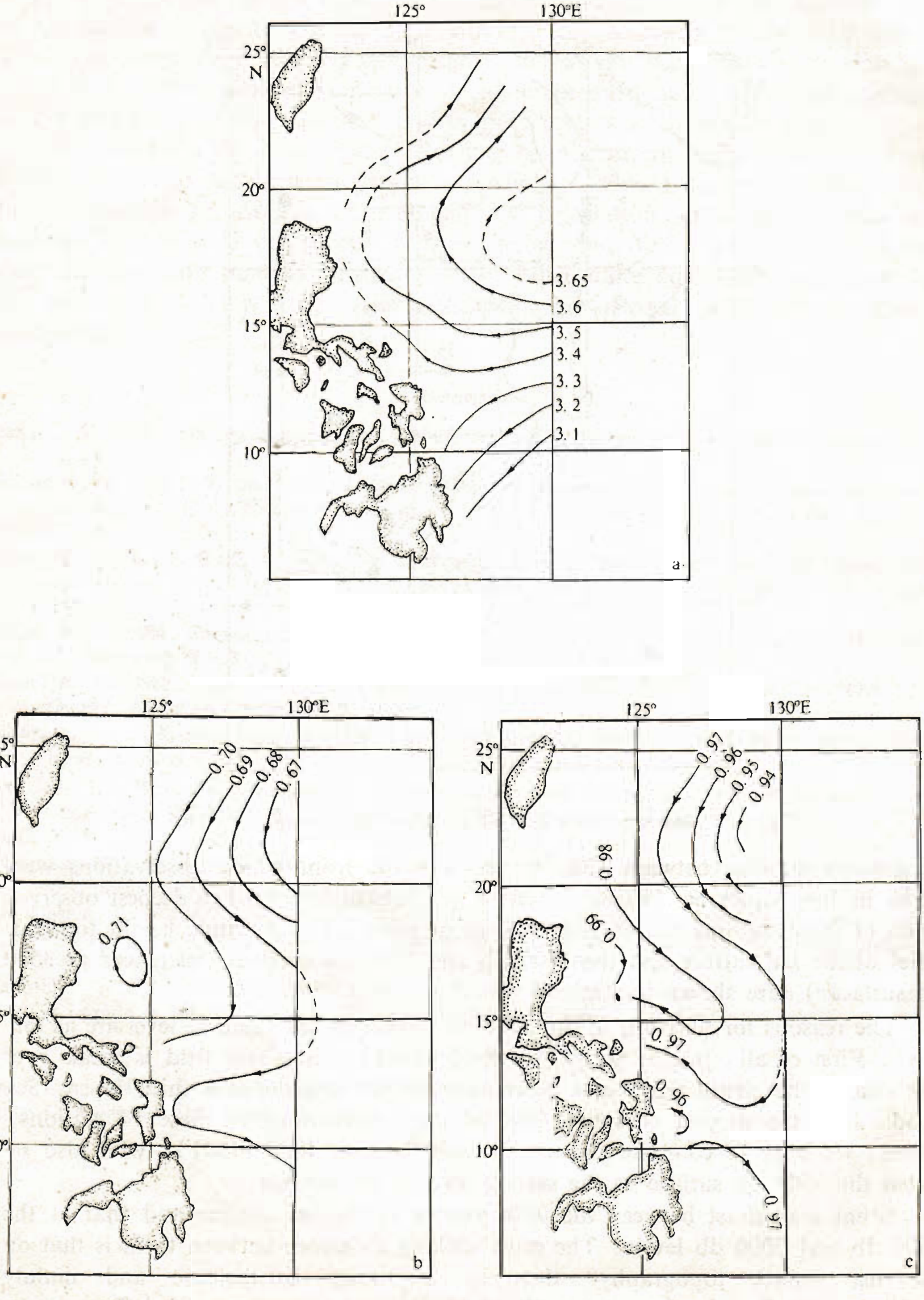

Fig. 4 Geopotential topographies (referred to 3500 db) of the sea surface (a), 2000 db surface (b), and 1500 db surface (c), in dyn·m.

In order to compare the results with those of Reid (1981), we will discuss the flow pattern of the 2000 db surface in some detail. It is evident from Fig. 4b that the steric height topography of the 2000 db surface slopes up westward, that is, on the east side, the dynamic height relative to 3500 db is less than 0.7 dyn. m., while, on the west side, it is equal to or more than 0.7 dyn. m. Therefore, there exists a southward deep flow, though it is very weak. The 0.7 dyn. m. contour indicates a southward current in the area east of Taiwan and the Philippines. It is the same as in Reid's map of the area east of 125 °E. But, as concerns the area close to the western boundary (west of 125 °E), the 0.7 dyn. m. contour on Reid's map indicates a northward flow.

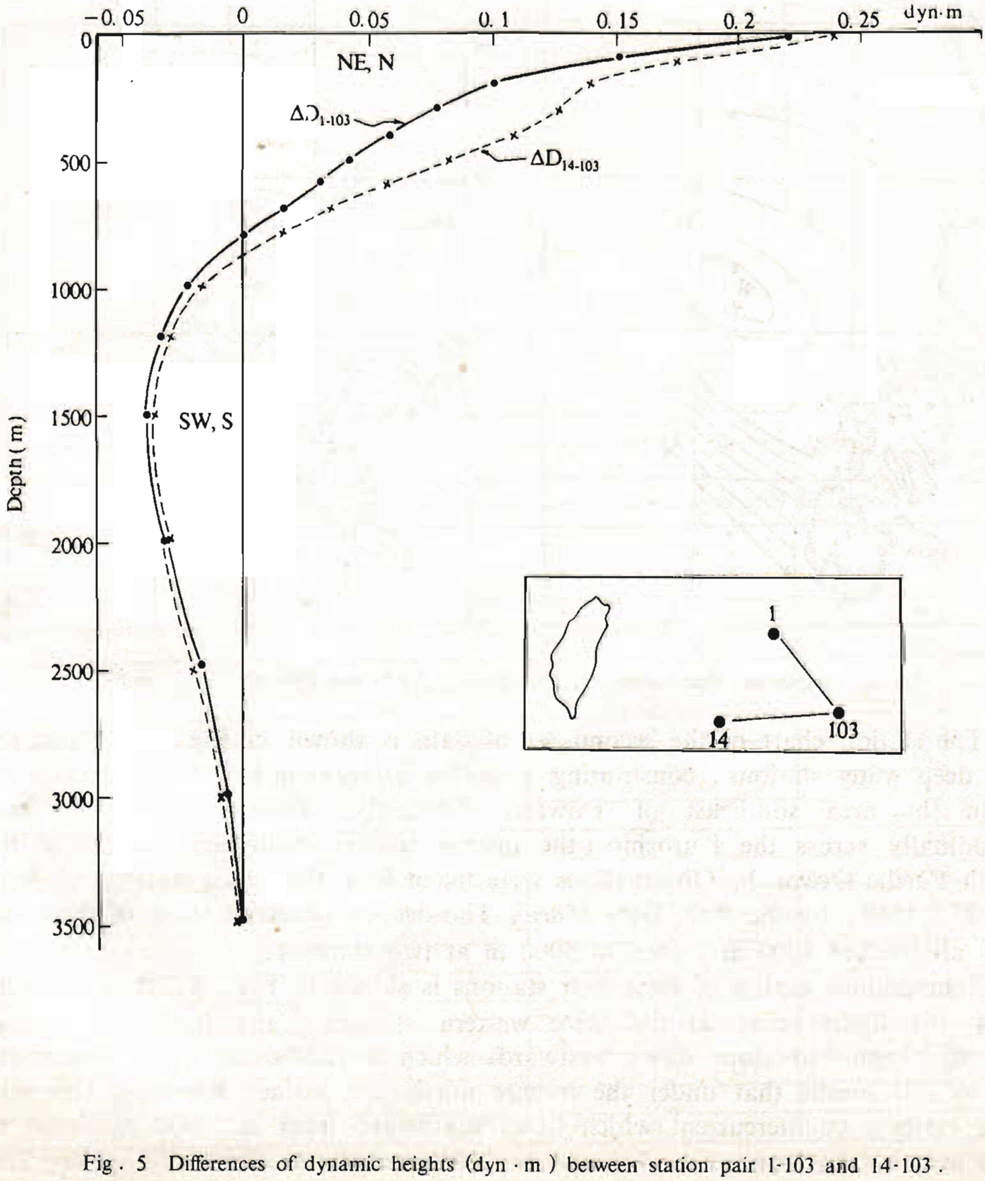

Fig. 5 Differences of dynamic heights (dyn · m) between station pair 1-103 and 14-103.

The vertical profiles of geostrophic velocities between Station pair 1–103 and 14-103 show that the boundary between the upper northward flow and the deep southward flow is located at the ca. 800–900 m depth. The thickness of the counter flow is about 1500 or more meters (Fig. 5).

The striking difference between the flow pattern at the sea surface and that at the deep level is consistent with the mass fields corresponding to the upper and deep level waters. Temperature distributions at 200 m and 2500 m are shown in Fig. 6. Evidently, the cyclonic southward flow in the northern part of the 2000 db surface is closely related to a large patch of cold water mass below that surface (2500 m depth).

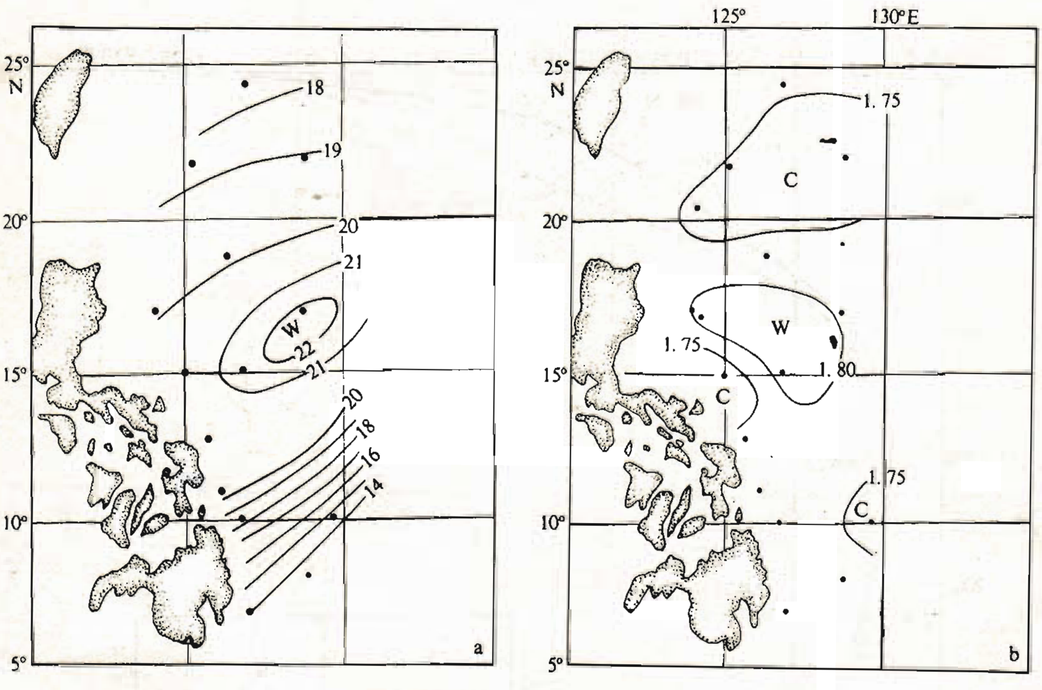

Fig. 6 Temperature distributions (℃) at 200 m (a) and 2500 m (b) depths

The station chart of the second set of data is shown in Fig. 7. There are four deep water stations, constituting a section approximately along 21°30′–22° N in the area southeast of Taiwan. Evidently, this section partly cuts latitudinally across the Kuroshio (the intense western boundary current of the North Pacific Ocean). Observations were taken from these four stations on May 24–27, 1969, by the *R/V Seifu Maru*. The deepest observed levels of these stations all reached 4000 m, even to 5000 m at two stations.

Temperature section of these four stations is shown in Fig. 8. It is evident from the figures that at the three western stations, the isotherms below 700 m begin to slope down westward, which is quite contrary to those above 700 m. It means that under the intense northward surface Kuroshio Current, there exists a countercurrent which flows southward from ca. 600 m down to 2000 m (between Stations 4–3) and to 3500 m (between Stations 3–2). The

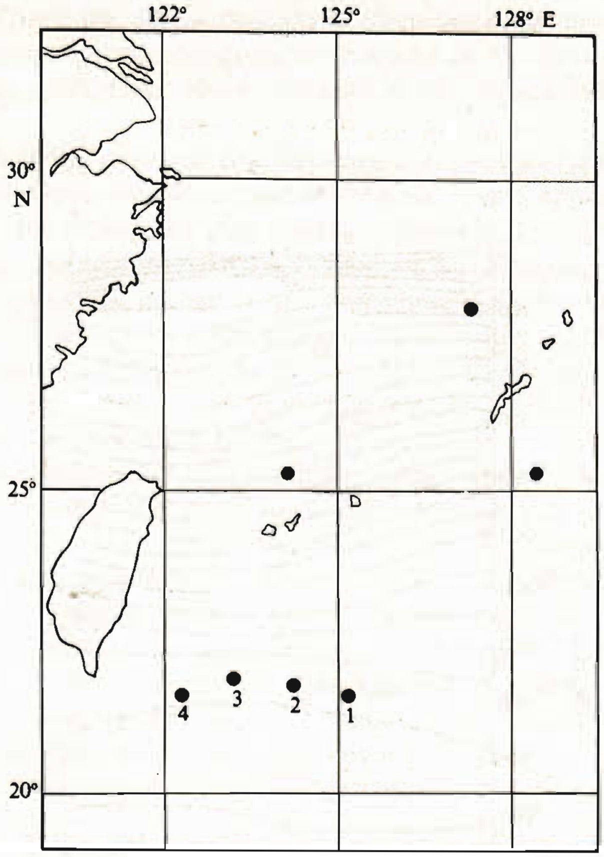

Fig. 7 Station map of the *R/V Seifu Maru* (May 7—June 14, 1969)

Table 1 Geostrophic current velocity (cm/s) (Relative to 3500 db surface)

Depth (m) \ St. pair	No. 4-3	No. 3-2	No. 2-1
0	15.5	24.0	−22.5
50	16.3	23.9	−22.8
100	17.5	22.1	−23.2
150	16.6	18.3	−21.2
200	15.7	13.9	−18.8
250	14.9	10.2	−16.5
300	13.4	7.9	−15.0
400	8.6	3.6	−11.4
500	3.1	1.0	− 7.6
600	−0.9	−1.2	− 3.4
700	−2.4	−1.7	− 2.3
800	−2.6	−2.0	− 1.5
1000	−2.4	−3.4	0.8
1200	−3.9	−3.4	1.5
1500	−4.5	−2.7	0.8
2000	−1.8	−2.4	− 0.8
2500	−0.5	−1.5	− 0.9
3000	−0.3	−0.5	− 0.4
3500	0	0	0

(Positive northward, negative southward)

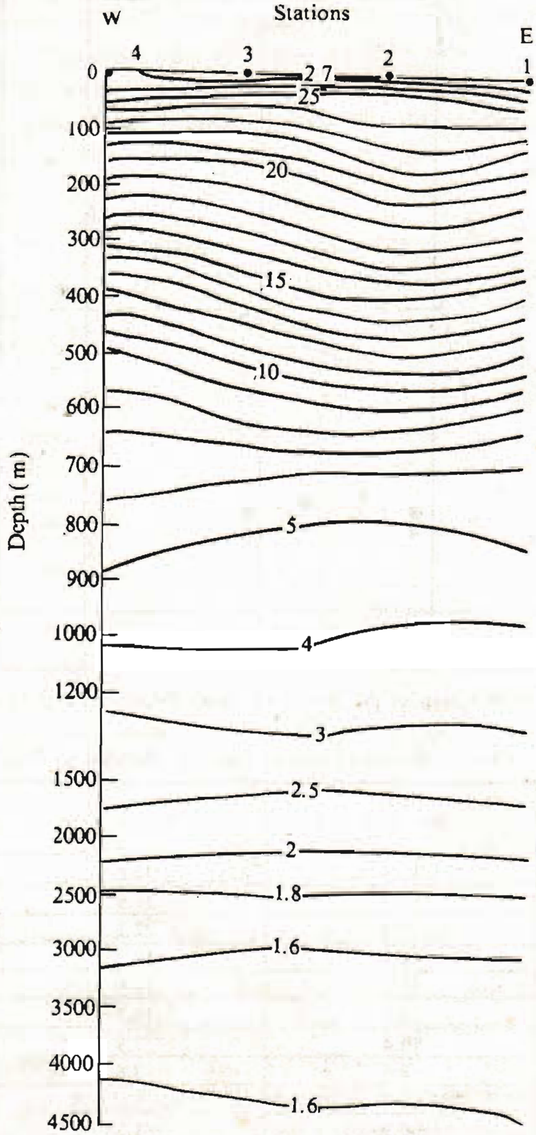

Fig. 8 Temperature (℃) section southeast of Taiwan.

southward current between Stations 2 – 1 penetrates deeply too.

To quantify the velocity structure of the Kuroshio Current, the geostrophic current velocities (cm/s) between station pairs of this section were calculated (referenced to 3500 db surface) and are shown in Table 1. The maximum countercurrent velocity below 600 m may reach 4.5 cm/s. The thickness of the countercurrent under the Kuroshio is very large, about 2500 – 3000 m.

The results from the above two sets of deep sea observation data are in agreement and show that at mid-depth or deep waters in the area east of Taiwan and the Philippines, southward countercurrents of the above surface northward currents exist.

Concerning the existence of countercurrents in the coastal area east of Taiwan, Fan (1979) and Guan (1984) held that, owing to the opposite directions of the inclinations of the isotherms below and above 200 m (Fan) or 600–700 m (Guan), there might be a reversal of the current direction under the northward flowing surface boundary current in the immediate vicinity of the Taiwan coast.

The possible mechanism of the appearance of southward flowing current under the northward flowing surface Kuroshio Current and its neighbouring currents may be the blocking effect of the submarine ridge east of Suao and that of the Ryuku Islands Shelf on the northward flowing surface and upper currents.

The submarine ridge east of Suao runs nearly perpendicular to the extension direction of the east coast of Taiwan. Its depth decreases abruptly from 1000–2000 m at the northern and southern sides to ca. 500 m; the shallowest part at its western end is less than 200 m (Guan, 1978). Therefore, although the upper (500 m thick) water column of the Kuroshio can flow over the ridge towards the East China Sea, a considerable part of the deep Kuroshio water cannot pass over the ridge owing to the blocking effect of the submarine ridge, so when it collides with the submarine ridge, it sinks down and rebounds backward to form a southward deep recirculation as shown in Fig. 9.

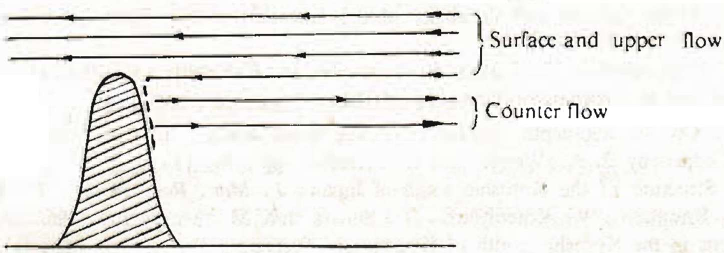

Fig. 9 Schematic diagram of the flow pattern

The above mechanism can also be used to elucidate the blocking effect of the Ryukyu Islands Shelf which stands as a barrier or wall to the northward flowing surface currents in the area east of the Kuroshio.

Of course, the possible occurrence of a deep eastward or northeastward current along the barrier or wall is not excluded, but such observational data are not available as yet.

Deep countercurrents under the strong surface Kuroshio Current were observed in the area south of Japan by Worthington and Kawai (1972), Taft (1978), and Fukasawa and Teramoto (1986), and in the area south of Kyushu by Takematsu et al. (1986). Therefore, it is reasonable to deduce that a countercurrent under the surface Kuroshio Current may also exist in the area east of Taiwan.

But, deep-bottom current measurements in the area of the Okinawa Trough (depth = 1060 m) in the East China Sea in June- October, 1984 (Yamashiro and Ichikawa, 1985) showed that even at great depth and near the bottom layer (1000 m), the current direction was still northeastward, or the same as that of the surface Kuroshio Current. As concerns the Kuroshio in the East China Sea, a countercurrent in the deep-bottom layer has not been observed to date.

It is a baffling problem for us to elucidate the different causative mechanisms of the occurrence of these currents and countercurrents in the above areas.

The existence of a southward flowing countercurrent under the northward flowing Kuroshio and adjacent currents is wholely deduced from the consideration of the relative geostrophic current and by calculation, though the reference surface (3500 m) is very deep. It is suggested that direct measurements of the deep currents with moored currentmeters or other more advanced instruments in the area east of Taiwan and the Philippines are needed to clearify the above phenomena.

References

Fan, K. L., 1979. On upwelling along the southeastern coast of Taiwan. *Acta Oceanogr. Taiwanica*, **10**: 151-159.

Fukasawa, M. and T. Teramoto, 1986. Characteristics of deep currents off Cape Shiono-misaki before and after formation of the large meander of the Kuroshio in 1981. *J. Oceanogr. Soc. Japan*, **42** (1): 53-68.

Guan, B. X. (Kwan, P. H.), 1978. The topographic effects of Taiwan Island, China and adjacent bottom relief on the path of the Kuroshio. *Studia Marina Sinica*, **14**: 1-21 (in Chinese, with English abstract).

Guan, B. X., 1984. Current path in a deep layer of the Kuroshio east of Taiwan — a case study of the observation result of February to March, 1940. *La mer*, **22** (3-4): 156-162.

Guan, B. X., 1988. Major features and variability of the Kuroshio in the East China Sea. *Chin. J. Oceanol. Limnol*. **6** (1): 35-48.

Moriyasu, S., 1972. Deep waters in the western North Pacific. In: Kuroshio — Its Physical Aspects (Edited by H. Stommel and K. Yoshida), University of Tokyo Press, pp. 387-408.

Reid, J. L., 1981. On the mid-depth circulation of the world ocean. In: Evolution of the Physical Oceanography (Edited by B. A. Warren and C. Wunsch), pp. 70-111.

Taft, B. A., 1978. Structure of the Kuroshio south of Japan. *J. Mar. Res*. **36** (1): 77-117.

Takematsu, M., K. Kawatate, W. Koterayama, T. Suhara and M. Mitsuyasu, 1986. Moored instrument observations in the Kuroshio south of Kyushu. *j. Oceanogr. Soc. Japan*, **42**, (3): 201-211.

Worthington, L. V. and H. Kawai, 1972. Comparison between deep sections across the Kuroshio and the Florida Current and Gulf Stream. In: Kuroshio-Its Physical Aspects (Edited by H. Stommel and K. Yoshida), University of Tokyo Press, pp. 371-385.

Yamashiro, T. and N. Ichikawa, 1985. Currents in the deep layer of the Okinawa Through. In: Abstracts of Lectures in Spring Assembly of Oceanographic Society of Japan, pp. 109 (in Japanese).

Data Source

Japan Oceanographic Data Center, 1967. Preliminary Data Report of CSK, pp. 1-59.

Japan Oceanographic Data Center, 1971. Data Report of CSK, pp. 1-6.

Fig9

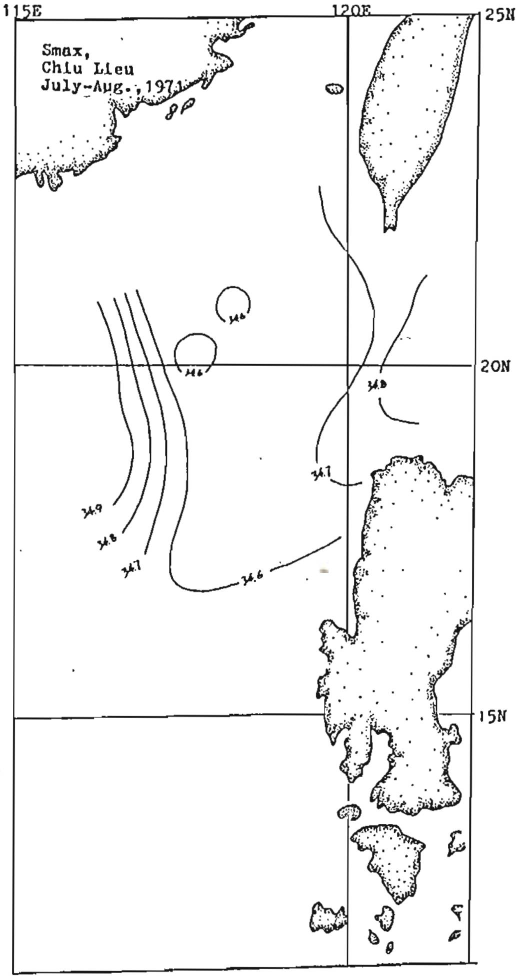

图 9. 盐度极大值 (Smax,‰) 分布

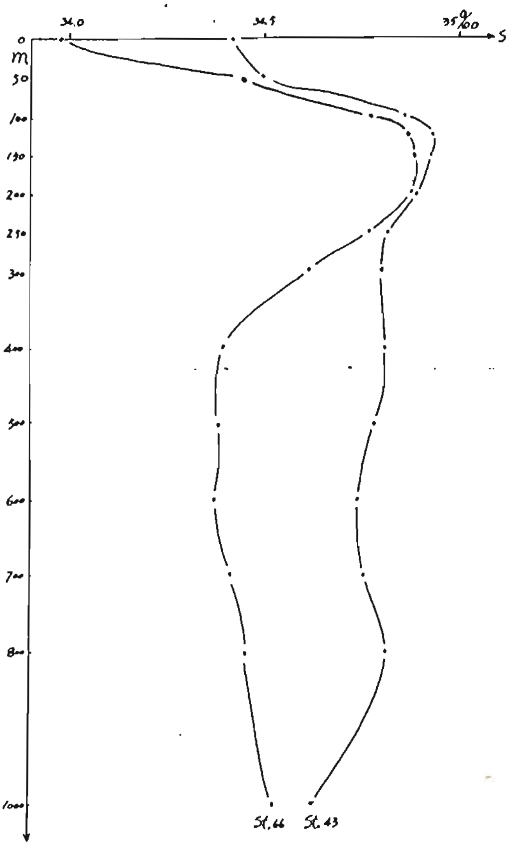

图 10. 黑潮水和冷涡水的盐度 (‰) 垂直分布

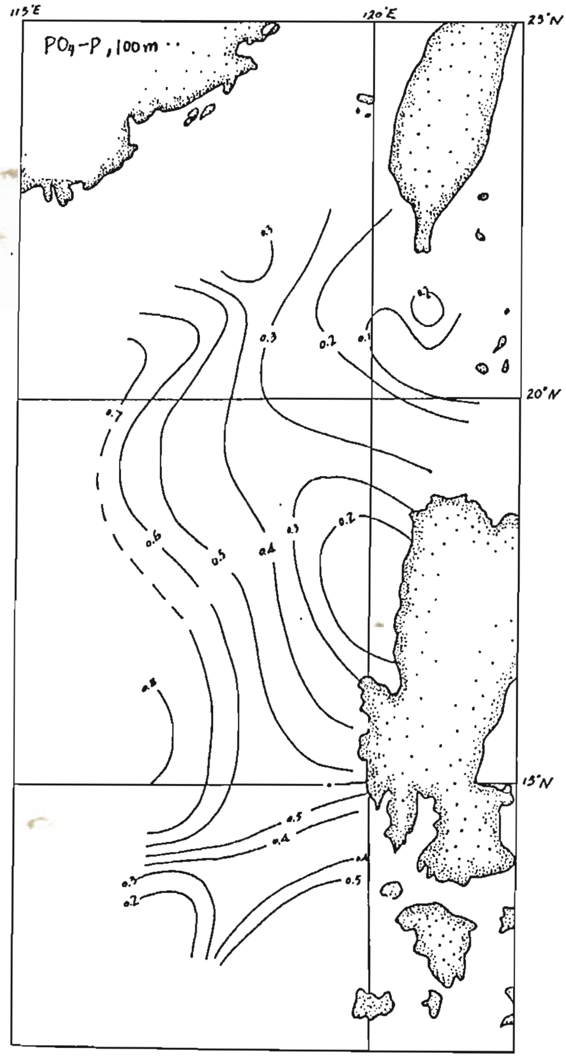

Fig.11.

图 11. 100m 层 PO_4—P (μg—at/L) 分布

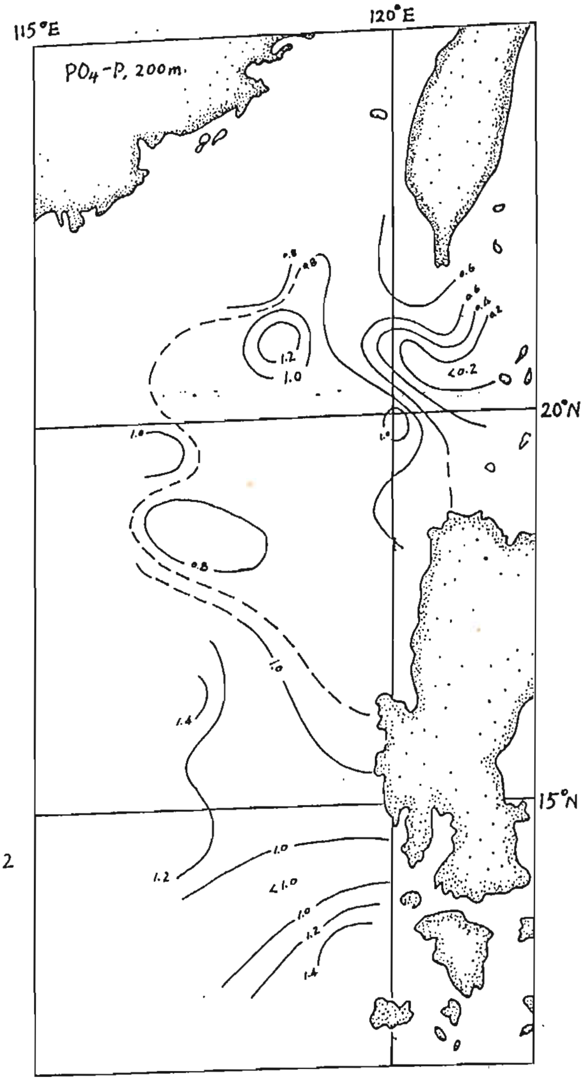

Fig.12

图 12. 200m 层 PO_4—P (μg—at/L) 分布

Fig 13

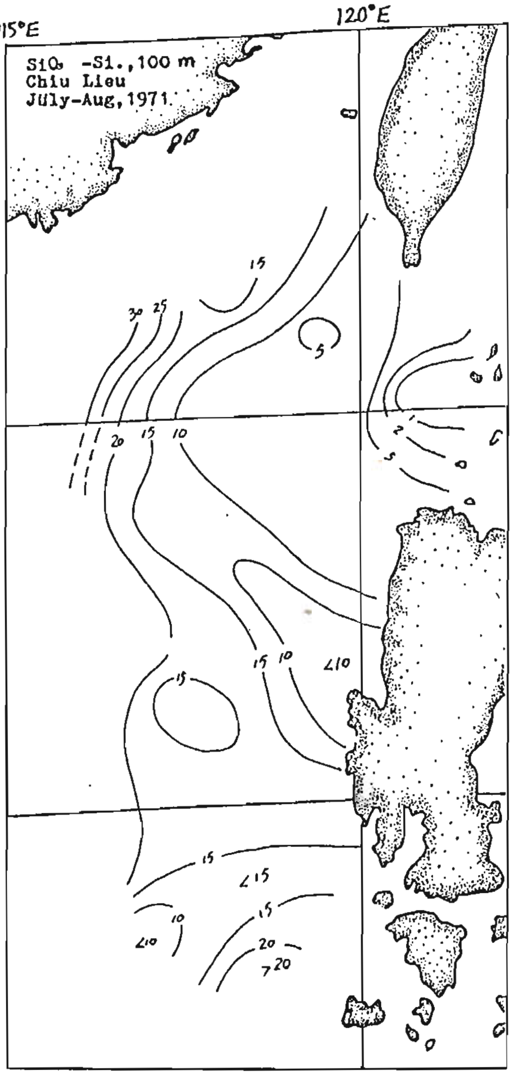

图 13. 100m 层 SiO_3—Si (μg—at/L) 分布

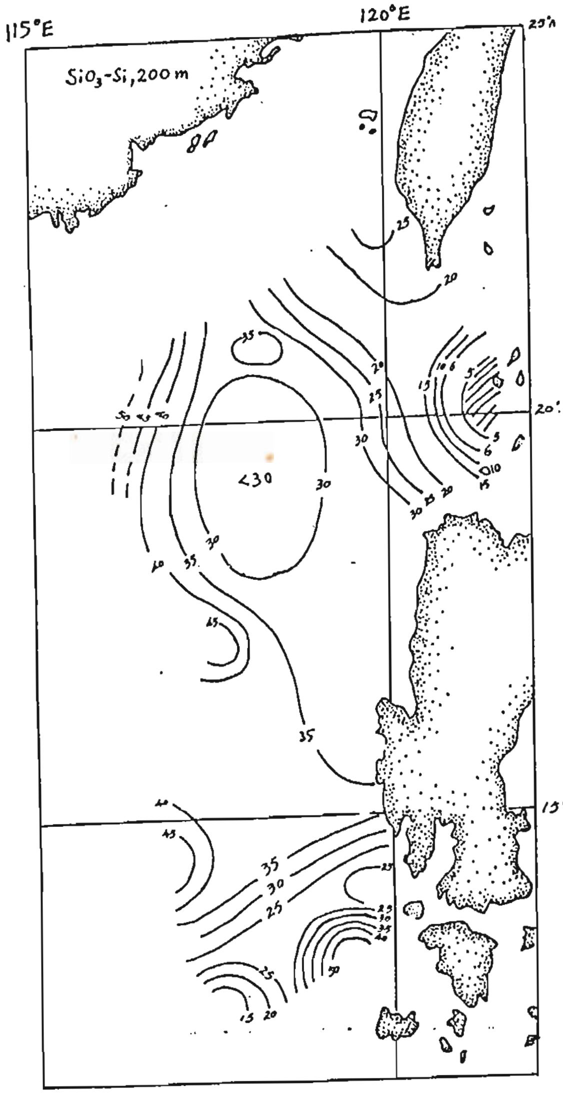

图 14. 200m 层 SiO_3—Si (μg—at/L) 分布

第5卷第4期 黄渤海海洋 Vol.5 No.4
1987年 JOURNAL OF OCEANOCRAPHY OF HUANGHAI & BOHAI SEAS 1987

副热带逆流二十年研究概况

管秉贤
(中国科学院海洋研究所)

副热带环流系统(或副热带流涡，Subtropical Gyre)是世界大洋总环流最显著的特征之一。长期以来，人们认为它是一个由单一的顺时针转动(北半球情况)的环流系统(即"单涡")所组成，其西边界海流(如黑潮或湾流)强而窄，东边界海流(如加利福尼亚海流或Canary流)弱而宽，内区则为微弱的西向流且少变化。70年代发现大洋内区存在着强有力的中尺度涡这一现象剧烈地动摇了人们对大洋环流结构的传统认识。这确实是海洋学中头等重要的事件。然而，不应遗忘60年代后期吉田和城所〔Yoshida & Kido-koro（以后简写为YK),1967〕[40, 41]发现的：在大洋（首先是在北太平洋）副热带环流系统内区(特别是西部20—30°N之间)存在着一支东向流，即副热带逆流（以后简写为STCC)，从而单涡的副热带流系可能分裂为南北两个系统(即"双涡")，这也该是60年代海洋学发展中的重要事件，同样动摇了人们对大洋环流结构的传统认识。经过20年来的努力，副热带逆流的研究已取得了较大进展。当然，其细致和深入程度不能和中尺度涡的研究相比，但其广度是相当大的。现已确认，这支首先在北太平洋北回归线附近发现的东向流，不仅在北大西洋，还有南印度洋，甚至南太平洋和南大西洋同样纬度区域都存在着。因而，可以说，副热带东向逆流是一种带有全球性的现象，可能是大洋环流的最基本特征之一。不仅如此，它还存在于副热带环流内区以外的同样纬度区域(如南中国海北部发现的"南海暖流")。本文拟对20年来副热带逆流研究的进展作一梗概的回顾。

一、副热带逆流发现经过

在1967年前，吉田和城所[40, 41]曾根据各季风应力资料(Hidaka, 1958)[13]从理论上计算并绘制了北太平洋温跃层深度与平均深度偏差分布图。这种图实际上就是上层环流图。它最吸引人的一个特征就是在冬、春季(特别是在3—5月)，在副热带西部区域(20—25°N)出现出人意料的东向流。而在其他季节及全年平均图上却未出现(附图1)。吉田开始注意到了这一新现象，并认为这支东向流与风应力负涡度(反气旋式的Curlz τ)经向分布曲线上的极小值(即"槽"，trough)相对应。

1967年4月在日本海洋学会召开年会之际，宇田和莲沼(Uda & Hasunuma)提出了一篇关于西北太平洋副热带水的很有意义的文章[32]，指出在20—25°N间很可能存在着一支东向流，它可能扩展到很东处(一般，这里的海流由东向西流动)。这一新证据的提出，对吉田印象很深，启发他提出副热带逆流的概念。起初，吉田用"北太平洋中的

本文于1987年7月25日收到，修改稿于1987年9月29日收到。

副热带逆流(STCC)——副热带辐聚区域附近的一支东向流"命题的[40]，即STCC的存在有区域性，限于北太平洋。后来进一步发现在其他海域(如北大西洋中的马尾藻海，Voorhis & Hersey，1964)[34]也有类似的东向流，认为STCC带有全球性，又以"副热带逆流——副热带较低纬区海域的东向流的预测"为题发表了第二篇论文[41]。

所以，不象Cromwell海流(太平洋赤道潜流)，首先是从渔人的延绳钓中发现其存在，而后由Cromwell等人(1954)观测予以证实；STCC是日本学者通过理论计算和资料分析发现这支东向逆流，而后再得到实测(主要是温盐度观测)证实的。

二、吉田·城所模式(YK，1967a，b)基本特征

他们引用Hidaka (1958)[13]风应力资料绘制的北太平洋南部风应力及其涡度随纬度的变化曲线(春季及年平均)如附图2所示。春季风应力涡度曲线在25°N附近处有一个"槽"(附图2a)，这与东向的副热带逆流相对应；而在年平均曲线中却没有出现这个"槽"(附图2b)。这就是一般用年平均风应力资料计算大洋环流模式时，副热带环流系统呈"单涡"型的原因。从春季温跃层深度的分布图上可以看出，在副热带流涡内的广大区域出现一个狭窄的纬向槽(附图1a)。在传统的经典模式中，副热带流涡区域的温跃层一般是深的，附图1a分为两个深的跃层区域，中间为一相当狭窄的较浅温跃层带所分隔。相应地，上层环流将在20—25°N附近(西部)或25—30°N附近(东部)，即北太平洋副热带较低纬区出现第二支向东输送的海流。赤道逆流被认为是与赤道无风带的存在有关，即与2—12°N附近信风强度曲线中的"槽"相当。基于这种相似性，与反气旋风应力涡度分布曲线中的"槽"相当的这支东向流，吉田称之为"副热带逆流"。

反气旋风应力涡度的"槽"在冬及春季都出现，但东向流以春季更为明显，平均流速的量级为1—10$cm \cdot s^{-1}$，但个别区域的流速可大得多，且流幅狭窄和不连续。当年YK并不要求在这一纬度范围和这部分时间内都应出现连续而十分明确的东向流。他们只是指出，自冬及春在风应力反气旋涡度的分布中出现这一特征"槽"，这槽至少对出现东向流是有利的。关于风应力反气旋涡度经向分布曲线中出现特征"槽"的问题，将在下面讨论副热带逆流的成因时，引用我们自己的计算结果再予论述。预先指出，Wyrtki及Meyers(1975)发表的风应力资料[39]，为讨论这个问题提供了更可靠的证据。

当年西北太平洋的资料较少，尚不能证实这是一支向东流动的明显而连续的海流。所以，吉田认为，毋宁说这是一支与某些不规则涡旋有关的东向流。由于在北太平洋20—30°N之间的海区存在许多海脊，所以，即使资料确实证明在这纬区内出现东向流，海脊的影响也可使东向流为之中断而呈不连续状。他们认为，东向的副热带逆流，仅仅是时间、空间上统计的平均特征，相对于传统概念中的环流来说，它是第二性的特征。由于副热带"槽"的稳定性较差，副热带逆流也可能是稳定性、持久性和连续性更差或竟是半永久性的一种流动[40]。

吉田曾绘制了两幅副热带环流系统的模式图(附图3)。其一代表传统概念，他称之为"旧模式"；另一为出现副热带逆流的"新模式"。旧模式的副热带海洋具有这样的特征：这是一个海面高而温跃层深的海区，大约在30°N附近有一个海面最高和温跃层最深的

中心区域。与这些平均密度和压力分布相对应，出现一个具有大尺度反气旋环流的副热带流系。新模式认为副热带流系并非单涡，而是整个副热带区域有时或多或少地分割为两个反气旋式涡，中间隔着一个狭窄的气旋式涡。分隔常常是不完整和部分的。因此，平均流线不会呈现出自西向东连续的单一东向输送，而是呈现出大的弯曲流型。

20年来的研究进展表明，当年YK提出的副热带逆流很可能是大洋环流最基本特征之一的一种表现(Yoshida，1977)[44]。它将在其他大洋信风和西风的边界附近区域出现，因而具有全球性质，而不是一种局部现象(Yoshida，1970)[42]。同时，现有资料证实，在20—25°N之间，这种东向输送可与西向输送相比拟，而且东向输送以带状结构出现，即是多枝的东向流[42]。从热盐结构来看，这支东向副热带逆流的存在，又与热锋(thermal front)，特别是副热带辐聚紧密相联。因此，本文将着重论述这支海流的这些基本特征。

三、副热带逆流的基本特征

(一)全球性分布

副热带逆流首先是在北太平洋西部的较低中纬区域发现的。20年来，已先后在北大西洋西部及南大西洋、南太平洋、南印度洋的副热带区域等发现有类似的东向逆流存在。正如吉田早所预言的，从理论上讲，副热带逆流可能穿过整个世界大洋。他生前更期待能发现某些过去未曾知道的这种海流[41，44]。下面按各大洋择要阐述那里已发现的副热带逆流。

1．北太平洋

(1) 宇田和莲沼(1969)首先通过历史资料，包括1965—1966年的黑潮联合调查(CSK)资料的分析，发现在北太平洋西部的副热带区域，大致沿北回归线(20—25°N)明显地存在着一支新的东向流，即“副热带逆流”。其途径与100m层上的21—24℃等温线相一致。逆流流速约为0.2—1.3节(平均0.5节)，它在地转流场上整年存在。宽度和厚度分别约为100海里及300米。流量为黑潮的10—20％。可自122°E追踪到160°E或更东。在日本水路部的表面海流图(根据1924—1934年的船舶定位资料编制)上，在20—25°N间四季都出现东向逆流。与副热带逆流相关联的次表层热锋位于北回归线附近的100—200m层上。他们引用两幅沿140°E的温度断面图分析了与副热带逆流有联系的海水质量结构。其一是1939年8月观测的，另一是1966年3月CSK观测的。两者都显示出随着纬度增加，温跃层深度向北加深。但在16°N附近，跃层开始分为上、下两个。上跃层在20—22°N开始向北上升(变浅)，形成次表层热锋，这就是副热带逆流存在的主要水文结构。次表层热锋再向北形成季节性跃层；下跃层在副热带区域形成主跃层。在20—22°N观测到次表层热锋处，可以看到主跃层也向北上升。这与断面其他部分主跃层向北加深的趋势正相反。这种热结构在北太平洋西部所有断面上几乎都存在。这与副热带逆流紧密相关联。在副热带逆流南北两侧为西向流。在副热带逆流之北，跃层分为季节性跃层和主跃层两种，中间(100—400m)为几乎均匀的海水，即是副热带模态水(Subtropical Mode Water)(附图4)。

(2) Seckel(1968)[21]在分析夏威夷群岛东北的148°W断面资料时指出,在20—24°N间存在着狭窄的东向流，这是0—200m层热锋的贡献。Reed(1968)[16]则根据沿160°W断面资料指出，23—26°N之间也存在着东向流，流速约为20cm·s^{-1}，其南为西向流，在20°N处又出现第二支东向流。上述两例的观测时间皆含9月。所以，在夏威夷群岛附近，即使在夏末秋初也出现副热带逆流。

(3) Robinson(1969)[17]根据温深仪(BT)及颠倒温度计资料，从逐月温跃层深度的分布，证实北太平洋西部从140°E远到160°W，在北赤道流以北存在着东向流，可能是整年存在的，但以1—5月为最强。这时，可能在较长距离上东向流是连续的，而在其他时间则较弱和不连续。

(4) Wyrtki(1975)[38]应用当时所有的水文资料绘制的太平洋海面动力高度分布图(0/1000×10^{4}帕，附图5)上，出现一个明确的“北赤道脊”，其北坡即为东向的副热带逆流。它自台湾以东大致沿20°N向东延伸。其南部为西向的北赤道流。副热带逆流在年平均、3—4月和11—12月的动力高度分布图上特别显著。

(5) 全国海洋综合调查(1958—1962)发现,在南海北部汕头和海南岛以东近岸海域，冬季在流向西南的沿岸流外缘，存在着逆风流向东北的海流，当年称为“南海暖流”。这是在YK(1967a、b)提出副热带逆流以前，用实测资料证实，南海北部副热带区域冬季存在着东向流的文献(管秉贤，陈上及，1964)[7]，管(1978)[8]还引用CSK中Cape St. Mary号调查船1966—68年冬季的水文资料,从地转流场上发现广东外海较深海域冬季存在着一支逆风流动的、流幅狭窄而流速较强的海流。相比之下，50年代底60年代初发现的南海暖流，仅是这支海流的左翼部分。同时还指出，这支冬季出现在南海北部的东向流，在地理纬度(19—22°N)，水文特征(具有强陡温跃层，其途径与100m层上的19—23℃等温线相一致)，流速结构(流幅80余海里，厚度300m)等方面都与文献[40，41]提出的副热带逆流相类似，故可称为“南海中的副热带逆流”(管秉贤，1978)[3，4]。后又从冬季水温的垂直结构分析了这支冬季逆风海流的特征，指出这支海流的流动与上下温跃层的走向相反有着密切的联系(管秉贤，1981)[5]。最近又根据水温历史资料阐述了这支冬季逆风海流的时-空分布特征，指出逆风海流以南海东北部为最稳定和强大，海南岛以东次之，中间区域较弱和不稳定。这些变异特征又与副热带逆流的相似。这种在地转流场上发现的东北向逆风海流，已为强寒潮天气下深海浮标站多日海流连续观测结果所证实[1，2]。

2. 南太平洋

(1) Merle等(1969)[15]在调查170°E断面的纬向地转流时报道，在15—20°S之间出现东向流，其最大流速为5—35cm·s^{-1}。这支海流主要位于海面至200m水层处。GEK和海流计的观测结果也与这支东向的地转流相符。Merle等把这支东向流称为南热带逆流(South Tropical Countercurrent)。Rotschi(1973)[20]认为这支海流与北太平洋的副热带逆流相当，但是Merle等所观测到的南热带逆流实是20—35°S处较宽阔的东向流的向赤道部分，这从Reid & Arthur(1975)和Wyrtki(1975)[38]的动力高度分布图上可以看得很清楚。

(2) Tsuchiya(1982)[29]的研究表明，南太平洋副热带环流仅系一巨大的反气旋式

单涡，它横贯东西，大致与北太平洋副热带环流中向赤道一侧的流核相对称。Tsuchiya[29]认为，南太平洋副热带环流看不出有明显的迹象存在着向南极一侧的流核。但他又指出,有这样两个特征也许能作为存在着极向流核的证据。一个特征是澳大利亚以东35°S附近出现一个动力高度高值的小核区。虽然这个流核比北太平洋那个极核要小得多，但与后者很相似。另一个特征则是假说性的反气旋环流，它由40—45°S处的西向流及更南处的东向流所组成。我们认为，由于南太平洋资料稀少，为了确证极核的存在，进一步的调查是很有必要的。

3．北大西洋

(1) 早在YK[40，41]的首创性论文发表前，Voorhis & Hersey(1964)[34]就曾指出，在马尾藻海(22—32°N)，西起Bahama Bank，东到55°W，观测到许多热锋，时间为1958—1963年的1—6月和11—12月，出现最频繁的是1—3月(附图6)。所以，热锋都不是在盛夏(7—9月)观测到的，6月测得的也很弱。Voorhis(1969)[33]后又发现，1964年1月在中央马尾藻海出现一大尺度锋面。1965年1—5月也观测到类似的热锋。锋面出现在21.5—23.5℃等温线之间，间距小于1 km；在26—29°N间锋面呈东西弯曲状，延伸几近1000km。马尾藻海的锋面水文观测均配备有同步的GEK表层流观测，为验证副热带逆流是否具有地转性提供了有力依据。

(2) Schroeder(1965)[22]通过对北大西洋20°N以北月平均温度断面图的分析，也发现有一类似的热锋，预示存在着东向流。热锋向更东方延伸，在这些纬度上几乎可穿过整个大西洋。

4．南大西洋

(1) Stone(1981)首先指出，在海面动力高度分布图($0/1000\times10^4$帕)上，南大西洋副热带环流分裂为两个单独的高脊，30°S附近间隔着一个低槽。

(2) Tsuchiya(1985)[30]根据同样型式的分布图也指出南大西洋副热带流涡分裂为两核，中心分别位于南美洲海岸外的22°S及32°S附近。两核有时在西边界处互相连接，有时则否。南大西洋副热带环流的这一特征是与300m层以下的等比容线其总趋势向极加深而浅层的等比容线有相反的趋势有关。在25°S附近处反向趋势特别显著,这里出现东向流(附图7)。

5．南印度洋

在南印度洋20—26°S附近，无论是在西南季风或东北季风期间，都出现副热带逆流。根据Montgomery的建议，南印度洋的副热带逆流改称为热带逆流(Tropical Countercurrent)(Sharma，1976；Sharma等，1982)[23，24]。

1964年5—6月沿65°E经向断面的温度分布表明，在西南季风时期，在22—26°S之间纬向流指东，这是因为此时这里出现一个与副热带辐聚区有关的热锋，通过热锋，温度向北增加，才形成这支东向地转流，两边则为西向流。这支副热带逆流较宽较强，逆东南信风而流动，可能是整年沿印度洋的这一纬带而存在的。

国际印度洋调查的动力高度分布图表明，在东北季风期内(1961—1964，1967年的1—2月、11—12月)，副热带逆流出现在20—26°S之间的所有经线上，向东延伸达60个经度，流速约$12cm\cdot s^{-1}$。

Sharma认为，印度洋中的副热带逆流与YK[40, 41]在北太平洋中从理论上发现的副热带逆流相似。

Mathew等(1982)引用1976年3月及12月分别沿90°E及60°E的断面资料(站距各为1纬度)计算了地转流速(相对于1000×10^{4}帕)，进一步指出南印度洋的副热带逆流也具有明显的带状结构(附图8)。

综上所述，除了北印度洋因地形特异，副热带海域甚小，北回归线以北几乎均为陆地所占，以致迄今尚未发现类似的这种海流外，在世界三大洋的北及南副热带较低纬度带内均已发现了东向逆流，副热带逆流的全球性分布已是十分明显的了(附图9)。

(二)带状结构和"多涡"假说

在CSK以前，副热带纬度区域的观测甚少。系统的CSK资料为验证副热带逆流的存在以及阐明它具有带状结构提供了可贵的情报。CSK期间(1965—1966)冬季200m层上温度经向梯度图(附图10)表明，温度向北递减(即密度向北递增)的区域呈带状出现，这里即是出现东向副热带逆流的区域。所以，在西北太平洋(130—155°E，20—30°N)这支东向的副热带逆流具有纬向的带状结构，其间距约为3°。在此区域内可分为3—4个东向流带状，中间隔着3个西向流带。每带自西而东基本上是连续的。σ_t及动力高度分布图与温度梯度图相似，均显示出相同的结构。

在垂直方向上也是这样。在与温度经向梯度图相对应的地转流速断面分布图(附图11)上，流速的带状结构更为明显：间距约为3个纬度，东向流分别出现在21—22°N，24—25°N及27—28°N上，每带至少深达1500m，表层流速约10—20cm·s^{-1}。此图以2000×10^{4}帕为零面，是将1965—1966年冬季观测的各经向断面(127—155°E)加以平均得出。其他季节按较浅零面的计算结果显示了大致相似的图景。所以，在各种平均分布图上，副热带逆流明确地显示出具有多枝东向流的特征，而并非单支海流。这是吉田(1970)根据CSK资料的分析得出的结论。

由于CSK资料囿于155°E以西，吉田(1970)还用其他来源的资料分析了副热带逆流在160°E以东的连续性及延伸性。在他应用"信风带海洋学试验研究"(1964—1965)资料所绘制的148°W地转流经向断面分布图上也显示了类似的带状结构：20°N以北东向流很明显，时间-空间上也较连续，但限于100m以浅的近表层。20°N以南出现2—3个深层东向潜流，带状结构的间隔也略宽一些。当然，带状结构的间隔在很大程度上视站距而定。此外，在日本水路部早年出版的表面海流图上，除了可以明显地看出存在着东向的副热带逆流外，也可看出它具有带状结构。

吉田(1970)曾引用稳定内波的理论试图阐释副热带逆流带状结构的机制。他得出：如取温跃层厚度约为500m，则相应的带状结构的波长分别为4(15°N)，3(20°N)，2(35°N)个纬度。还认为有越来越多的证据表明东向流出现在副热带较低纬区，它并具有带状结构。由于这种多枝的东向流在西部最为显著，故上述特征对黑潮源地区域更显得重要。吉田(1972)再指出，副热带流涡南半部所发现的这支东向流，最终可能与黑潮途径的变异有联系。

我们在研究南海北部冬季的流场时也曾指出，自海岸向外，西南向的沿岸流—东北向

的南海暖流侧翼—西南向流—东北向的南海暖流主流等依次沿等深线相间分布。这表明位于副热带较低纬区域的海流具有带状结构(管秉贤，1978)[3，4]。

综上所述，从北太平洋西部现有的资料来看，副热带逆流具有带状结构是毫无疑义的。White & Hasunuma (1982)[35]的研究还进一步认为，北太平洋西部包括副热带逆流在内的平均纬向地转流的带状结构具有准稳定性。20—30°N之间的副热带逆流包含两个高速核(分别位于23°N及28°N)，中间隔着零速区。最近作者对沿137°E经向断面六个冬季(1967—1972)海面动力高度(0/1000×10⁴帕)平均值的分析表明：通过137°E的副热带逆流由三支东向流所组成，它们的宽度约为2个纬度，中心分别位于19°N，23°N及27°N附近。每两支东向流之间隔着一支西向流(附图16)。所以，副热带逆流呈现出明显的带状结构(Guan，1987)[11]。

副热带逆流的发现加深了人们对副热带流涡结构的认识，所以在阐述副热带逆流的带状结构时，简略介绍一下有关整个副热带流涡结构的“多涡”假说，是有必要的。

1974年2—3月日本调查船白凤丸在134°E以西和15—26°N海域的观测结果(莲沼和吉田，1978)，进一步揭示了北太平洋副热带流涡西部结构的基本特征。这两位日本学者指出，北太平洋西部副热带流涡既不是由“单”涡，也不是由“双”涡组成，而是可能分裂为三个次级流涡，后者分别由一对东向流和西向流所组成(见表1)。

不仅在天气式的动力高度分布图上有几个带状脊，在长期平均的海面动力高度分布图(0/1000×10⁴帕)上也是这样，副热带流涡分裂为两个或多个次级流涡，这表明它至少是一种半永久性特征(附图12)。这就是莲沼和吉田近年提出的“多涡”假说。

表1　次级涡及组成海流名称

流涡	次级流涡	东、西向流对
西北太平洋副热带流涡	1.黑潮脊或次涡 (副热带槽)	(1)黑潮(东向流) (2)黑潮逆流(西向流)
	2.热带脊或次涡 (热带槽)	(1)副热带逆流(东向流) (2)副热带逆流之南的西向流
	3.北赤道脊或次涡	(1)与脊北坡有关的东向流 (2)北赤道流(西向流)

应该指出，副热带流涡虽分裂为几个次级流涡，但其天气式“细”结构并非固定不变，而随季节或年际而变，1965—1966年冬季就是两脊一槽模式充分发展的一个时期(Guan，1987)[11]。

(三)与热锋并存

关于热锋及其与副热带逆流相依并存的关系，Uda(1955)[31]，Uda & Hasunuma (1969)[32]，Schroeder(1965)[22]，Voorhis & Hersey(1964)[34]及Evans(1971)等都作过许多研究。一般讲来，当海面温度梯度大于1℃/10km时，即称为热锋(thermal front)。垂直水柱中温度水平梯度大于1℃/10km的地方称为锋面区(thermal frontal zone)。

由于副热带逆流具有显著的地转性，所以它与热锋相一致是必然的。宇田和莲沼(1969)在分析副热带逆流的特征时指出，副热带逆流与该海区的次表层热锋及主温跃层相关联。在20—22°N附近，次表层热锋(100—300m)和主温跃层均自南向北上倾，即为东向流的标志，两侧伴以西向流。副热带逆流的途径与100m层上的21—24℃等温线相一致，通过这一热锋时，水温向北锐减。作者(1978)在分析南海暖流时指出，这支海流与该海区内较强陡的温跃层(即次表层热锋)相关联。后者以19—22°N附近为最显著。那里温跃层自东南向西北上倾，即为东北向流的标志，两侧亦伴以西南向流。南海暖流的途径也与100m层上的19—23℃等温线相一致。通过这一热锋时，水温亦向北锐减。

南海暖流的实测结果表明，南海北部较深海域冬季的流场以斜压性流为主，亦即地转流具有较好的代表性(管秉贤，1985)[6]。这一论述从另一方面证实了副热带逆流与热锋相依并存的关系。

在大西洋，60年代初期马尾藻海的海洋热锋观测，是最早证明热锋与副热带逆流相依并存的工作。附图13显示了1962年12月10日Chain号调查船用测温链得出的30m层温度及用GEK测得的表层流速。热锋很强，自海面向下扩展至少达混合层之底(约80m)；在横越热锋仅5km的范围内温度变化达1.5℃。表层流沿等温线亦即热锋自西向东流动，流幅狭窄，流速颇强，可达60cm·s^{-1}，冷水位于流向左侧，锋面近乎地转平衡[34]。

(全文未完待续)

A SKETCH OF THE STUDY OF THE SUBTROPICAL COUNTERCURRENT IN THE PAST TWO DECADES

Guan Bingxian

(*Institute of Oceanology, Academia Sinica, Qingdao*)

第6卷第1期 黄渤海海洋 Vol.6 No.1
1988年 JOURNAL OF OCEANOGRAPHY OF HUANGHAI & BOHAI SEAS 1988

副热带逆流二十年研究概况(续)

管 秉 贤

(中国科学院海洋研究所)

四、副热带逆流的可能成因

关于副热带逆流形成的原因，迄今尚无一个完满的普遍接受的解释。20年来，不少学者提出了几种有关逆流成因的可能解释，主要的有：1）吉田和城所[40，41，43]的风应力反气旋涡度的"槽"理论；2）杉ノ原伸夫(Suginohara，1973)[25]的风生大洋环流三层模式；3）竹内谦介(Takeuchi，1983；1984)的副热带锋及副热带逆流的形成机制和数值模式；4）Cushman-Roisin(1984)[10]的不考虑Ekman辐聚的副热带锋生成论；5）White & Walker(1985)的夏威夷群岛的影响论等。总的讲来，吉田和城所的理论提出最早，引用较为普遍。但对副热带反气旋涡度的"槽"结构在形成逆流中到底具有什么作用(主导因子或次要因子)争议较多。其他各家的理论，进一步考虑了除风应力涡度以外的其他机制，比较全面，但尚未最后定型。现对上述五家的学说分别简介如下：

(一)吉田·城所的风应力涡度"槽"理论

他们根据两层海洋中风生环流的动力分析预言了这支新的东向流的存在。这支海流存在的原因归结为风应力涡度(反气旋式)经向分布曲线上出现"奇异点槽"所致。同时，风应力涡度分布只在冬、春两季的月份出现此槽，所以吉田又预言，东向流也只有在这几个月才存在。象经常所假设的，当风应力为正弦分布时，风应力涡度在30°N达到极大值而无"槽"出现；与此相对应的流场是在15—45°N之间出现一个单一的反气旋流涡。但实际上从现有风应力资料来看，西风和信风之间的边界是与风应力涡度的极小值或"槽"相当。反气旋风应力涡度经向分布中的这个槽，是较低副热带区域出现东向逆流的原因所在。槽及副热带逆流是海面风应力产生的，而不是风场本身结构产生的。风应力的平方定律($\tau \sim W^2$)是出现这槽的主要因素。

在整个副热带区域，$\frac{\partial \tau_x}{\partial y}$的气候式平均值为正，相当于风应力涡度为负(反气旋式)。这是因为假定$\tau_y \to 0$时，$\mathrm{Curl}_z \vec{\tau} = \frac{\partial \tau_y}{\partial x} - \frac{\partial \tau_x}{\partial y} \sim -\frac{\partial \tau_x}{\partial y}$。$\frac{\partial \tau_x}{\partial y}$约在30—35°N间出现极大值。这里即是西风区转为东风区的纬度所在。但这是年或一般的平均情况。在冬、春季这里出现一槽，具有相当低的$\frac{\partial \tau_x}{\partial y}$值，而将$\frac{\partial \tau_x}{\partial y}$曲线分成两个位于"槽"点两侧的高值区，副热带流涡才由单涡结构分裂成北、南两个流涡，从而在中间(与"槽"相

本文于1987年7月25日收到，修改稿于1987年9月28日收到。

应处)出现副热带逆流。具体地讲，在西风和信风边界之南出现东向流，即副热带逆流。

当用这样的风应力涡度值按Sverdrup输送量公式计算海流时，在槽点附近将出现副热带逆流，但这槽只在冬、春季出现，其他季节和年平均图上都不出现。这也是过去的气候式平均海流模式图上没有出现STCC的原因。

当年吉田曾用Hidaka(1958)[13]，Hellerman(手稿)及Fofonoff & Dobson(1963)三种风应力资料分别计算了风应力涡度的经向分布及海流输送。虽然，槽所在的纬度及其出现季节，各种资料所得结果不尽相同，但仍互相类似。吉田(1972)[43]后来指出，我们对风应力值的认识是很不充分的，看来需要重新计算风应力，以便能对理论模式进行严密的检验。

太平洋信风场资料(Wyrtki & Meyers，1975)[39]的出版为检验当年吉田的设想提供了重要的依据。我们根据这种风应力资料又计算了相应的风应力涡度Curlz $\vec{\tau}$(管秉贤，刘举平，1987)[8]。北太平洋风应力涡度(沿纬向平均值)的23年(1950—1972)平均值的经向分布如附图14所示。可以看出，在24°N附近，各双月及年平均值曲线上均出现一个槽点，年平均值约为-0.5×10^{-8}dy/cm³，除7—8，9—10月外，各双月平均值均在-1.0—-0.5×10^{-8}dy/cm³之间，以1—2月为最大，可达-1.0×10^{-8}dy/cm³。这项风应力涡度的计算结果与吉田当年得出的，无论在纬度位置及量值上均趋于一致。特别值得指出的是我们这项计算结果几乎在各双月和年平均值曲线上都出现槽结构。由于这项风应力资料是迄今最好和最新的一份资料，其多年平均值具有良好的气候式图景代表性。所以，如果风应力涡度槽理论成立的话，与此相应的副热带逆流当具有比较稳定或准稳定的性质。

这份风应力资料的另一个重要优点是经向间隔为2个纬度，远较吉田当年所分析的间隔(5个纬度)要细，有可能揭示风应力涡度经向分布的较细结构，从而也有可能阐明上述副热带逆流的成因。我们应用137°E断面上动力高度偏差(ΔD,0/1000×10⁴ Pa)六个冬季(1967—72年1—2月)观测平均值与相应的风应力涡度($\mathrm{Curl}_z\vec{\tau}$)七个冬季(1966-72年1—2月)平均值作了比较(如附图15所示)，可以明显地看到两者的经向分布几乎相互平行。即当风应力涡度向北增加时，相应地，动力高度偏差向北减少。这是东向流情况；反之，是西向流情况。如上所述，副热带逆流由三支宽度为2个纬度的东向流(分别位于19°N，23°N及27°N附近)所组成。它们分别与$\mathrm{Curl}_z\vec{\tau}$的三个正梯度带(中心位于17°N，23°N及27°N)相对应。在两支相邻东向流之间，有一西向流区，它与$\mathrm{Curl}_z\vec{\tau}$的负梯度带相对应。除了19°N附近的东向流与以17°N为中心的正梯度带位置略有偏移外，两者的关系显然十分紧密(附图16)。这一关系表明，副热带逆流的带状结构是与上空风应力涡度的结构相一致的，并且逆流的形成机制确与风应力涡度经向分布上的“槽”结构相关联。换言之，上述“槽”结构在副热带逆流形成中起了重要作用(Guan，1987)[11]。从Wyrtki & Meyers这份风应力资料中所得出的上述结果予吉田和城所(1967a，b)[40,41]早年提出的风应力涡度槽理论以有力的支持。

虽然，多种证据对证实这支东向副热带逆流的存在以及吉田·城所理论模式的可能成立予以支持，这是令人鼓舞的，但看来问题并非如此简单。首先人们考虑这样一个问

题：除了可用风应力涡度经向分布上出现的"槽"来阐释这支副热带逆流外，它是否还可用其他机制来阐释？

无论是在太平洋、大西洋或是印度洋，这支副热带逆流都与副热带热锋，或再确切点说，与次表层热锋同时存在。所以，有理由这样说，副逆带逆流和副热带热锋是同一个现象的两个分量，阐明了副热带热锋的生成机制也就等于阐明了副热带逆流的成因。因为副热带逆流可以用与横越副热带热锋的温度水平梯度有联系的斜压性热流(baroclinic thermal current)来解释。(2)—(4)项工作就是朝着这个方向发展的。应该提到的是，Stommel对副热带逆流的成因也很感兴趣。在1968年美国地球物理流体动力学夏季讨论会上，Stommel曾向吉田提出可否试作这样一种模式：Ekman漂流与混合层热结构的相互作用可能在某些纬度处产生东向流。这一概念在下面几位学者的工作中得到了发展。

(二)杉ノ原伸夫的大洋风生环流三层模式

他构作这一理论模式的基本思想导源于宇田·莲沼(1969)[32]提出的"东向的副热带逆流与次表层热锋相关联"这一概念。次表层热锋终年存在，因此，副热带逆流在地转流场上也可能是一永恒特征，而成为各季大洋总环流的一部分。他试图用层化效应来阐明副热带逆流，即将副热带逆流认为是Sverdrup输送中的内模态运动(an internal mode of motions)。他考虑了三层模式，即表层暖水(含Ekman层)、温跃层及深层。即在常用的两层模式上加上一层暖水。驱动力为具有简单正弦分布的纬向风应力。表层暖水和温跃层具有同样量级的厚度(分别为200,300m)，深层为4500m。由于最上层的辐散效应，可望在上面两层发生内模态运动。

附图17为大洋中部经向断面的典型流速分布。从图上可以看出，在最南处运动只限于表层暖水，向SW流动。在表层暖水突然向北变薄处(约22—24°N)，表层暖水的运动方向变为NE。东向流随深度的平均流速向西递增，在西边界(离东边界7000km处)最大值可达20cm·s^{-1}。

计算得出的热结构与观测到的主温跃层的特征相似。与次表层热锋有关的东向流出现在较低中纬度的表层暖水内，它可能与副热带逆流相当。在此逆流下面有西向流(迄今尚未有观测证据)。因为假定总输送量满足Sverdrup关系，所以副热带东北向逆流及其下的西南向流呈现为与次表层热锋有关的内模态运动。

本模式没有考虑吉田·城所的风应力分布的特殊结构"槽"(YK，1967a,b)[40,41]，但也模拟出了在较低副热带处的表层出现东向流。所以，槽结构并非是产生东向流的必要条件。但Rooth等(1978)[19]指出：杉ノ原伸夫(1973)在东边界附近的计算中存在错误，才导致产生次表层热锋并伴以东向表层流及西向次表层流。亦即次表层热锋是他数值计算的结果，而并非真实的物理特征。但杉ノ原伸夫仍然认为他的工作是可能有其应用价值的(Suginohara，1978)。

(三)竹内谦介的副热带锋及副热带逆流的数值模式

竹内用多层数值模式，假定北太平洋(0—50°N)为一矩形平底海洋，受到海面风(动力学)和海面热通量(热力学)的偶合作用，在这些条件下模拟出了副热带锋和副热带逆

流。数值计算结果表明，沿密度锋有一浅薄的东向流，西起风应力涡度最大值出现纬度的稍南处，倾斜地向东北延伸。这与副热带逆流相当(Takeuchi，1983)[27]。

在竹内的这项研究中，虽然有关副热带锋和副热带逆流的详细机制尚未清楚，但他发现，下列两个因子对副热带锋和逆流的形成机制并非是必不可少的。首先，他的模式结果表明，副热带风应力涡度经向分布上的“槽”结构，对副热带锋和逆流的形成并非必需，因为他的模式没有考虑“槽”结构也能很好地模拟出副热带热锋和东向逆流。其次，经向Ekman辐聚同样不是必需因子。不过，他着重指出，在他的工作中并没有否认，上述两种因子(即风应力涡度“槽”结构和经向Ekman辐聚)对副热带锋和逆流的形成会有所贡献。他认为这两种因子确实会强化副热带锋,但它们仅仅是起配角作用而已。他对什么是副热带锋和逆流形成的主导作用这个问题也未能给出明确的答复。他的研究只表明，副热带锋的形成乃是风生环流和加热差异两者综合作用的结果(Takeuchi，1984)[28]。

(四)Cushman Roisin不考虑Ekman辐聚的副热带锋生成论

他基于副热带逆流与纬向密度锋(即副热带锋)相关联这一事实，试图用一种包括简单作用力以及简单几何学的模式来复制副热带锋-逆流的结构。早些时候，包括Cushman-Roisin(1981)在内的一些学者曾试图将副热带锋的形成与由西风和信风引起的Ekman漂流的辐聚作用相联系。但是，这项理论难以解释若干观测事实。例如，在北太平洋西部，副热带锋位于比西风和信风边界要低几度的纬度处，而这项理论预测锋形成于边界上。其次，风场季节性的南-北向移动约10个纬度，而副热带锋如有移动的话,也不会超过5个纬度。再者，如纬向风为经向风所取代，而保持风应力涡度分布不变，也可得出类似结果。考虑到上述种种情况，Cushman-Roisin(1984)[10]转而认为Ekman输送的辐聚作用，虽能使副热带锋加强，但不可能是副热带锋存在的主要原因。他建立了一个稳定、三维、垂直平流-扩散的温跃层模式。他的模式得出了海面温度和表层流的分布。从海面温度分布图上可以清楚地看出有一条热锋，西起25°N附近，并向东北方上倾延伸。这与海面温度卫星照片(1977年3月15日，Roden，1980)[18]上所确定的水平温度梯度大的区域(它可解释为副热带锋)相一致。与这种温度分布相联系的流场是一支沿热锋向东流动的斜压、热驱动地转流，它叠置在正压、风生顺时针环流之上形成了较传统认识要复杂得多的副热带流涡。所以Cushman-Roisin的这个简化模式能很好地复制副热带锋及副热带逆流。

(五)White·Walker的夏威夷群岛影响论

如上所述，副热带逆流位于北太平洋西部副热带流涡的中部，它至少由三支狭窄的东向地转平均流所组成。White及Walker着重用夏威夷群岛的影响来阐释这些东向平均流的带状结构。平均讲来，这些带状结构西起菲律宾海(约140°E)，向东延伸达到夏威夷群岛(约160°W)。而在夏威夷群岛以东未曾发现带状结构。他们认为，早年吉田·城所[40, 41]试图用Sverdrup(1947)模式来解释东向副热带逆流的成因而没有成功，主要有这样两个原因：(1)那时风应力涡度的分辨度很粗(5个纬度/经度)，不可能分辨宽度只有1—2个纬度的狭带结构；(2)没有认识到东向流带状结构向东扩展只到夏威夷群

岛经度附近这一事实。他们针对这些问题应用 2 个纬度/经度网格的多年平均(1968—1980)风应力，并将夏威夷群岛作为一个"有效屏障"插入在Sverdrup模式中。这一屏障对来自群岛以东海域伸透入北太平洋西部的风生环流，施加了有效的影响。模拟结果表明：(1) 在不考虑夏威夷群岛影响的情况下，模拟不出东向平均流的带状结构；(2) 当夏威夷群岛出现时，在20°、26°及24°N附近处模拟出东向平均流的带状结构，只是在24°N处显得较弱而已(附图18)。White及Walker(1985)[37]的结论是：20°及25°N附近处的东向流带状结构是由于夏威夷群岛(它作为大洋东、西部分之间的一个有效屏障)的存在所致的。他们最后指出，为了进一步了解东向流带状结构的来源，有必要再构作分辨度更高的长期平均的风应力涡度场。

通过20年来的努力，副热带逆流的研究，无论在结构的调查剖析和机制的探索阐释上，都取得了许多实质性的明显进展。副热带逆流是一种带有全球性的现象，它可能是大洋环流的最基本特征之一，这些概念已越来越为人们所接受。对于它的形成机制，也提出了若干种创新见解。为了进一步把这支副热带东向逆流的研究推向一个新的境界，继续开展较系统而长期的调查(特别是南太平洋西部的调查)和更深入的动力学机制研究，对阐明副热带流涡中的这个新的重要分量的特征和变异，都是必需的。

参　考　文　献

〔1〕郭忠信、杨天鸿、仇德忠：冬季南海暖流及其右侧的西南向流，热带海洋，4(1)1985：1—9。
〔2〕郭忠信、黄羽庭：寒潮对南海暖流的影响，热带海洋，2(2)1983：102—107。
〔3〕管秉贤：南海暖流的新证据，海洋科学，(增刊)1978a：100—103。
〔4〕管秉贤：南海暖流—广东外海一支冬季逆风流动的海流，海洋与湖沼，9(2)1978b：117—127。
〔5〕管秉贤：南海北部冬季水温垂直结构的重要特征，海洋与湖沼，12(4)1981：311—320。
〔6〕管秉贤：南海北部冬季逆风海流的时—空分布特征，海洋与湖沼，16(6)1985：430—438。
〔7〕管秉贤、陈上及：中国近海的海流系统，全国海洋综合调查报告，1964：1—85。
〔8〕管秉贤、刘举平：北太平洋信风场风应力资料，科学出版社，1987：220。
〔9〕Basil Mathew, R. N. Nair & Sharma, G. S.:
Band structure of Tropical Countercurrent in the Indian Ocean.
Indian Jour. Mar. Science 11(3)1982：208—211.
〔10〕Cushman-Roisin:
An explanation for the subtropical front-without Ekman convergence. *Ocean modelling*. 54, 1984, Feb.：5—7.
〔11〕Guan Bingxian：
Current structure and its variability in the area east of Taiwan and Philippines in winter. in "*Proceedings of 19th IUGG Meeting*" (abstract). 1987.
〔12〕Hasunuma, K. and Yoshida, K.
Splitting of the Subtropical Gyre in the western North Pacific. *Jour. Oceanogr. Soc. Japan*, 34(4) 1978：160—172.
〔13〕Hidaka, K.:
Computation of the wind-stress over the oceans. *Rec. Oceanogr. Wks. Japan*. 4(2)1958：77—123.
〔14〕Katz, E. J.:
Further study of a front in the Sargasso Sea. *Tellus* 21,1969：259—269
〔15〕Merle, J., Rotschi, H. and Voituricz, B.
Zonal circulation in the tropical western South Pacific at 170° E.
Bull. Jap. Soc. Fish. Oceanogr. (*Uda pap.*), 1969：91—98.
〔16〕Reed, R. K.:
Indications of Subtropical Countercurrent near Hawaii, *Trans. Amer. Geophy. Union*, 49(4)1968：702.
〔17〕Robinson, M. K.:

Theoretical predictions of Subtropical Countercurrent confirmed by Bathythermography (BT)Data. *Bull. Jap. Soc.Fish. Oceanogr.(Uda pap.)*1969：112—121.

〔18〕 Roden, G. I.：
On the variability of surface temperature front in the western Pacific, as detected by Satellite. *J. Geophys. Res.*,85,1980：2704—2710.

〔19〕 Rooth, C. , Stommel, H. and Veronis, G.;
On motions in steady, layered, geostrophic models. *Jour. Oceanogr. Soc. Japan*, 34(6)1978:265—267.

〔20〕 Rotschi, H.;
Hydrology at 170° E in the South Pacific. in"*Oceanography of the South Pacific*."1972, R. Fraser. comp., New Zealand National Commission for UNESCO. Wellington. 1973; 113—128.

〔21〕 Seckel, G. R.;
A time-sequence oceanographic investigation in the North Pacific trade-wind Zone. *Trans. Amer. Geophy. Union* 49(1)1968; 377—387。

〔22〕 Schroeder, E. H.;
Average monthly temperatures in the North Atlantic Ocean. *Deep-Sea Res.*, 12(3)1965; 323—343

〔23〕 Sharma, G. S.;
Water characteristics and current structure at 65° E during the southwest monsoon. *Jour. Oceanogr. Soc. Japan*, 32(6)1976; 284—296.

〔24〕 Sharma, G. S. , R. Narendran Nair and Basil Mathew;
Current structure in the Intertropical Indian Ocean during the northwest monsoon. *Indian Jour. Mar. Sciences*. 11(1)1982; 7—14.

〔25〕 Suginohara, N.;
An eastward flow at lower middle latitudes derived from a three-layer model of a wind-driven ocean circulation. *Jour. Oceanogr. Soc. Japan*, 29, 1973; 227—235.

〔26〕 Suginohara, N.;
Comment to "On motions in steady, layered, geostrophic models" by C. Rooth, H. stommel and G. Veronis
Jour. Oceanogr. Soc. Japan, 34(6)1978; 268.

〔27〕 Takeuchi, K.;
Two layer model of subtropical front. *Geophys. Bull. of Hokkaido Univ.*, 42,1983; 229—238.

〔28〕 Takeuchi, K.;
Numerical study of the Subtropical Front and Subtropical Countercurrent. Doctoral dissertation, *Jour. Oceanogr. Soc. Japan*, 40, 1984; 371—381.

〔29〕 Tsuchiya, M.;
On the Pacific upper-water circulation. *J. Mar. Res.*, 40(suppl.), 1982; 777—799

〔30〕 Tsuchiya, M.;
Evidences of a double-cell subtropical gyre in the South Atlantic Ocean. *J. Mar. Res.*, 43(1)1985; 57—65。

〔31〕 Uda, M.：
On the Subtropical convergence and the currents in the north-western Pacific. *Rec. Oceanogr. Wks. Japan*, 2(1) 1955; 145—150.

〔32〕 Uda, M. and Hasunuma, K.：
The eastward Subtropical Countercurrent in the western North Pacific Ocean.
Jour. Oceanogr. Soc. Japan. 25(4)1969：201—210.

〔33〕 Voorhis, A. D.;
The horizontal extent and persistence of thermal front. in the Sargasso Sea。
Deep-Sea Res., Suppl. to 16, 331—337(Fuglister Vol.),1969.

〔34〕 Voorhis, A. D. and Hersey, J. B. ：
Oceanic thermal fronts in the Sargasso Sea. *J Geophys. Res.* 69, 1962: 3809—3814.

〔35〕 White, W. B. and Hasunuma, K.：
Quasi-stationary banded structure in the mean zonal geostrophic current regimes of the western North Pacific. *Jour. Mar. Res.* 40(4)1982：1035—1046.

〔36〕 White, W. B. , Hasunuma, K, and solomon. H.
Large-scale seasonal and secular variability of the Subtropical Front in the western North Racific from 1954 to 1974.
Jour. Geophy. Res., 83(C9),1978：4531—4544.

〔37〕 White, W. B. and Walker, A. E. ：

The influence of the Hawaiian Archipelago upon the wind-driven Subtropical Gyre in the western North Pacjfic.
Jour. Geophys. Res. 90(C4)1985：7061—7074。

〔38〕 Wyrtki, K.：
Fluctuations of the dynamic topography in the Pacific Ocean. *J. Phys. Oceanogr.* 5, 1975: 450—459.

〔39〕 Wyrtki, K. and Meyers, G.：
The trade wind field over the Pacific Ocean, Part Ⅱ, Bimonthly fields of wind stress, 1950-1972, Hawaii Institute. *Geophys.*, *Rep.*, (HIG-75-2) 1975：16, 138Figs.

〔40〕 Yoshida, K. and Kidokoro, T.：
A Subtropical Countercurrent in the North Pacific--An eastward flow near the subtropical convergence, *Jour. Oceanogr. Soc. Japan*, 23(2)1967a：88—91

〔41〕 Yoshida, K. and Kidokoro, T.:
A Subtropical Countercurrnt (Ⅱ)--A prediction of eastward flows at lower subtropicl latitudes. *Jour. Oceanogr. Soc. Japan*, 23(5)1967b：231—246

〔42〕 Yoshida' K.：
Subtropical Countercurrents：Band structure revealed from CSK Data, In *"The Kuroshio--A Symposium on the Japan Current"*. 1970：197—244.

〔43〕 Yoshida, K.：
Some aspects of theoretical studies on the Kuroshio—A review. In *"Kuroshio--its physical aspects"* (edited by Stommel H. and K. Yoshida), 1972：443—440.

〔44〕 Yoshida, K.：
Physical Oceanogrophy in Japan--Some topics on the activities during the last ten to twenty years--Science Council of Japan, *Recent Progress of National Sciences in Japan.* 2, 1977：73—82.

A SKETCH OF THE STUDY OF THE SUBTROPICAL COUNTERCURRENT IN THE PAST TWO DECADES

Guan Bingxian
(Institute of Oceanology, Academia Sinica)

Abstract

Two decades have elapsed since the existence of an eastward flow at lower latitudes (the Subtropical Countercurrent) has been discovered from the surface wind stress and hydrographic data (Yoshida & Kidokoro, 1967 and Uda & Hasunuma, 1969). This new finding has deepened the understanding of the circulation structure of the world ocean. It is one of the most important events in the history of the ocean circulation study. Through the efforts of the worldwide oceanographers, an essential and significant progress has been achived. The idea that the Subtropical Countercurrent is quite widespread and not a local phenomenon, and it could be a manifestation of one of the very basic features of the ocean circulation has more and more been accepted by the people.

The study on the Subtropical Countercurrent in the past twenty years is briefly reviewed in this paper. Emphases are laid upon to show the investigations of the basic features of the Subtropical Countercurrent, such as the characteristics of its global distribution, band structure and coexistence with the Subtropical Front. Finally, some possible mechanisms of the Subtropical Countercurrent suggested by some authors are also briefly introduced.

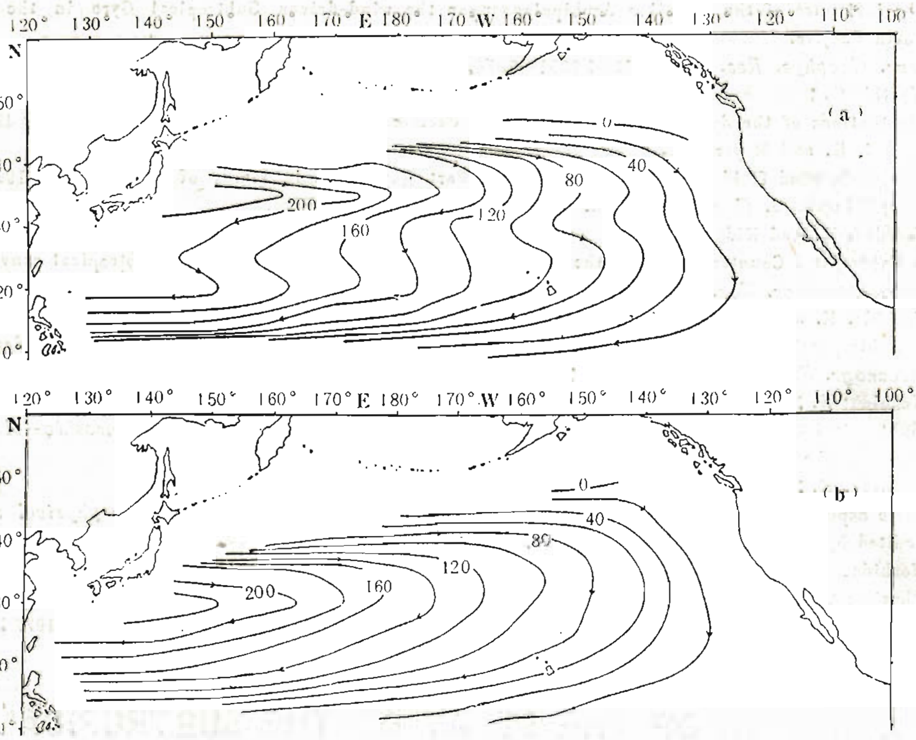

附图 1　北太平洋温跃层深度相对于平均深度的偏差分布图

数字单位为m，箭头表示上层环流方向

(a)——春季(3—5月)　(b)——年平均(根据YK，1967b)

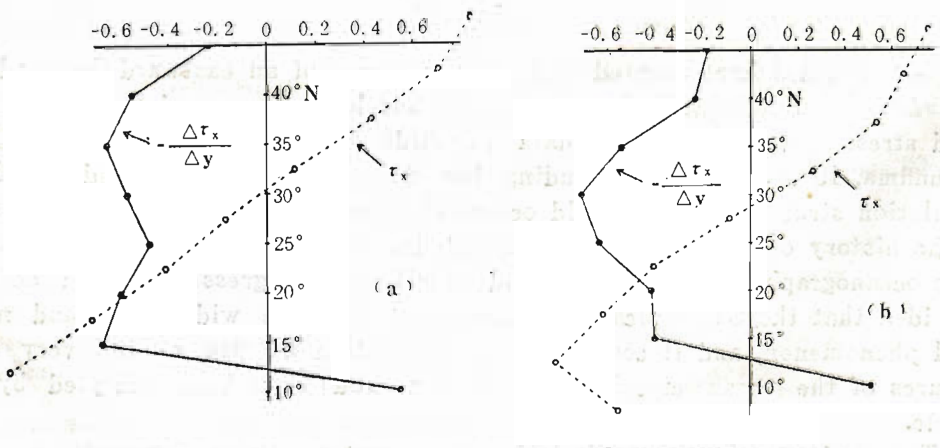

附图 2　纬向风应力(τ_x)及其涡度($-\frac{\partial\tau_x}{\partial y}$)随纬度的分布

(a)——3—5月平均　(b)——年平均　τ_x单位为dy/cm^2　Curl$_z\tau$为$2\times10^{-8}dy/cm^3$

其值均指沿纬圈平均值(根据YK，1967a)

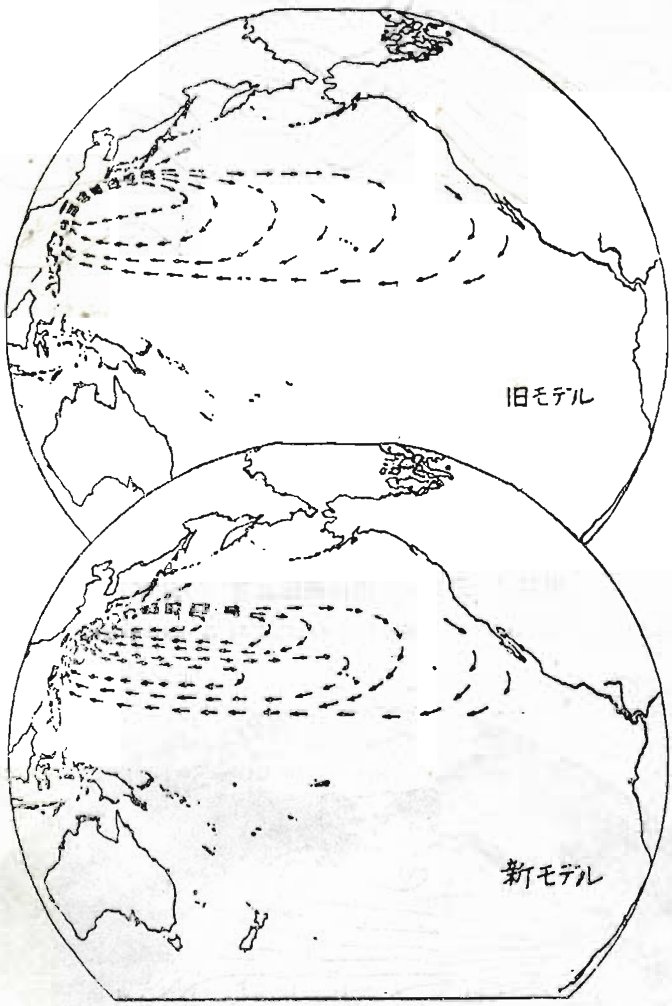

附图 3　吉田描绘的北太平洋副热带流涡新(下)及旧(上)模式

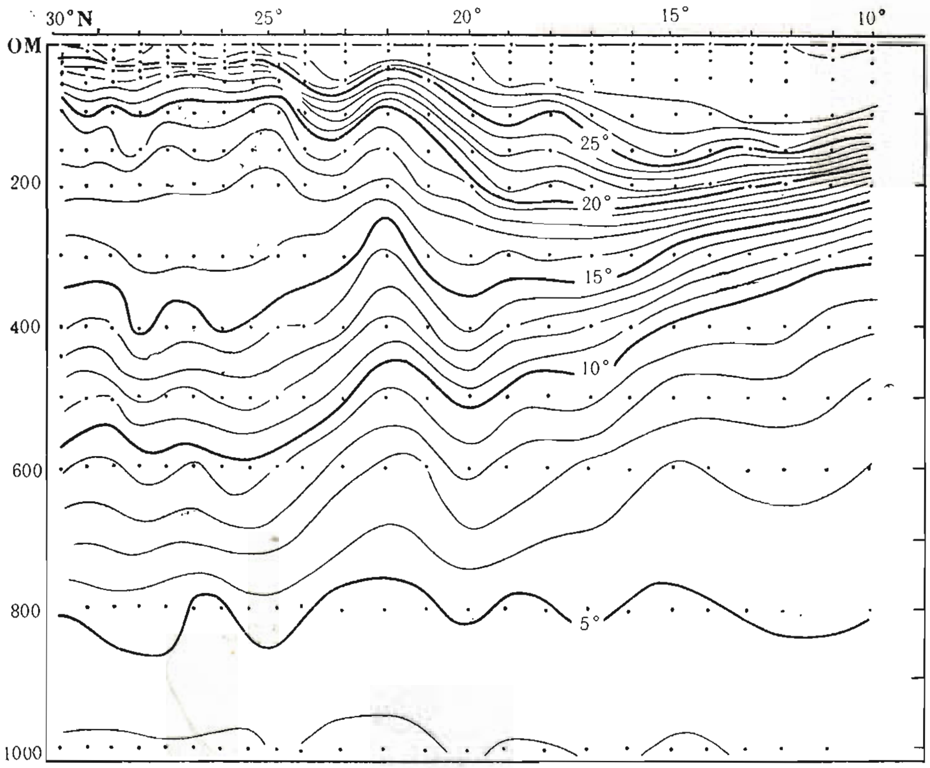

No. 10 Takunan Maru, 140°E, August 1939.

附图 4 沿140°E经向断面温度(℃)分布

1939年8月Takunan 10号丸调查船观测(根据Uda & Hasunuma, 1969)

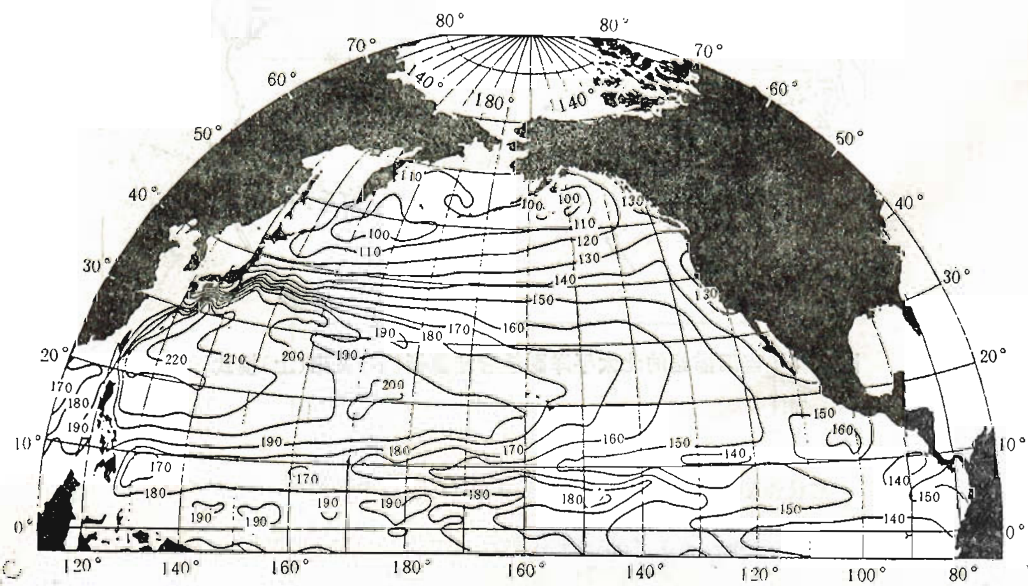

附图 5 北太平洋海面动力高度图

(0/1000×10⁴Pa, dyn·cm, 根据Wyrtki, 1975)

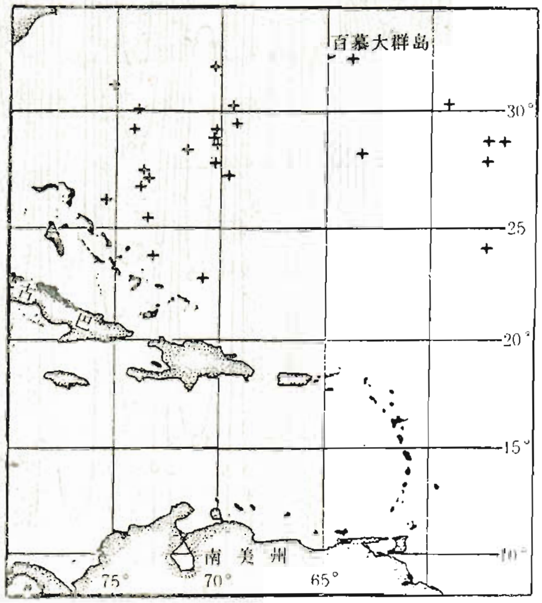

附图 6　北大西洋西部1958—1963年间曾观测到热锋的测站(+)
(根据Voorhis & Hersey, 1964)

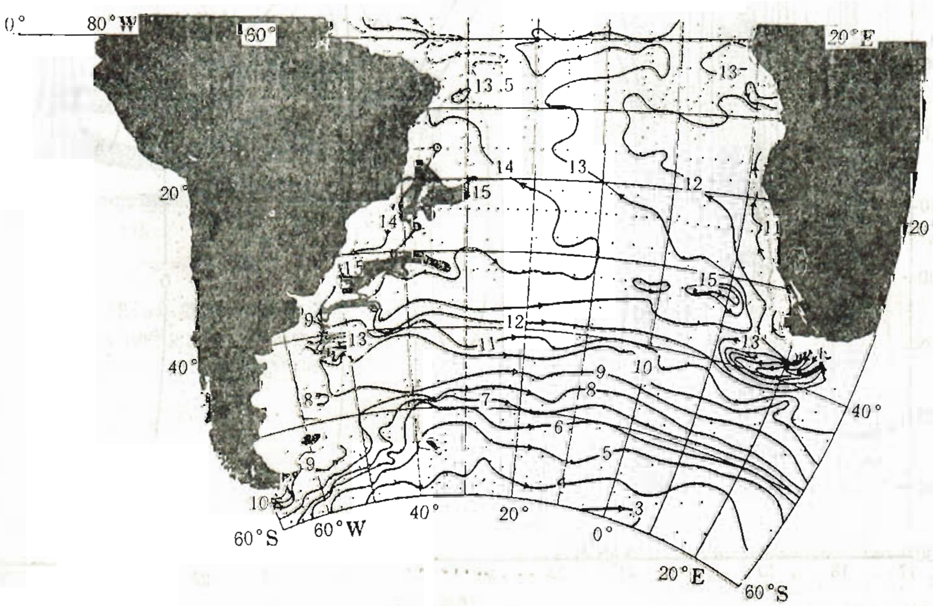

附图 7　南大西洋海面动力高度
(0/1000×10⁴Pa，单位$m^2 \cdot s^{-2}=0.1dyn \cdot m$)(根据Tsuchiya，1985)

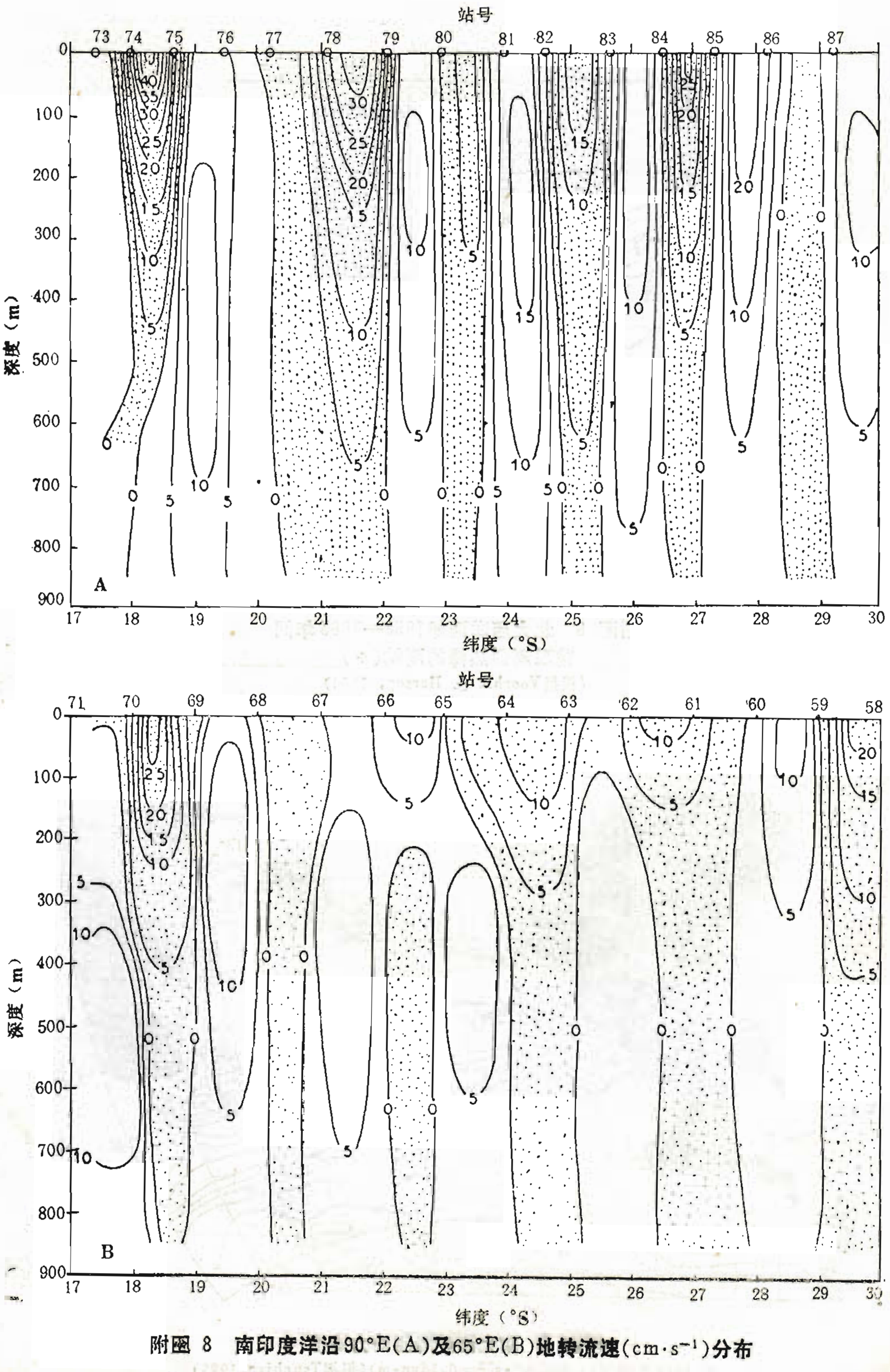

附图 8 南印度洋沿90°E(A)及65°E(B)地转流速(cm·s⁻¹)分布

(相对于1000×10⁴Pa,阴影区流向指东，根据Basil Mathew等,1982)

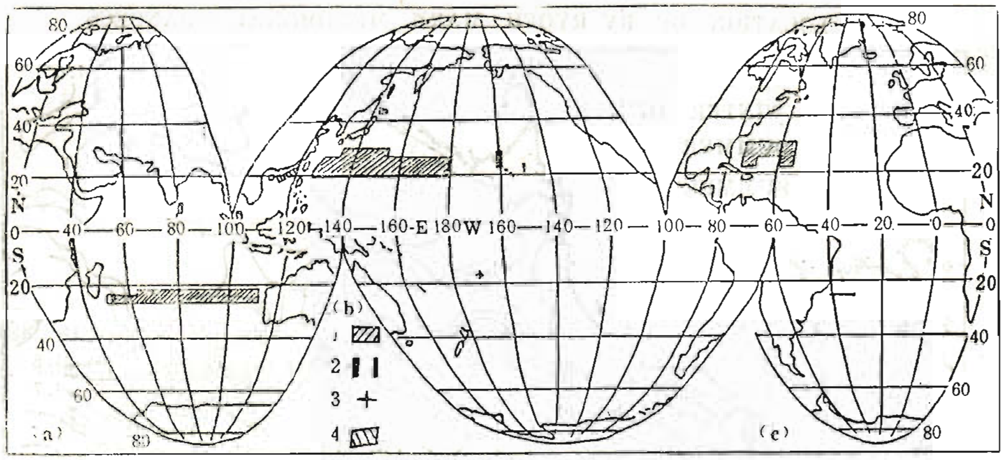

附图 9　副热带逆流的全球性分布

(a)——Sharma(1976,1982),22—26°S,5—6月；20—26°S, 50—110°E, 11—12月

(b)——1. YK(1967a, b), Uda & Hasunuma(1969), White & Hasunuma(1982)

　　2. Seckel(1968), Reed(1968)　3. Merle et al(1969)　4. 管(1978),管、陈(1964)

(C)——Voorhis & Hersey(1964),Voorhis(1969),Katz(1969),22—32°N,57—75°W；

　　——Tsuchiya(1985)

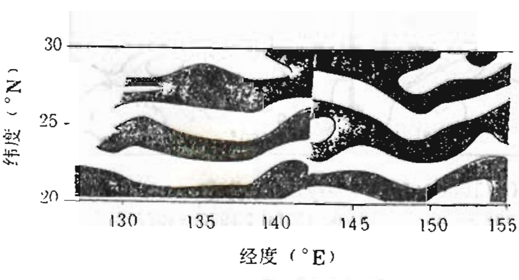

附图10　1965—1966年冬200m层上温度经向梯度

阴影区域表示温度向北减少，即为密度正梯度及东向流(根据Yoshida,1970)

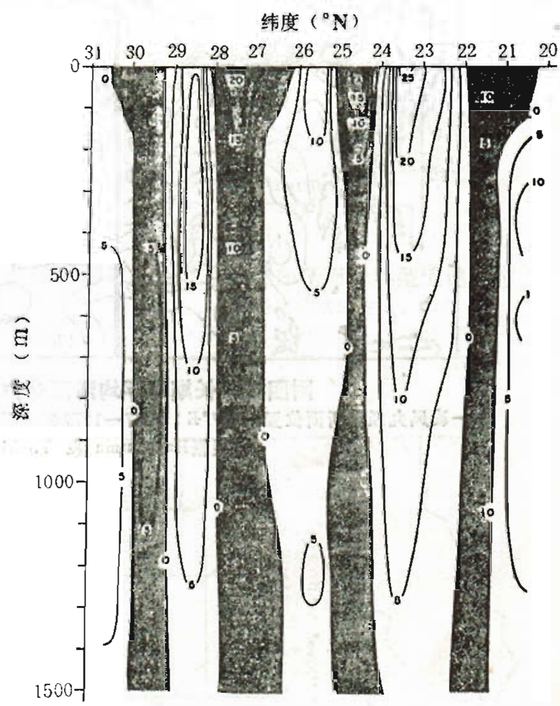

附图11　1965—1966年冬127—155°E间纬向平均地转流速(cm·s⁻¹，相对于2000×10⁴Pa面)分布

(根据Yoshida,1970)，阴影区域流向指东

LOCATION OF RV RYOFU MARU MERIDIONAL TRANSECS

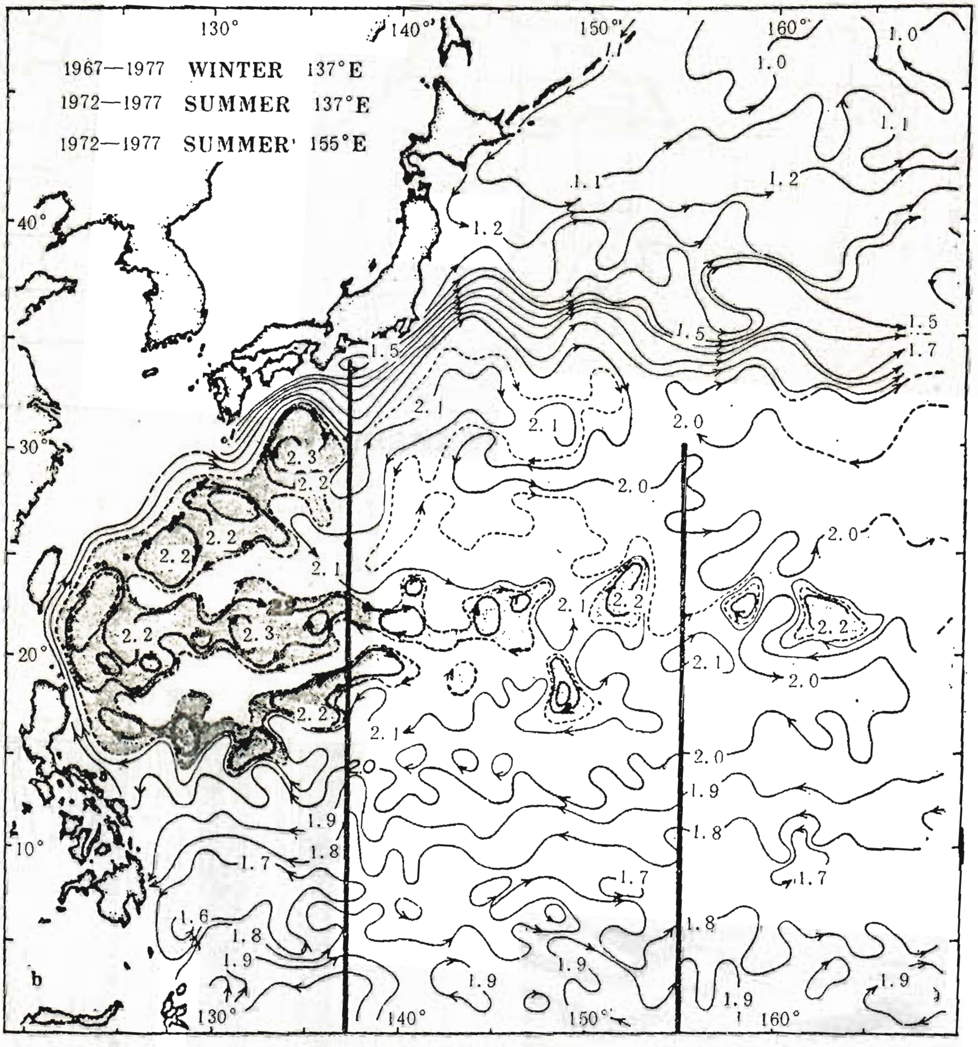

附图12 长期年平均海面动力高度($0/1000\times10^4$Pa, dyn·m)分布

——凌风丸经向断面位置；137°E：1967—1977冬季观测、1972—1977夏季观测；155°E：1972—1977夏季观测

（根据Hasunuma & Yoshida,1978）

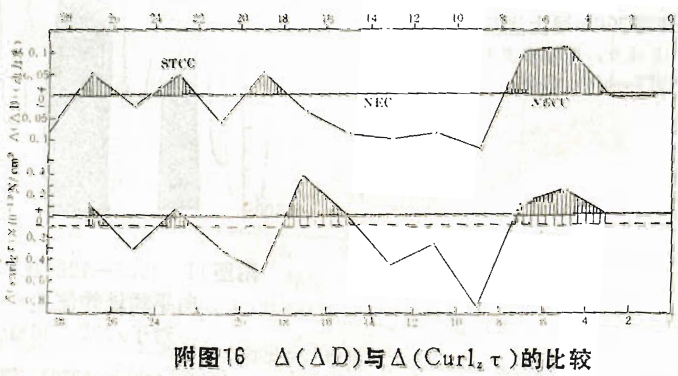

附图16 Δ(ΔD)与Δ($\mathrm{Curl}_z\,\tau$)的比较

（图中横坐标为°N）

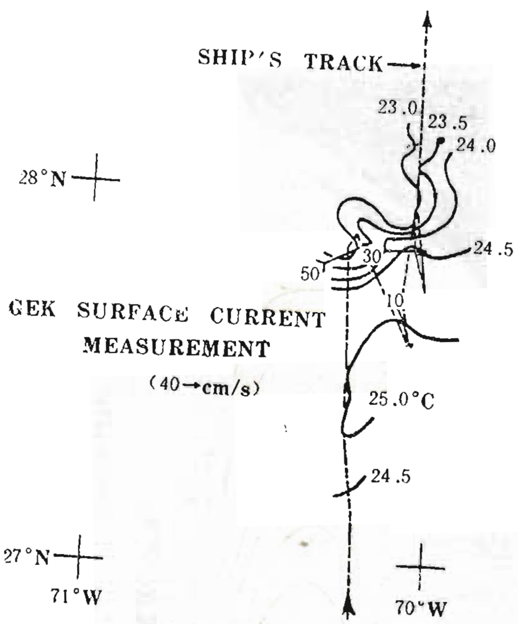

附图13　1962年12月10日 Chain 号测得的 30m层温度(℃)及表层流($cm \cdot s^{-1}$)

…→航线　40›—→GEK表层流观测结果($cm \cdot s^{-1}$)
(根据Voorhis & Hersey, 1964)

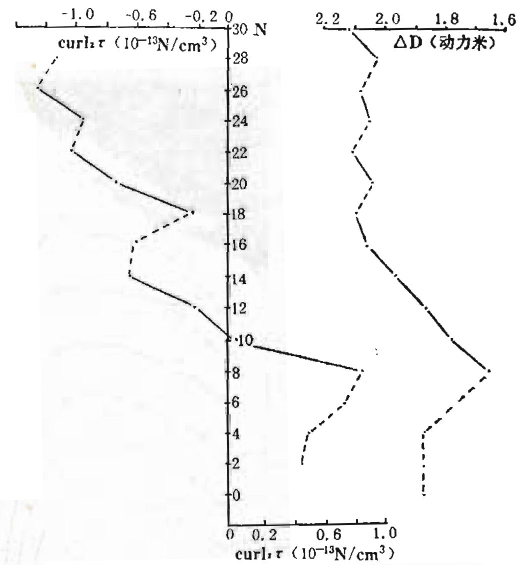

附图15　海面动力高度偏差(ΔD, 沿137°E)与风应力涡度 $Curl_z\tau$)两者经向分布的比较

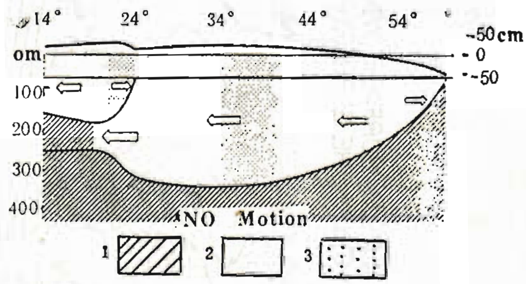

附图17　大洋中部经向断面的典型流速分布

箭矢表示各层经向输送的方向，影区流向指东(根据Suginohara,1973)

1 ——无运动　2 ——西向流　3 ——东向流

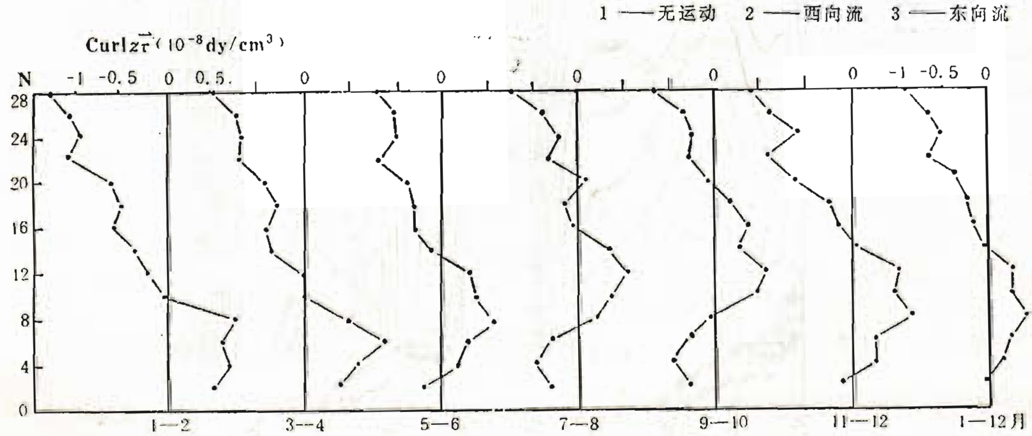

附图14　纬图平均(1950—1972)风应力涡度($Curl_z\vec{\tau} \times 10^{-13}N/cm^3$)经向分布曲线

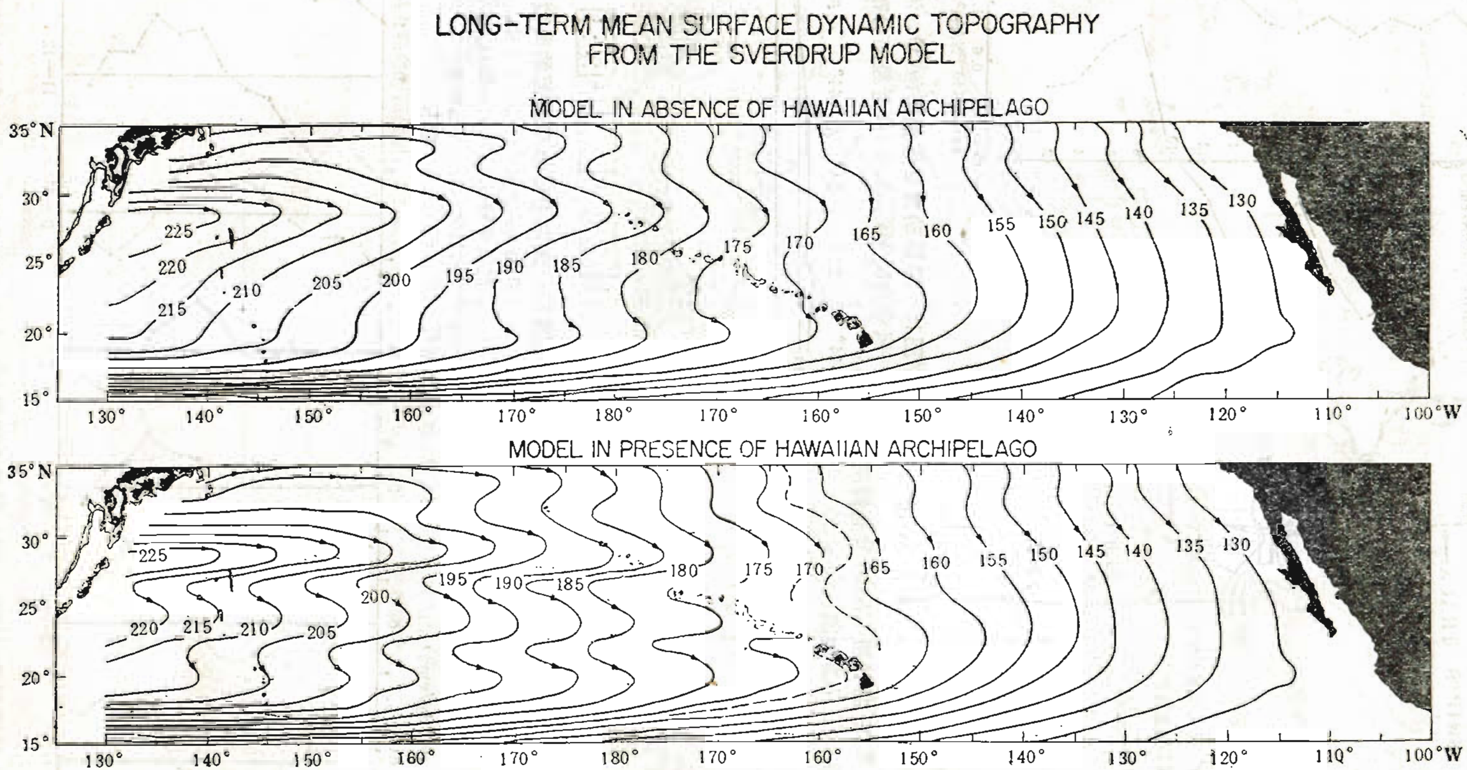

附图18 北太平洋副热带区域海面动力高度模式图

不考虑夏威夷群岛(上)及考虑夏威夷群岛(下)的情况(根据White & Walker,1985)

北太平洋西部低纬区域环流结构和海--气相互关系的若干特征

管 秉 贤

(中国科学院海洋研究所，青岛)

这是指赤道以北，35° N以南，西边界以东，150° E以西的海域。主要风带有赤道无风带，东北信风带，北部还带上西风带的一点边。 主要流系自北向南有黑潮 (K)，北赤道流 (NEC)，北赤道逆流 (NECC) 及赤道潜流 (EUC)，还有 60 年代下半期发现的位于副热带较低纬度处的副热带逆流 (STCC)。 按传统的概念，北赤道流 -- 黑潮 -- 黑潮延续体 -- 北太平洋流 -- 加里福尼亚流构成了副热带流涡 (Subtropical Gyre)。与我国关系密切且感兴趣的是副热带流涡的西端部分 (Western S G)。 北赤道流，北赤道逆流及赤道潜流构成了北太平洋赤道流系。下面根据作者近年来在这方面的工作， 简述有关这些流系结构及海 -- 气相互关系的一些特征，供研究大洋环流问题参考。

1．副热带流涡西端部分的结构

副热带流涡的西端部分 (W S G) 是北太平洋西部环流最显著的特征之一。传统上认为，副热带流涡是单一结构，此即“单涡”说。 Stommel (1948) 和 Munk (1950) 的模式就是这样的。 自从副热带逆流被发现后,吉田和城所 (Yoshida & Kidokoro, 1967) 提出 W S G 不是单一的，而是分裂为两个反气旋涡,中间隔着一个狭窄的气旋涡这种观点。 这就是吉田的“双涡”或“二脊一槽”说 [18]。 这是 60 年代海洋学发展史上的重要事件，动摇了人们对大洋环流结构的传统认识。

后来，蓮沼和吉田 (Hasunuma & Yoshida, 1978) 根据长期平均资料及 1974 年 2 -- 3月的天气式调查资料又进一步提出 W S G 含有三脊二槽， 并且三脊在其西端相联。 三脊即黑潮脊 (K R)，热带脊 (T R) 和北赤道脊 (N E R)。 二槽即副热带槽 (S T T) 和热带槽 (T T)。 这就是“多涡说” [10]。

二十年来对副热带逆流的研究发现， 东向的副热带逆流是一种带有全球性的现象，可能是大洋环流的最基本特征之一 [1，2]。 所以，大洋环流中的副热带流

刊于《海洋环流研讨会(北京,1989)论文选集》

涡模式不应是单涡而应是多涡。

但是到底是双涡或三涡，这问题还没有一个共同的认识。

测站最密，观测时间最接近的 1965 ~ 1966 年冬季海面动力高度（ 见图 1, 0 / 1000 db ）分布表明，在 140° E 以西及 15° N 以北海域，W S G 确实不象传统概念所描述的为单一流涡，但其结构又与莲沼和吉田（ 1978 ）的“三脊二槽”模式有所不同。 从这一时期的分布来看，W S G 为二脊一槽，即黑潮脊（ K R ），副热带槽（ S T T ）和北赤道脊（ N E R ）。 而且副热带槽向西深展， 所以二脊在西端并不相联结。 热带脊和热带槽甚弱或不明显。 这种分布与吉田和城所 (1967) 的模式更为近似（ 管，1989 b ）[4]。 所以，W S G 虽非单涡， 而分裂为二个或多个，但其天气式的“细”结构并非固定不变，却随季节或年际而变（管，1989b) [4]。 这种变异的机制是北太平洋环流研究中的一个重要问题。

早年，吉田和城所（ 1967 ）在解释副热带逆流的形成原因，即双涡机制时，曾认 为 这 支 东向流与风应力负涡度经向分布曲线上的极小值（ 即“槽”）相对应 [13]。 也就要说，双涡结构是由风应力涡度经向分布上出现“槽”导致的。 但是，后来的研究，如杉ノ原伸夫（ Suginohara, 1978 ）[14]， 竹内谦介（ Takeuchi, 1984 ）[15], Cushman-Roisin（ 1984 ）[5], White & Walker （ 1985 ）[16] 等却认为风应力涡度经向分布上没有“槽”结构，也能形成副热带逆流，即流涡会分裂成多个。 迄今为止，关于“双涡”或“多涡”的机制问题，还没有得到圆满的解决。

2． 地转流的带状结构

本海域上层的纬向地转流，边界分明，呈明显的带状结构。 虽然，用风应力涡度经向分布上的“槽”结构来阐明副热带逆流的形成机制还没有为大家所广泛接受，但是，地转流的带状结构与风应力涡度分布有着密切的关系，这是十分明确的（ 管，1989b ）[4]。

图 2a 给出了海面动力高度偏差（ ΔD, 0/1000db ）和相应的纬向平均风应力涡度（ Curl τ ）两者的经向分布。 站距均为 2 个纬度。 ΔD 是沿 137° E 断面六冬（ 1967-72 ）的平均值，Curl τ 是七冬（ 1966-72 ）的平均值。

比较表明，风应力涡度和海面动力高度两者的经向分布几乎互相平行。即当风应力涡度向北增加时，相应地动力高度偏差向北减少，这是东向流的情况。反之，是西向流的情况。

我们又比较了动力高度偏差和风应力涡度两者的经向梯度（$\Delta(\Delta D)$, $\Delta Curl\,\tau$）的关系，如图 2b 所示。这种动力高度偏差的经向梯度就代表了纬向流。自赤道向北相继出现：

1）东向的北赤道逆流（3° -- 8° N），与 Curl τ 的正梯度带（3° -- 7.5° N）相对应；

2）西向的北赤道流（8° -- 18° N），与Curl τ 的负梯度带(7.5° -- 15° N)相对应。

3）三支宽度各为 2 个纬度的东向流（中心位于 19° N，23° N及27° N附近）与Curl τ 的三个正梯度带（中心位于 17° N，23° N 及 27° N 附近）相对应。这三支东向流组成副热带逆流。在相邻两支东向流之间，各为一西向流，它与Curl τ 的负梯度带相对应。除 19° N 附近的东向流与以 17° N 为中心的 Curl τ 的正梯度带位置略有偏移外，两者的关系十分紧密，几乎是一一对应的（管，1989b）(4）。

所以，定性地讲，自赤道至 28° N，主要平均纬向地转流沿 137° E 的带状结构是与纬向平均风应力涡度的经向分布紧密相关的，这是大尺度海--气相互关系的一个好例（管，1989b）(4）。从这一结果可以引伸出，副热带流涡西端部分的结构（为“双涡”或“多涡”）主要当视上空的风应力涡度场而定。风应力涡度场若有变异，W S G 的结构亦将随之而异。

3．棉兰老冷涡的变异与 El Nino 的关系

棉兰老气旋型涡旋（简称冷涡）是棉兰老岛与新几内亚岛之间最突出的现象之一。它与黑潮在巴士海峡以东的暖涡，在机制上有相似之处，但它比后者更为复杂。首先，它位于西向的北赤道流，南向的棉兰老流和东向的北赤道逆流之间。同时，它毗邻西太平洋的热库（Warm pool），后者被认为是引发 El Nino 的关键性区域之一。冷涡的变异当受到这些因素的影响。

这个冷涡早在 30 年代，肥沼宽一 (Koenuma, 1937) [11] 就已指出过。后来，Wyrtki (1961) [17] 也作过研究。冷涡核心部分的水文结构是一个具有低温和低盐特征的水体。在 200m 层上，冷涡中心的温度 < 10° C，盐度低于34.4‰。所以，这个冷涡与一般的冷涡有所不同，它不是低温高盐，而是低温低盐。同时它在垂向上延伸不深，大概只有 400~500m 深 (管，1989a) [3]。

研究发现，这个冷涡的变异与 El Nino 有着密切的关系。图 3 给出了 1965 - 1966，1967，1968 及 1969 四个冬季海面动力高度偏差 (0/1000db) 的分布。在北赤道流与北赤道逆流最西端之间出现了一个趋于封闭的低槽。1967 年由于 130° E 以西缺少资料，只见半个涡。图中带影线的是冷涡核，涡核中心位于 7° N 附近。在非 El Nino 年 (1967，1968)，冷涡在不同程度上向西收缩，并趋于封闭，1967 年冬季收缩最甚。在 El Nino 年 (1965-1966，1969)，冷涡在不同程度上向东扩展。在 1965-1966 年中等型 El Nino 期间，冬季冷涡向东扩展最远而呈带状。在 1969 年弱型 El Nino 期间，冬季冷涡亦较非 El Nino 年 (196 8) 为扩展。所以，在这四个冬季，冷涡向东扩展或向西收缩的程度是与这几年是否出现 El Nino 及其强弱相联系的 (管，1989a) [3]。

对于 70 年代及 80 年代初期的几次 El Nino，没有类似的海面动力高度图可资比较。但可利用 137° E 断面的水文观测资料以及 Malakal 站 (7° 20'N，134° 28'E) 的月平均水位资料，对上述关系作出类似的检验。Malckal 站位于帕劳群岛上，是最接近冷涡的一个海岛水位观测站，可以监测冷涡的变化。检验发现，上述关系仍然存在。即：在 El Nino 年期间，冷涡低比容水位 (即低动力高度) 范围向东扩展和 (或) 冷涡毗邻区域的水位比正常偏低，因而冷涡变得较强。反之，在非 El Nino 年期间，冷涡低比容水位的范围向西收缩和 (或) 冷涡毗邻区域的水位比一般偏高，因而冷涡变得较弱。当然，冷涡强化的程度并非总与 El Nino 的强度相对应。这显然是由于 El Nino 仅是影响或控制冷涡变化的主要因素之一而已。这个冷涡显然还要受到周围流场，即北赤道流、棉兰老流和北赤道逆流的影响 (管，1989a) [3]。

上述关系的机制可用赤道太平洋热结构对大气扰动力或风场变异的响应来阐明。在一般信风情况下 (即非 El Nino 年)，水位向西上升，温跃层加深，亦即海面比容水位升高，低比容水位范围缩减，即冷涡变弱。在信风衰弱而西风增强时 (即 El Nino 年)，海水向东倾泻，导致西太平洋水位下降和温跃层上升，亦即海面比

容水位下降，低比容水位范围扩大，因西部受阻于边界，才向东展延，即冷涡变强（管，1989a）[3]。

所以，结论是：棉兰老冷涡的上述变化与 El Nino 之间的这种局部性中尺度关系是与赤道太平洋海--气变异之间的总的大尺度关系相一致的（管，1989a）[3]。

4．赤道潜流的变异及其与 El Nino 的关系

从 1972 -- 1983 年间冬、夏两季的海流实测资料中可以看出，太平洋西端部分（以 137° E 线为例）的赤道潜流与其以东部分（以 155° E 线为例）的赤道潜流是大有不同的（Guan，1986）[7]。

在 155° E 线上，在赤道及跃层深度处，为强而典型的东向赤道潜流，流速结构与赤道对称，最大流速可达 90 cm/s 以上（1973 年 6 月）。

在 137° E 线上，在赤道及跃层深度处，除个别时期外，大部为西向流。在赤道以北（1° - 2° N）才观测到东向流。同时，与 155° E 线上的东向赤道潜流相比，137° E 线上的东向流尺度较小，流速较弱。这里的东向流，我们称之为"赤道潜流之源"（Origin of EUC）。我们认为，赤道潜流之源的位置偏于赤道以北与 137° E 线赤道离新几内亚岛海岸很近（＜60 海里）有关，使得东向流核北移（Guan，1986）[7]。海岸对赤道潜流的位置发生如此明显的影响，值得从动力学上进一步予以研究。

1981 年 1 -- 2 月（图 4a）及 6 -- 7 月（图 4b）间的海流观测资料为赤道潜流之源位于赤道偏北 1° -- 2° N 处提供了最明显的证据。在这两幅图上还可以看到与潜流之源相邻的南赤道流（S E C），北次表层逆流（N S C C）和北赤道逆流（N E C C）等等。

潜流之源在 1972 - 83 年间也经历了显著的变化。特别是在 1982 年夏季（6 月 30 日 -- 7 月 2 日），潜流之源在赤道附近处（1° S -- 2° N）突然消失了，这里为西向流所取代，在赤道上最大的西向流速达到 60 cm/s（图 5）。

137° E 线上赤道潜流之源在 1982 年 6 -- 7月间突然消失，这不是孤立事件。在这之后，在中太平洋（ 159° W ）和东太平洋（ 110° W ），赤道上也相继出现东向潜流变弱或消失为西向流所取代的情况，也就是说， 赤道潜流的逆向现象是自西向东传播的（ Guan，1986 ）[7]。

159° W 线上：根据 Firing 等（ 1983 ）[6] 的观测，这一经度处的赤道潜流，在 1982 年 8 月，EUC 的上、中部消失；到 9 月至 10 月西向流出现在 EUC 的流核处。 这是海洋观测史上首次在中太平洋未能观测到 EUC。 同年 9 月进行的沿 159° W 经线的海流观测进一步表明，EUC 是真的消失，而不是移离赤道。 到 1983 年 1 月 EUC 很快在 159° W 线上再现。

110° W 线上：根据 Halpern（ 1983 ）[9] 的观测，这一经度处的赤道潜流是在 1983 年 1 月 10 日 -- 2 月 10 日期间转变为西向流的，整整消失了一个月。到 1983 年 2 月15 日东向流再次出现。

所以， 从 137° E，159° W 及 110° W 三个经线上看，赤道及其附近处潜流的消失现象自西向东传播：6 - 7 月在 137° E， 9 月在 159° W，潜流消失现象的传播速度约为 1.1 m/s（ Cuan，1086 ）[7]。 在 110° W 处这现象落后于 159° W 处的约 4.5 月，传播速度约为 0.5 m/s（ Halpern，1983 ）[9]。 所以，潜流消失现象自西太平洋向中、东太平洋传播的速度约为 0.5 - 1.0 m/s ， 这相当于斜压 Kelvin 波的传播速度。

根据 Firing 等（ 1983 ）[6] 的研究， EUC 1982 年 9 月在 159° W 经线上的消失现象与 1982 - 1983 年的强 El Nino 事件密切相关。 西太平洋和中太平洋出现的强西风导致了El Nino，并使整个海盆的海面坡度进行了调整。 这种调整与 EUC 的消失相一致。 他们还进一步认 为， 那 里 EUC 的消 失是与 Christmas 岛（ 157° W ）上当时水位出现峰值及局地信风消失相一致的，因而又与那里 EUC 流核处出现弱西向流相一致。

异常西风首先是在西太平洋（ 140° E ）于 6 月间出现的，而后向中太平洋及东太平洋传播。

我们认为， 1982 年 6 月 - 7 月 间 137° E 线上赤道潜流之源的消失是 与 1982 年 6 月 140° E 处首先出现异常西风密切相关， 即与 1982 - 83 年 的 强

El Nino 事件有关（ Guan，1986 ）[7]。 1972 年 7 月及 1976 年 7 月在 137° E 线上也曾观测到类似情况(图略)。 西太平洋的异常西风改变了137° E 线上海面的纬向坡度，从而也改变了海水中的压力梯度， 导致那里的东向流减弱或竟为西向流所取代。

所以， 在 1982 - 83 年 El Nino 期间，首先在西太平洋出现而后向中、东太平洋传播的洋流异常现象可与相应的大气异常现象相比拟。 El Nino 通常可用海面温度、水位、风、降水及水文结构的变异来描述。 上 述分析表明，赤道潜流在 El Nino 期间也象风向一样要逆转。 所以，El Nino 事件也可用赤道潜流的消失现象来描述。

5．台湾和菲律宾以东海域的深层流

上面简述了这一海区主要纬向流的特征，下面再简述西边界附近经向流的特征，这主要涉及台湾和菲律宾以东附近海域的深层流。

台湾和菲律宾以东附近海域的上层流， 包括著名的西边界强流黑潮都是自南向北流的，即极向的。 关于这里 2000 -- 3000 米深层处的海流，按照Stommel-Arons（ 1960、1971 ）的深层流模型，其西边界流也是北向的。 Moriyasu（ 1972 ）[12] 及 Reid（ 1981 ）[13] 的研究也得出了类似的北向流结果。

但是，最近我们分析了两组 1968 年及 1969 年观测的深水站（ 观测深度达到 3500 -- 4000 m 或以上 ）水文资料，却得出了不同的结果， 即在台湾和菲律宾以东附近的深层海域，存在着主要是流向南的，即赤道向的海流。 这是值得重视的（ 管，1990 ）[8]。

动力零面取得很深（ 3500db ）的地转流计算结果指出，在台湾东南海域， 在强大的黑潮上层流下面，自600 -- 700 m 以深即出现南向逆流， 流层很厚， 可达 2000 -- 3000 m，在 1500 m 层处最大逆流流速可达 4.5 cm/s。 在水文结构上，南向逆流的存在与台湾东南海域的等温线分布，自 700 -- 800 m 层以深， 由自东向西上倾变为自东向西下倾相对应（ 管，1990 ）[8]。

类似地，在 130° E 以西至 125° E，大约在 15° N 以北附近的海域， 这里的上层流主要为一反气旋环流，大部分海水自西南流向东北。 但在 1500 -- 2000 m 层上，相应区域却为气旋式流动，大部分海水自北流向南， 与上层形成了明显的不同（ 图 6a，b ）。 在水文结构上， 南向逆流的存在与 2500 m 深层上下出现一块低温水相对应（ 管，1990 ）[8]。

我们认为， 上述两例中上层为北向流而深层为南向逆流，其成因与上层流在北向流动中遇到了台湾东北角的海脊（ 苏澳 -- 与那国岛海脊 ） 以及以东的琉球群岛岛架有关，即主要是由于地形阻塞作用形成的， 使北向流遇到海壁有一部分海水下沉转为南向回流。 当然也有一部分海水将仍然沿着海壁向东或东北流去（ 管，1990 ）[8]。

通过这一深层西边界流特征的分析，可以看出，在边界附近地形的影响很重要，从而海流在垂直方向上的分层异向现象也很显著。 所以在海流的数值模拟中，应该采用分层模式。

参　考　文　献

[1] 管秉贤,1987。副热带逆流二十年研究概况。　黄渤海海洋　5(4):65-72.

[2] ------,1988。副热带逆流二十年研究概况(续)。黄渤海海洋　6(1):71-86.

[3] ------,1989a。棉兰老冷涡的变异及其与El Nino的关系。海洋与湖沼　20(2): 131-138.

[4] ------,1989b。台湾与菲律宾以东海域冬季的环流结构及其变异。海洋与湖沼 20(5):393-400。

[5] Cushman-Roisin,1984. An explanation for the subtropical front-without Ekman convergence. Ocean modelling 54(1984,Feb.):5-7.

[6] Firing,E.,R. Lukas,J.Sadler and K.Wyrtki,1983. Equatorial Undercurrent disappears during 1982-1983 El Nino. Science, 222: 1121-1123.

[7] Guan,B.X.,1986. Current structure and its variation in the equatorial area of the western North Pacific Ocean. Chin.J.Oceanol. Limnol.4(3):239-255。

[8] -----,1990. A note on the deep circulation in the area east of Taiwan and the Philippines. To appear in Chin.J.Oceanol. Limnol.8(2).

[9] Halpern,D.,1983. Variability of the Cromwell Current at 110° W before and during the 1982-1983 warm event. Trop.Ocean-Atmos. Newslett.21:31-34.

[10] Hasunma,K. and K.Yoshida,1978. Splitting of the subtropical Gyre in the Western North Pacific. Jour.Oceanogr.Soc.Japan, 34(4):160-172.

[11] Koenuma,K.,1937. On the hydrography of the southwestern part of the North Pacific and the Kuroshio. Part I:General oceanographic features of the region. The Memoirs of the Imperial Marine Observatory Kobe, Japan. 6(1):279-332.

[12] Moriyasu,S., 1972. Deep waters in the western North Pacific. In: Kuroshio-Its physical aspects (edited by H.Stommel and K.Yoshida), University of Tokyo Press, 387-408.

[13] Reid,J.L.,1981. On the mid-depth circulation of the world ocean. In: Evolution of the Physical Oceanography (edited by B.A. Warren and C.Wunsch), 70-111.
[14] Suginohara,N.,1973. An eastward flow at lower middle latitudes derived from a three-layer model of a wind-driven ocean circulation. Jour.Oceanogr. Soc.Japan.29:227-235.
[15] Takeuchi,K.,1984. Numerical study of the Subtropical Front and Subtropical Countercurrent. Jour.Oceanogr.Soc.Japan. 40: 371-381.
[16] White,W.B.,and A.E.Walker,1985. The Influence of the Hawaiian Archipelago upon the wind-driven Subtropical Gyre in the western North Pacific. Jour.Geophys.Res. 90(C4): 7061 - 7074.
[17] Wyrtki,K.,1961. Scientific results of marine investigation of the South China Sea and the Gulf of Thailand.1959-1961. Naga Report,2:1-195.
[18] Yoshida,K.,and T.Kidokoro,1967. A Subtropical Countrcurrent(II)-- A prediction of eastward flows of lower subtropical latitudes. Jour.Oceanogr. Soc. Japan, 23(5):231-246.

Some Features of the Current Structure and Air and Sea Correlation in the Area of low Latitudes of Western North Pacific Ocean

Guan Bingxian

(Institute of Oceanology, Academia Sinica, Qingdao)

Abstract

Baced upon the studies made by the author in recent years, some features of the current structure and air and sea correlation in the area of low latitudes of western North Pacific Ocean are briefly depicted in this paper. Emphases are laid upon the following topics:

(1) Current structure of the western Subtropical Gyre;
(2) Banded structure of the geostrophic current field;
(3) Variation of the Mindanao Cold Eddy and its relation with El Nino;
(4) Variation of the Equatorial Undercurrent and its relation with El Nino; and
(5) Deep currents in the area east of Taiwan and the Philippines.

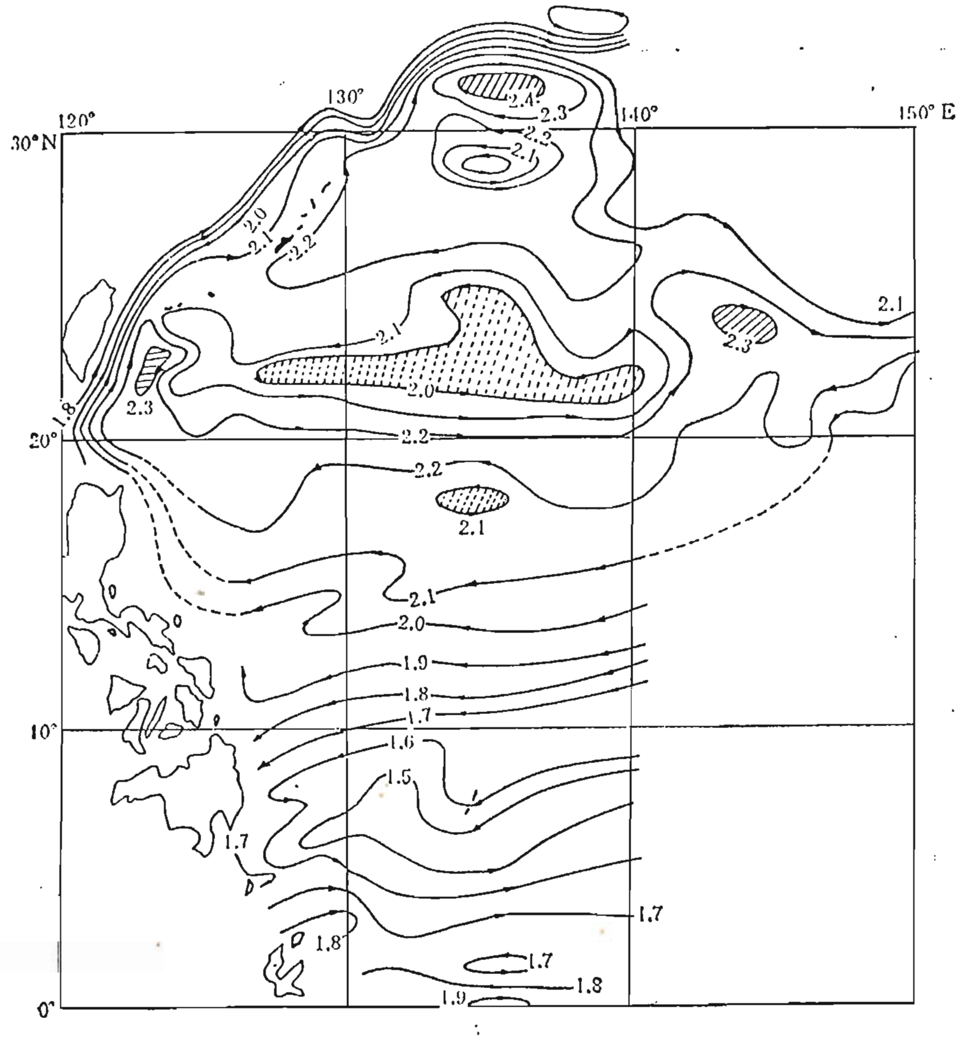

图1. 1965～1966年冬季海面动力高度(0/1000db, dyn.m)分布图（转引自管, 1989b）

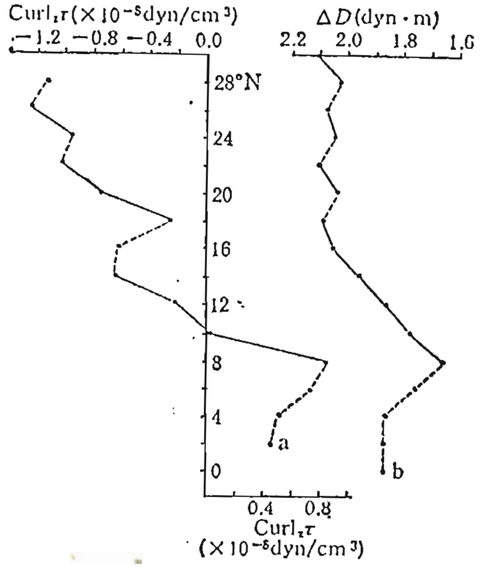

图2a. 风应力涡度(a, Curl$_z\tau$)及海面动力高度(b, △D)的经向分布(根据管, 1989b)

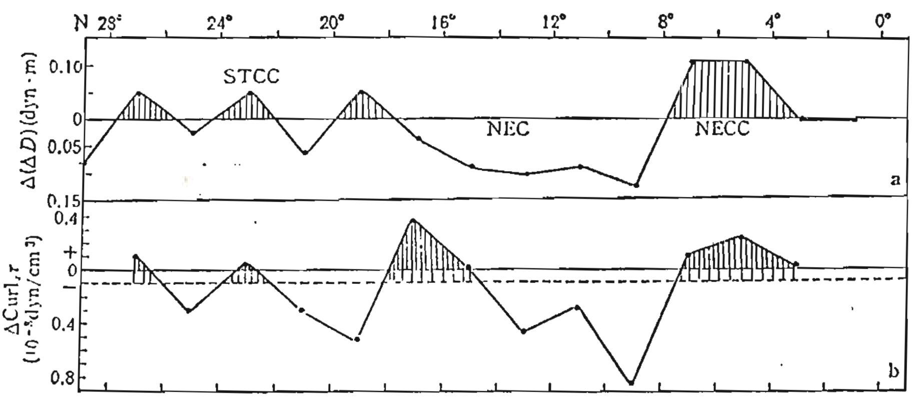

图2b. △(△D)(a)及△Curl$_z\tau$(b)的经向分布(根据管, 1989b)

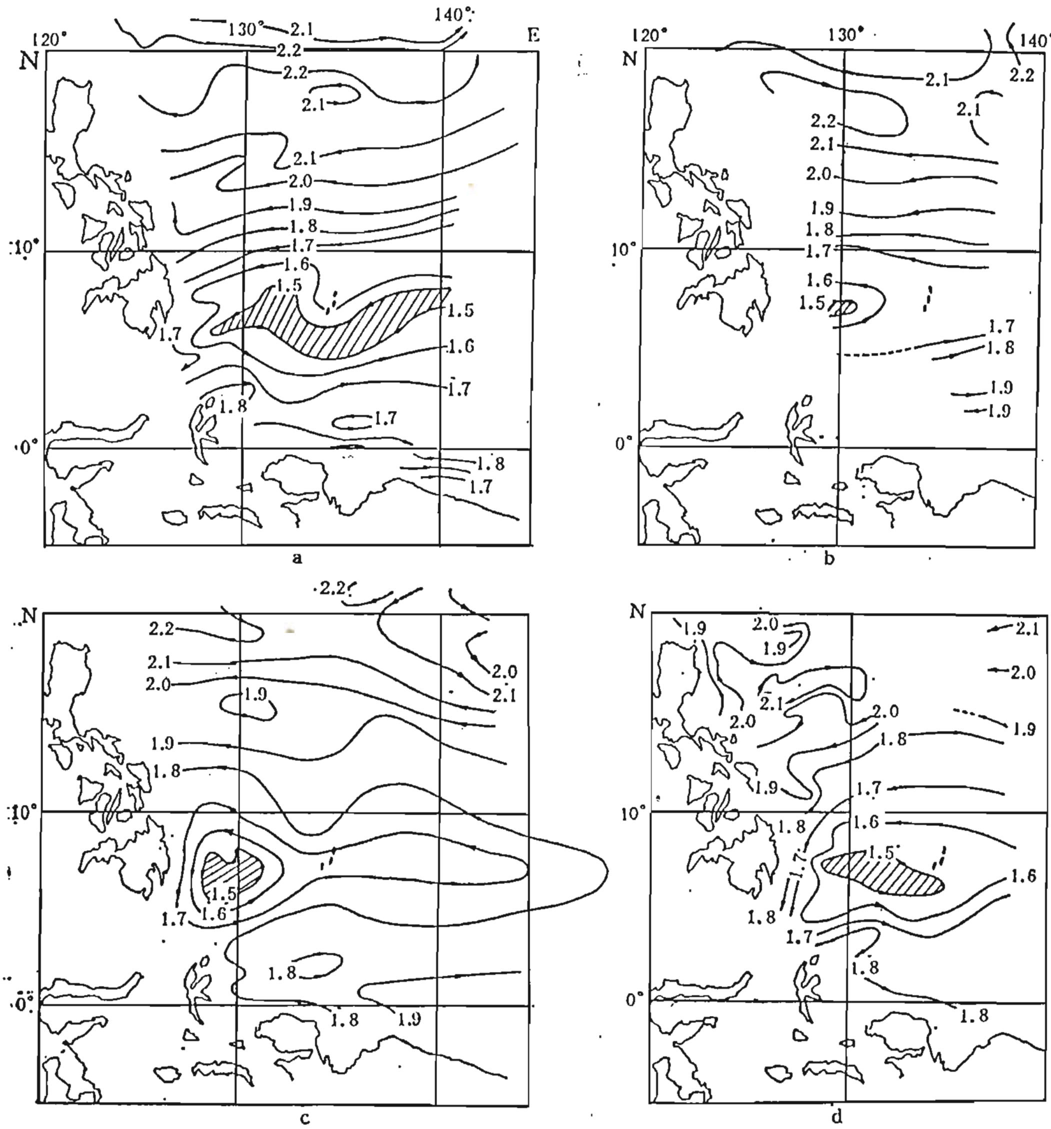

图3　棉兰老涡旋及其附近区域海面动力高度(0/1000 db, dyn.m.)的分布

a. 1965～1966年冬季；　b.1967冬季；

c. 1968年冬季；　d.1969冬季。

(转引自管，1989a)

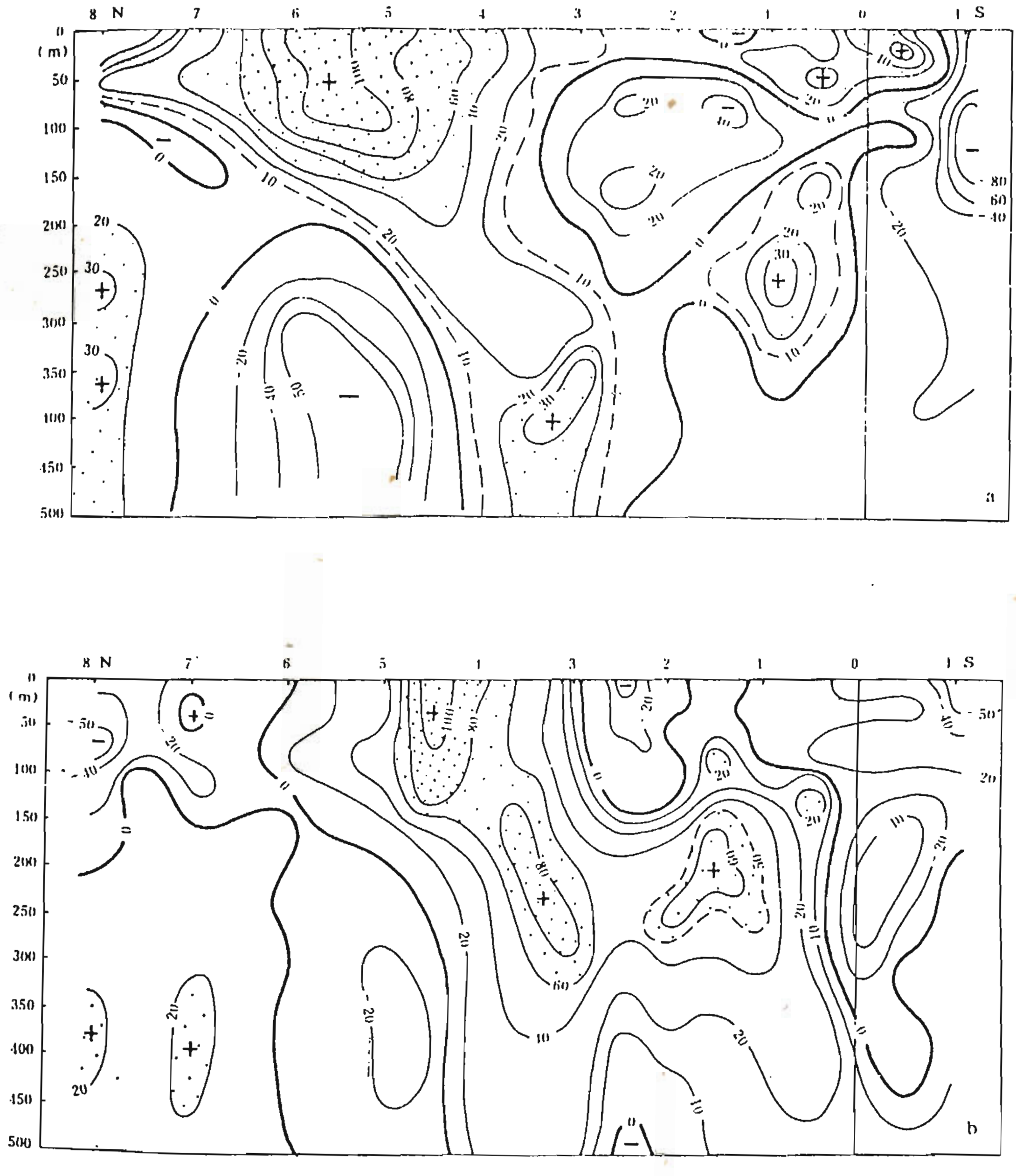

图4. 137° E线纬向流速分量($cm \cdot s^{-1}$,正值指东)的经向分布(根据管, 1986)

a.冬季(1981年1月31日—2月1日);

b.夏季(1981年6月30日—7月2日)。

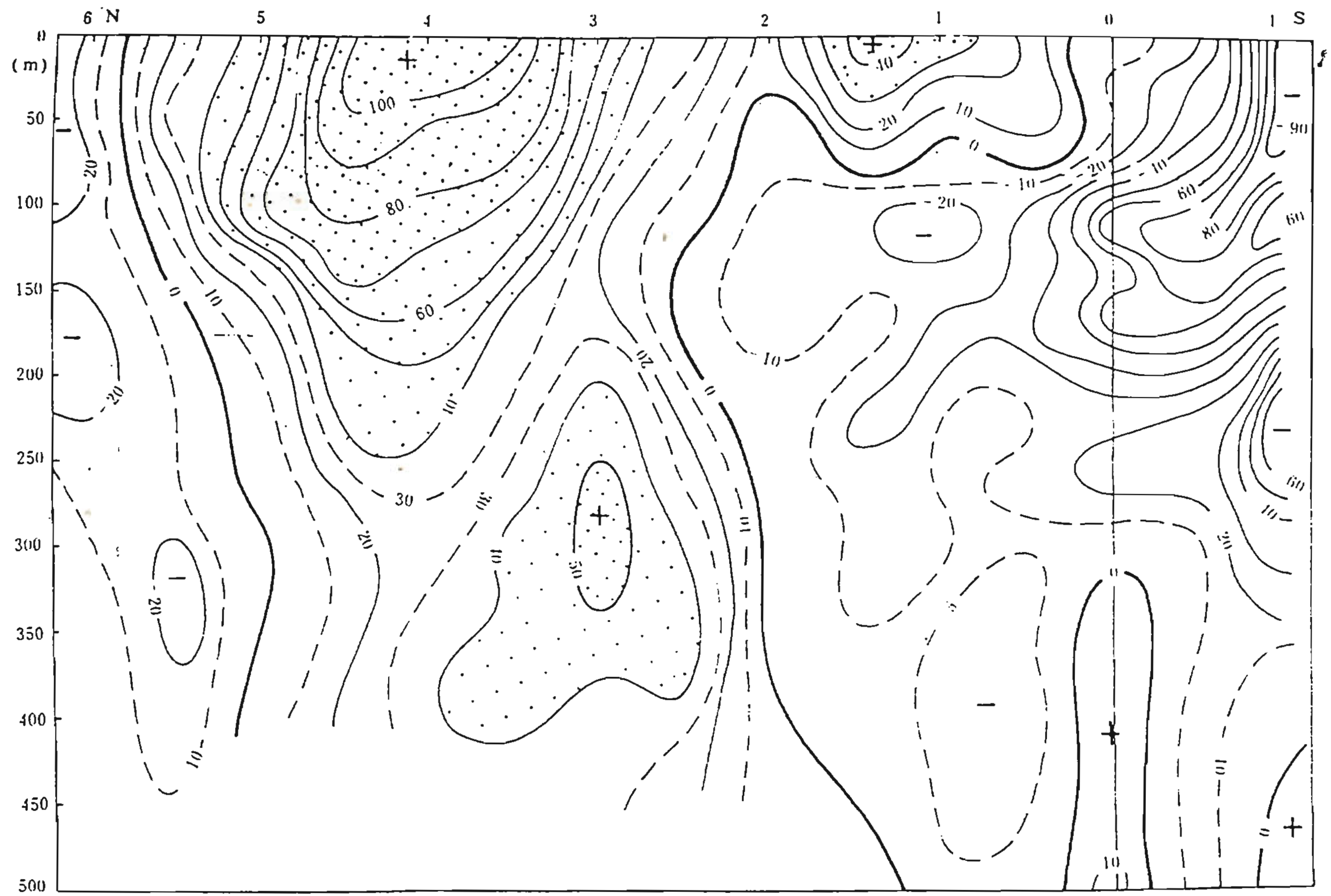

图5. 1982年夏季137° E线纬向流速分量(cm · s^{-1},正值指东)的经向分布。在6月30日—7月2日毗邻赤道处(1° S—2° N)"赤道潜流之源"消失(根据管，1986)。

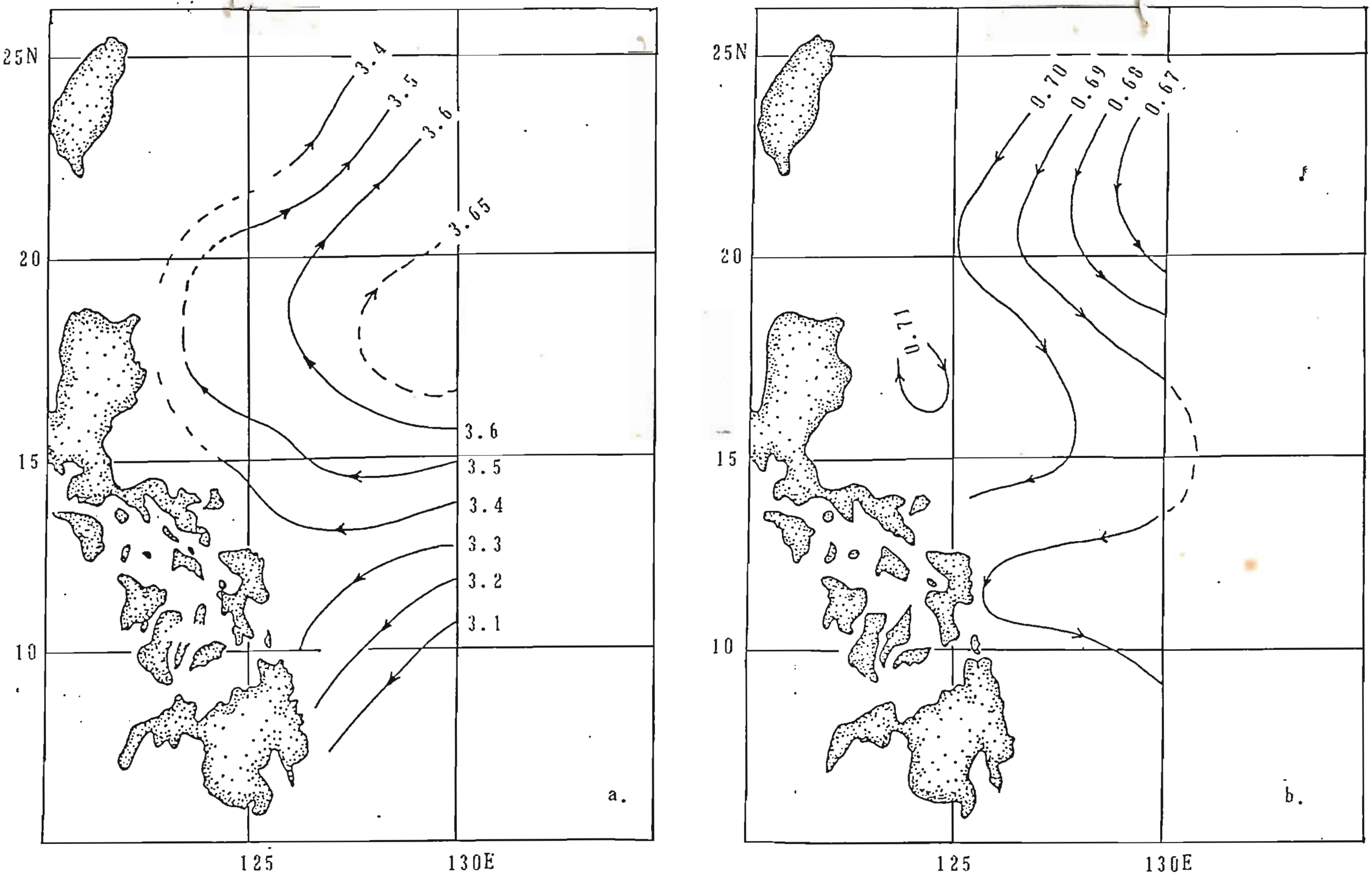

图6.　海面(a)及2000db面(b)上相对于3500db面的动力高度(dyn.m.)分布图(根据管，1990)。

国内关于厄尔尼诺及其对海洋和气候的影响研究概述*

管 秉 贤

（中国科学院海洋研究所，青岛）

厄尔尼诺是发生在赤道东太平洋南美沿岸的海面持续增暖现象，它会导致全球性的气候导常，造成巨大的经济损失。例如，1982－1983 年破记录的 El Nino 事件造成世界范围内的经济损失约达 200 亿美元。南方涛动指在南太平洋上的高压带与北澳大利亚到印尼的低压带之间的海平面气压波动。当这种波动较大时也会导致全球性的天气异常。研究表明，虽然厄尔尼诺发生在海洋上，南方涛动发生在大气，但两种现象紧密相关，通常把这两种现象作为一种事件来看待，简称 ENSO 事件。这是太平洋热带地区，特别是赤道地区海－气相互作用最集中的一个反映（黄荣辉，1990）。

由于 El Nino 对世界气候变异的巨大影响，吸引了全球海洋学家和气象学家的浓厚兴趣。还有最近两次发生的 El Nino，即 1982－1983 和 1986－1987 年的 El Nino 与 50 年代以来发生的其他几次 El Nino 具有不同的特征和发展过程，更促使人们对 El Nino 的形成机制进行深入的探索。

本文仅就我国学者近几年来对 El Nino 的研究，特别是 El Nino 对我国邻近海域水文和气候的影响这些方面的研究概况作一简略的介绍。

1、 最近两次 El Nino 事件的研究

人们对 1982－1983，1986－1987 年两次 El Nino 事件特别感兴趣，因为这两次事件的强度、发展时间和地点虽有差别，但海面温度场的空间分布和主要演变过程基本相似，而与前几次有明显的不同。张启文和王绍武（1986），武建平和李若纯（1988）及何有海等（1990）的研究均指出了上述特点。他们认为，在这两次 ENSO 事件中，赤道太平洋海温异常增暖不是象通常那样发生在春季和由南美沿岸向西发展，而是发生在秋季，且首先出现在赤道中太平洋日界线处，而后迅速向东发展。当然，这两次 El Nino 的强度是大有不同的。1982－1983 这次 El Nino 是 70 多年以来最强的一次 El Nino 过程，1983 年 6 月南美沿岸海温比常年竟偏高 6－7℃。而 1986－1987 年这次 El Nino 是一次中等或中等偏强的事件。根据王宗山等（1990）的估算，在这次 El Nino 期间，向东输送的暖水总量为 $11.4\times10^{14}m^3$，此值比 1976 年 El

* 本文得到国家自然科学基金的资助，曾在"海洋对气候变化调节与控制作用学术研讨会"（青岛，1990 年 8 月）上宣读过。

刊于《海洋对气候变化调节与控制作用学术研讨会论文集》

Nino 事件多 1/3 而比 1982－1983 年 El Nino 事件少 2/5。向东输送率为 $24\times10^6m^3/s$,表明 1986－1987 年 El Nino 为中等偏强事件。何有海等(1990)还分析了这两次 El Nino 强度差异的可能原因,认为与 1986－1987 年事件前,自西太平洋沿赤道东传的海温为负距平有关。

在 El Nino 期间,西北太平洋赤道和热带区域的流系结构也发生了异常。例如,管秉贤(1986)根据 137°E 线的实测流速资料,指出在 1982 年 6 月底－7 月初,赤道附近区域(2°N－1°S)东向的赤道潜流之源消失,而为西向流所取代。与中太平洋(159°W)和东太平洋(110°W)赤道区域赤道潜流类似的消失现象联系起来,可以认为,1982－1983 年 El Nino 期间的这一赤道潜流异常现象,以与斜压 Kelvin 波相当的速度(0.5－1.0m/s)自西向东传播。在 1986－1987 年 El Nino 期间,165°E 线上的赤道潜流也于 1987 年 10－11 月间经历了类似的消失过程。所以,赤道潜流的消失已成为 El Nino 事件的一个海洋特征现象。王宗山等(1990)又指出,在 1986－1987 年 El Nino 爆发前,南赤道流较强,暖水在西太平洋堆积;在爆发期内,则在 12.5 个纬度带内形成东向流,向东输送暖水;在 El Nino 结束后,在 12 个纬度带范围内变为西向流。

2、　El Nino **与西太平洋海洋现象之间关系的研究。**

El Nino 不仅与赤道和热带太平洋的流系变异有关,也与西太平洋其他一些海洋现象的变异有关。例如,蒲书箴和徐洪达(1987)根据 137°E 断面 1967－1983 年的水文资料分析比较了热带西太平洋水温对 El Nino 和反 El Nino 的不同响应。结果指出,在上述断面的深厚水体内的水温分布,El Nino 年呈现为冷年的特征;而在反 El Nino 年则为暖年。混合深度在 El Nino 年变浅,而在反 El Nino 年变深。同时,热带西太平洋的热库(Warm Pool),在 El Nino 年变弱,而在反 El Nino 年变强。林传兰(1990)研究了热带西北太平洋上层海洋热含量在 1964－1982 年间的变化特征,指出热含量的年际变化与 El Nino 事件相联系,在 El Nino 期间,平均温度出现大面积的负距平,高热含量海区的分布范围明显缩小。管秉贤(1989)根据 1965－1983 年的水温和水位资料分析了棉兰老冷涡变异与 El Nino 的关系,指出冷涡变异与 El Nino 有密切关系,在 El Nino 期间,冷涡向东扩展变得较强,而在非 El Nino 期间,冷涡向西收缩变得较弱。刘举平和管秉贤(1986)通过北太平洋信风场应力资料的分析发现,太平洋中两个最引人注目的海洋现象－黑潮大弯曲和 El Nino 都与北太平洋上空风应力涡度场的变化和大气热带辐聚带(ＩＴＣＺ)的南北移动有关。可以说,黑潮大弯曲和 El Nino 不是彼此孤立的,而是同一个大尺度海气系统变化的反映。

我国学者非常关心 El Nino 对我国邻近海域水文和气候的影响,在这方面主要研究了 El Nino 对台风活动、气温变化、海雾和水位等的影响,特别是前两者。

3、　El Nino **对西北太平洋和南海台风活动关系的研究。**

韩福荣等(1988)探讨了近百年来西北太平洋台风发生频数的时空分布主要特

征，指出在 El Nino 年台风位置发生异常，其高频区(145－155°E)比常年的高频区(140－145°E)偏东，同时在 El Nino 年台风发生的次数也较少。

不少学者研究了 El Nino 与南海台风活动的关系。例如，李崇银(1986)指出 El Nino 与南海台风活动有明显的关系，El Nino 年平均台风数偏少，反 El Nino 年平均台风数偏多，其异常主要发生在 8－11 月份；在两广沿海登陆的平均台风数也是 El Nino 年偏少，反 El Nino 年偏多，其异常以 10 和 11 月为最显著；在北部湾海域活动的台风多在 8－9 月，也是 El Nino 年偏少，反 El Nino 年偏多。陈特固和黎洁溪(1986)，施能和周家德(1989)得出了类似的结果。吕迎春和张其芳(1990)还研究了 El Nino 与影响我国北方海域(指 30°N 以北)的热带气旋的关系，指出在 El Nino 年热带气旋发生的平均纬度偏南，频数偏少，登陆偏早，早期路径偏西，转向点偏南，灾害性天气较弱。而在反 El Nino 年及非 El Nino 年期间情况则相反，对北方海域的袭击严重，灾害性天气剧烈。陈特固和周强(1990)专门研究了 1986－1987 年 El Nino 期间南海北部气候异常的主要特征有：台风活动显著减少，南海高压持续偏强，季风持续偏弱，寒潮冷空气入侵偏少，还有气温偏高，雨量与蒸发量偏少以及表层海温与盐度偏高等。

4、 El Nino 对我国气温影响的研究

赵振国(1989)从总的方面研究了 El Nino 与我国气温变化的关系，指出在 El Nino 当年的春夏季我国气温容易偏冷，冷月出现频率明显高于气候概率；在 El Nino 当年的秋冬季至次年春季我国气温偏暖的可能性大，暖月出现的频率明显高于气候概率。反 El Nino 年的情况正好相反，即当年春夏季我国气温容易偏暖，当年秋冬季至次年春季容易偏冷。上述关系主要表现在东部地区，而且夏季比冬季的关系更为明显。他特别指出，El Nino 现象与我国东北夏季低温冷害的发生有着非常密切的关系。李崇银(1989)专门研究了 El Nino 事件与我国东部气温变异的关系，得到了类似的结果。不仅如此，吴尚森等(1990)在对 El Nino 与华南气温变化关系的研究中也得到了类似的结果。他们还指出，广州月平均气温 2－3 年的振荡周期与 EL Nino 的关系甚为密切。

5、 EL Nino 对我国沿岸海平面影响的研究

李立(1987)通过对 1960－1982 年月平均水位资料的分析，研究了我国东南沿岸海平面对 EL Nion 的影响。发现 EL Nino 期间赤道太平洋海面的异常波动可以波及我国海域，我国东南沿岸在 El Nino 年的秋冬季海平面低于常年数到 10cm，呈负距平。月平均水位的年变幅也下降，年标准差出现最小值。EL Nino 造成的水位异常以台湾海峡为最显著，向北逐渐减弱。陈特固和詹小涌(1988)还分析了广东沿海 1963 年海平面异常低的原因，认为除了受大气环流异常的影响外，也与 1963 年是强 EL Nino 年，西北太平洋热带地区的海平面较常年明显偏低，从而波及广东沿海海平面也偏低。

6、 El Nino 与海雾天气关系的研究

许金镜(1989)分析了ENSO现象与台湾海峡西岸海雾天气的关系，指出El Nino的次年海雾天数偏多，反El Nino的次年海雾天数偏少。同时，南方涛动指数明显偏低的次年本海区海雾天数也偏多；反之，指数明显偏高的次年海雾天数偏少。所以，可以认为，ENSO现象对本海区次年海雾天数的多少有一定影响，两者相关关系较好。

7、 **El Nino与副热带高压及东亚寒潮关系的研究**

陈锦年(1990)用赤道东太平洋的平均水温来反映El Nino事件的发展过程，发现副高特征指数与赤道东太平洋水温的变化趋势是一致的，即当东太平洋水温增高(降低)时，副高将加强(减弱)，它们之间存在着明显的时滞(6—9月)关系。另一方面，李若纯(1988)还研究了东亚寒潮对ENSO的可能影响，认为东亚寒潮是通过对赤道西太平洋天气的影响而影响ENSO事件的。

8、 **其他**

王绍武(1989)研究了El Nino的时间序列，在1470—1987的近500年间共定出100次El Nino事件，总发生频率为19.3%。但其中有63次事件是跨两年的，所以共有163年为El Nino年或相邻年，约占总数的1/3。所以，从历史上看，El Nino的发生是相当频繁的。王绍武(1985)还从1860—1979年的120年中共定出31个El Nino年。张先恭(1988)根据El Nino的这一时间序列，研究了El Nino与太阳黑子活动的关系，发现在太阳黑子少的年份，即少于70个的年份，赤道东太平洋海区容易发生El Nino，在31个El Nino事件中，平均太阳黑子数少于70的，就有27个，约占87%。这表明，El Nino的发生确与太阳黑子活动有一定的关系。

总的讲来，在上面提到的许多论述中，大都是偏重研究El Nino与海气现象的相关关系，有关机制的研究显得不够。这应是今后的努力方向。

9、 **展望**

还有不少文章，用不同的理论预侧了El Nino可能发生的年份。例如，翁文洁和曹鸿兴(1989)运用灰色预测理论，预测下一次El Nino将发生在1992—1993年。但今年5月份日本气象厅根据观测就报称，当时南美秘鲁海面已出现El Nino现象的前兆，从而预言"今夏很可能发生El Nino"。符淙斌(1990)也报道称"一次新的El Nino事件即将发生"。最近，自有关方面获悉，1990年已发生了一次弱的El Nino，且目前正处于消衰阶段。但有些学者对1990年是否可列为El Nino年，仍有不同的看法，请大家留意这方面的新报道。

参考文献

[1] 王宗山，邹娥梅，John M. Toole, Linda J. Mangum, 徐伯昌，杨克奇，1990. 1986—1987年厄尔尼诺期间赤道太平洋的物理海洋学事件. 海洋学

报 12(2)：159－166.

[2] 王绍武，1989. 近 500 年的厄尔尼诺事件. 气象 15(4)：15－20.

[3] 刘举平，管秉贤，1986. 黑潮大弯曲与埃尔尼诺的关系初步探讨. 海洋学报 8(5)：541－546.

[4] 吕迎春，张其芳，1990. 埃尔尼诺与影响我国北方海域的热带气旋. 海洋预报 7(1)：

[5] 许金镜，1989. 厄尔尼诺和南方涛动现象与台湾海峡西岸海雾天气的关系. 台湾海峡 8(3)：211－214.

[6] 李　立，1987. 我国东南沿岸海平面对埃尔尼诺的响应. 台湾海峡 6(2)：132－138.

[7] 李若纯，1988. 东亚寒潮对 ENSO 的可能影响. 黄渤海海洋 6(1)：15－18.

[8] 李崇银，1986. 厄尔尼诺与南海的台风活动. 热带气象 2(2)：117－123.

[9] 李崇银，1989. El Nino 事件与中国东部气温异常. 热带气象 5(3)：210－219.

[10] 何有海，Warren B. White and Stephen E. Pazan，1990. 海面温度场对 1986－1987 年 ENSO 事件的响应. 热带海洋 9(2)：86－92.

[11] 吴尚森，黄成昌，薛惠娴，1990. 华南气温变化与 ENSO 的关系. 热带气象 6(1)：57－64.

[12] 陈特固，黎洁溪，1986. 厄尔尼诺与南海台风活动的初步分析. 热带海洋，5(2)：80－83.

[13] 陈特固，詹小涌，1988. 广东沿海 1963 年海平面异常低的原因分析. 热带海洋 2(2)：45－53.

[14] 陈特固，周强，1990. 1986－1987 年 El Nino 期间南海北部的气候异常. 热带海洋 9(2)：98－102.

[15] 陈锦年，1990. El Nino 与南方涛动及其对副热带高压的影响. 热带海洋 9(2)：71－77.

[16] 武建平，李若纯，1988. 1986－1987 年厄尔尼诺－南方涛动事件形成发展过程分析. 热带海洋 7(4)：27－35.

[17] 张先恭，1988. 厄尔尼诺与太阳活动的关系. 气象 14(2)：41－43.

[18] 张启文，王绍武，1986. 1982－1983 年埃尔尼诺现象与其他年埃尔尼诺现象的比较. 海洋学报 8(4)：429－435.

[19] 林传兰，1990. 1964－1982 年热带西北太平洋海洋上层热含量的变化特征. 热带海洋 9(2)：78－85.

[20] 赵振国，1989. 厄尔尼诺现象与我国温度. 气象 15(7)：26－30.

[21] 施能，周家德，1989. ENSO 与南海台风活动的统计分析. 气象 15(4)：9－14.

[22] 翁文洁，曹鸿兴，1989. El Nino 发生年份的灰色预测. 黄渤海海洋 7(4)：18－24.

[23] 符淙斌，1990. 一次新的埃尔尼诺事件即将发生. 大气科学 14(2)：232－233.

[24] 黄荣辉，1990. ENSO 及热带海气相互作用动力学研究的新进展. 大气科学 14(2)：234－242.

[25] 韩福荣，文其汉，赵绪孔，1988. 西北太平洋台风发生频数的时空变化特征与 El Nino 的关系. 黄渤海海洋 6(3)：23－27.

[26] 蒲书箴，徐洪达，1987. 热带西太平洋水温对埃尔尼诺的响应. 海洋学报 9(2)：262－266.

[27] 管秉贤，1986. 北太平洋西部赤道区域的海流结构及其变异. Chin. J. Oceanol. Limnol. 4(3)：239－255.

[28] 管秉贤，1989. 棉兰老冷涡的变异及其与 El Nino 的关系. 海洋与湖沼 20(2)：131－138.